WRC RESEARCH REPORT NO. 72

METHODOLOGIES FOR FLOW PREDICTION IN URBAN STORM DRAINAGE SYSTEMS

Ben Chie Yen
Associate Professor
Department of Civil Engineering
University of Illinois at Urbana-Champaign

F I N A L R E P O R T

Project No. B-043-ILL

September 1, 1969 - January 31, 1973

The work upon which this publication is based was supported by funds provided by the U.S. Department of the Interior as authorized under the Water Resources Research Act of 1964, P.L. 88-379
Agreement No. 14-31-0001-3078

UNIVERSITY OF ILLINOIS
WATER RESOURCES CENTER
2535 Hydrosystems Laboratory
Urbana, Illinois 61801

August 1973

ABSTRACT

METHODOLOGIES FOR FLOW PREDICTION IN URBAN STORM DRAINAGE SYSTEMS

Increasing public concern on urban storm water quantity and quality problems demands a thorough review of the methodologies for flow prediction and design of urban storm drainage systems and development of improved methodologies. In this study the urban storm drainage system is considered as an integrated system of components of urban surface, gutters, inlets, sewer branches, junctions, manholes, and other structures. The flow equations that can be used to solve storm drainage problems are critically reviewed and the mathematical methods for solving the St. Venant equations are compared. A method to routing the unsteady flow due to rainfall and other inputs through land surface and gutter to produce the inlet hydrograph is proposed. The results have been presented in nondimensional form for general uses. A mathematical simulation model for tree-type sewer networks is developed by using the St. Venant equations to route the inlet hydrographs through the network. An overlapping segment scheme is used to account for the backwater effects and mutual influences of the unsteady flow in the sewers. The results show clearly the importance of detention storage in the drainage system and the possibility of detention storage manipulation for flood peak attenuation. In addition to flow prediction purposes, the developed model can also be used for design of sewer systems. Furthermore, new approaches based on risk consideration are proposed for determination of design rainfall and for design of sewers and other hydraulic structures.

Yen, Ben Chie
METHODOLOGIES FOR FLOW PREDICTION IN URBAN STORM DRAINAGE SYSTEMS
Final Report to Office of Water Resources Research, Department of the Interior, Washington, D.C., Research Report No. 72, Water Resources Center, University of Illinois, Urbana, Illinois, August 1973, x + 150 pp.
KEYWORDS--design-hydraulics, drainage, *drainage systems, effluents-waste water, flood routing, flow characteristics-water, gutters, hydraulics, *hydraulic design, hydrographs, inlets, *mathematical models, *open-channel flow, overland flow, *risks, runoff, safety factor, simulation, *storm water, surface flow, *unsteady flow, *urban runoff

ACKNOWLEDGMENTS

This report is a summary of the accomplishments and activities of a research project financially supported by the Office of Water Resources Research for the amount of $28,984 and matched by the University of Illinois for the amount of $30,507.50 under Grant Agreement No. 14-31-0001-3078, Project No. B-043-ILL.

Throughout the duration of this project, many people whose names appear in Appendix 2 have participated in the project, particularly the contribution by Messrs. A. S. Sevuk and A. O. Akan, to whom the author would like to express his thanks. Cooperation from Drs. B. B. Ewing and H. G. Wenzel, Jr. Director and Assistant Director, respectively, of the Water Resources Center of the University of Illinois, for matters related to the progress of the project is appreciated. The author is also grateful to the secretarial support in typing to meet the seemly endless deadlines throughout the project period.

CONTENTS

LIST OF FIGURES

LIST OF TABLES

NOTATION

A = area of channel cross section (Fig. 1);

B = width of gutter (Fig. 9);

b = free surface width of channel cross section;

C_f = constant in Eq. 18;

D = hydraulic depth = A/b; also, diameter;

E_f = work done due to fluctuating nonhomogeneous fluid as defined in Eq. 4;

E_u = work done due to fluctuating nonhomogeneous fluid as defined in Eq. 5;

F = function;

$\mathbb{F}$ = Froude number;

f = Weisbach resistance coefficient given in Moody diagram;

$f_e = 8gRS_e/V_1^2$, energy dissipation coefficient;

$f_f = 8gRS_f/V_1^2$, frictional resistance coefficient;

$f_H = 8gRS_H/V_1^2$, total head loss coefficient;

g = gravitational acceleration;

H = approximate total head as defined in Eq. 10;

H_B = cross sectional total head of flow measured from horizontal reference datum in terms of γ_a (Eq. 7);

H_c = reference total head as defined in Table 4;

H_L = piezometric head, with respect to horizontal reference datum, of lateral flow when joining or leaving channel flow (Eq. 8);

H_L' = local fluctuation or turbulence velocity head of lateral flow when joining or leaving channel flow (Eq. 9);

H_p = cross sectional average piezometric head;

H_v' = velocity head due to fluctuating nonhomogeneous fluid as defined in Table 4;

h = depth of flow, measured along y direction;

i = rainfall intensity, also, coordinate direction;

j = index; also, coordinate direction;

K = piezometric pressure correction factor as defined in Table 3;

K' = ambient piezometric pressure correction factor as defined in Table 3;

k = surface roughness;

k_p = surface roughness of pavement;

L_g = length of gutter;

N = directional normal of a surface, positive outward; also, a number;

n = Manning's roughness factor; also, a number;

P = $p + \rho g y \cos\theta$, local piezometric pressure with respect to channel bottom; also, wetted perimeter; also, probability;

p = local pressure intensity;

Q = discharge;

Q_b = base flow rate; also, reference design discharge;

Q_o = discharge at gutter exit;

Q_p = peak discharge;

Q_{pu} = peak inflow rate at upstream of gutter;

Q_s = $iA + Q_{pu}$;

q = time rate of lateral flow per unit length of σ;

R = hydraulic radius;

$\mathbb{R}$ = $V_1 R/\nu$, Reynolds number;

r = normal displacement of σ with respect to space or time projected on a plane parallel to A, positive outward;

S = storage;

S_e = dissipated energy gradient (Eq. 6);

S_f = friction slope as defined in Table 3;

S_H = $-\partial H/\partial x$, total head gradient;

S_o = $-\partial z_b/\partial x = \sin\theta$, channel bottom slope;

T = force due to internal stresses $\bar{\tau}_{il}$ acting on A as defined in Table 3; also, return period;

t = time;

t_i = duration;

t_u = duration of gutter upstream inflow hydrograph;

U = velocity of lateral flow when joining channel flow;

u_i = local velocity component along x_i-direction;

u_i' = turbulent fluctuation of the i-th component of local velocity with respect to $\overline{u}_i$;

V = velocity;

V_i = i-th component of channel flow velocity averaged over cross section; also, cross sectional averaged velocity for i-th sewer;

$\overline{V}^2 = \overline{u}_i \overline{u}_i$

W = a symbol referred to conservative work done by internal and surface stresses as defined in Table 4;

W_p = length of pavement along transverse direction of street;

w = safety judgement factor;

$x = x_1$, longitudinal coordinate along channel bottom direction;

x_i = coordinate along i-th direction;

y = coordinate perpendicular to x on vertical plane, measured from channel bottom; also depth of flow in sewers or junctions;

y_m = maximum flow depth;

Z = height of drop at junction;

z_b = elevation of channel bottom with respect to horizontal reference datum;

α = convective kinetic energy flux correction factor as defined in Table 4; also, risk;

β = momentum flux correction factor as defined in Table 3;

β' = turbulent momentum flux correction factor as defined in Table 3;

γ = specific weight of fluid;

$\gamma_a = \rho_a g$, cross sectional average specific weight;

ϵ = error in flood volume conservation;

ζ = unsteady pressure correction factor (Eq. 3);

η = convective potential energy flux correction factor as defined in Table 4;

θ = angle between channel bottom and horizontal plane;

λ = density correction factor as defined in Table 2;

λ' = fluctuating density correction factor as defined in Table 2;

μ = dynamic viscosity of fluid;

ν = kinematic viscosity of fluid;

ρ = mass density of fluid;

ρ_a = cross-sectional average mass density;

σ = perimeter bounding cross sectional area A; also, standard devi

$\overline{\tau}_{ij}$ = temporal mean stresses, as defined in Table 4 for incompressib shear stresses for $i \neq j$, normal stresses for $i = j$;

ϕ = transverse angle of the gutter made with horizontal plane; and

ϕ_p = angle between pavement and horizontal plane.

olog fo

drai

deve pi

the

and t

faci

fect ir

amou

ific io

work n

tima

(196 .

pend

grow g

It w

sour

stru io

seve

be s nt

expe

unsa f

lack f

λ = density correction factor as defined in Table 2;

λ' = fluctuating density correction factor as defined in Table 2;

μ = dynamic viscosity of fluid;

ν = kinematic viscosity of fluid;

ρ = mass density of fluid;

ρ_a = cross-sectional average mass density;

σ = perimeter bounding cross sectional area A; also, standard deviation;

$\overline{\tau}_{ij}$ = temporal mean stresses, as defined in Table 4 for incompressible fluid, shear stresses for $i \neq j$, normal stresses for $i = j$;

ϕ = transverse angle of the gutter made with horizontal plane; and

ϕ_p = angle between pavement and horizontal plane.

I. INTRODUCTION

The main objective of this research is to develop an improved methodology for quantitative prediction of storm runoff at various locations in urban drainage systems. Auxiliary objectives are to investigate the possibility of developing techniques for optimum design of storm sewer systems and to reveal the inadequacy of existing sewer design methodologies.

Metropolitan areas, in Illinois as well as elsewhere in the Nation and in the world, are growing at an unprecedented rate. Among the vital facilities related to the urban living environment, storm drainage systems affect directly the quantity as well as quality of disposed urban water. Large amount of money and resources are involved in the design, construction, modification, operation and maintenance of urban storm sewer systems. Cost of work on storm drainage systems and storm water damage in urban areas is estimated to be of the order of $100 million annually in the State of Illinois (1967). The American Public Works Association (1966) estimated that the expenditures before the year 2000 for storm drainage facilities to serve the growing population of the Nation will exceed 25 billion dollars (1966 value). It was recorded in an American Society of Civil Engineers Urban Water Resources Research Program (1969) report that the estimated average public construction cost for storm sewers is 2.5 billion dollars annually for the next several years. Rawls and Knapp (1972) estimated that 20 billion dollars will be spent on urban drainage facilities in the next decade. Yet, despite the expenses and efforts involved, urban storm drainage projects are often found unsatisfactory, due partly to the insufficient knowledge on storm runoff and lack of reliable flow prediction and design methodologies.

Urban storm drainage systems consist of urban surface areas, gutters and inlet devices, sewer conduits, junctions, manholes, and other control and regulation facilities. Traditionally, in the design of a storm drainage system each of its components is considered individually by assuming the flow to be steady and uniform without due consideration to the backwater and detention storage effects. In other words, it is assumed that the flows in the system can be combined linearly without considering the mutual effects on the flow characteristics in the various components of the drainage system. Typical examples of such design techniques can be found in the widely adopted manuals such as those by ASCE (1969) and Wright-McLaughlin Engineers (1969) for the metropolitan area of Denver, Colorado.

However, natural rainstorms are of finite and usually short durations with rainfall intensity varying both spatially and temporally. Consequently, the flow in storm drainage systems is unsteady. Time is needed to transform the rainfall to runoff from surface through gutters, inlets, sewers, junctions and manholes to the points of disposal, such as into channels, rivers, reservoirs, lakes and treatment plants. During this transformation process a certain amount of water is inevitably stored at various parts of the drainage system to be released at a later time. The detention storage and the backwater effects modify significantly the propagation of the storm runoff in the drainage system. Thus, the conventional design method of using estimated steady condition peak discharge as the design flow usually gives an unbalanced and uneconomic results, and under certain unfavorable conditions it may be costly and unsafe, such as the cases of simultaneous meeting of attenuated peak discharges which are greater than the offsetted unattenuated flows.

Lately, attention has also been focused on the total amount of storm runoffs and their time distributions because of the public concern on water pollution problems and preservation and possible improvement of the living

environment. Traditional flow prediction methods provide only the peak discharge but not the runoff hydrographs. Recently the importance of effects of unsteadiness of the flow and the detention storage in the drainage system has been recognized, and attempts have been made to apply the one-dimensional equations of momentum and continuity, i.e., the St. Venant equations or their various simplified forms, to the components of storm drainage systems for prediction of flow (e.g., Ackers and Harrison, 1964; Schaake, 1965; ASCE Urban Water Resources Program, 1968; Harris, 1970a, 1970b; Yevjevich and Barnes, 1970).

Even with the recent development in computer capabilities and numerical techniques, at present it is impossible to develop a single highly accurate comprehensive simulation model for both flow prediction and design purposes for the entire drainage system because of the limitation of the size of the existing computers. Fortunately, hydraulically the characteristics of certain components in drainage systems, such as inlet catch basins, provide flow controls that enable the decomposition of the entire system into individually manageable but related subsystems.

The size and geometry of inlet catch basins depend mainly on local conditions and therefore there is no standard specification for them. Yet, their height is a control factor in determining the detention storage in the inlet catch basin and the time lag of the gutter flow into the sewers. The flow entering an inlet catch basin does not depend on the depth of water in the basin nor on the discharge into the sewer unless the basin is completely filled and submerged which rarely occurs. Therefore, it is desirable in this research to divide the urban storm drainage system into two major components; namely, (a) the surface storm runoff system considering the transformation of rainfall to the inlet catch basin inflow hydrographs; and (b) the storm sewer network

system downstream from the inlet catch basins. The two components are related by the fact that the inflow hydrographs into the sewer network system are obtained from the inlet catch basin inflow hydrographs adjusted by the storage and time of fall in the catch basins. Furthermore, in sewer networks, facilities such as drops, chutes, and pumps often behave hydraulically as flow control sections. Thus, they provide a means to divide the sewer network into individual sequential subsystems for hydraulic analysis. This division of a storm drainage system by using hydraulic control sections into individual sequential components in this research considerably simplifies the analysis without sacrificing the accuracy and usefulness of the results. It also makes possible for the problem to be handled numerically within the capability of the existing large computers with considerable savings in computation time.

This report is a summary of the research results obtained from the OWRR project, B-043-ILL, "Methodologies for Flow Prediction in Urban Storm Drainage Systems." Most of the research findings from this project have been published previously in papers and theses and this report furnishes to provide an integrated overall view of the research together with some additional new information. A brief review of existing urban storm runoff models is first presented. Next, the flow equations used in solving urban storm drainage problems are critically examined and the mathematical methods to solve the simplified forms of these equations are compared. Simulation models for storm runoffs in the surface flow system upstream from the inlet catch basins and the sewer network system downstream from the catch basins are then presented. Finally, the determination of design rainfall and a new approach of sewer design based on risk analysis is reported. It is believed that the research results can be applied separately or integratedly for the purposes of flow prediction, drainage system design, improvement of existing drainage systems, and identification of the effects of urbanization and local storages.

II. EXISTING URBAN STORM RUNOFF MODELS

Numerous rainfall-runoff mathematical simulation "models" have been proposed by previous investigators. Many of these models are applicable to urban environment. It would be tedious to list all these models in this report. Fortunately, many of them are only modifications or slight variations of the better known models which for discussion purpose, can be classified here into three categories; namely, the overland component models, the sewer component models, and the integrated system models. Several early methods in each of the three categories have been widely accepted and used in the design and operation of urban drainage systems. However, many more rational and sophisticated models have been developed and proposed only recently. They need to be tested, and if proven worthwhile, introduced to engineers for practical applications.

An excellent review of some of the models mentioned in this chapter can be found in a report by Linsley (1971). It should be noted herein that a number of the stream network routing models such as the USDA Hydrograph Laboratory Model (Onstad and Jamison, 1960), the stream flow simulation and reservoir regulation model (Rockwood, 1958, 1968), and the Sugawana model (1961) do not seem to be applicable to urban settings.

II-1. Overland Runoff Models

There are two different approaches to estimate overland runoff due to rainfall. The black box (lumped system) approach produces output from a given input without considering what is happening within the overland surface. The hydraulic routing (distributed system) approach routes the rainfall excess through the overland surface to produce the runoff hydrograph.

The models using the black box approach can again be subdivided into four groups; namely, the rainfall-intensity coefficient formulas, the frequency

formulas, the monograph methods, and finally, the hydrograph methods. The first three groups give only the magnitude of the peak rate of storm runoff, Q_p, and cannot provide any information concerning the time of occurrence of Q_p nor the runoff rate at any other time. The last group, the hydrograph methods, gives information on the time distribution of runoff and hence is more useful in solving urban drainage problems.

Among the rainfall-intensity coefficient formulas the rational formula is undoubtedly the most famous, popular, enduring, and perhaps the oldest (Chow, 1964). Others in the group applicable to or strictly for urban settings include the Adams, Burkli-Ziegler, Cramer, Gregory, Gregory-Arnold, Gregory-Hering, Grunsky, Hawksley, McMath, and Parmely formulas summarized in Group 5 of Appendix 1 in a report by Chow (1962). All of these formulas were derived on the basis of regional observed data and have limitations on basin size, region, and other geographical conditions of application. They are all dimensionally nonhomogeneous which will impose a minor problem in view of the possibility of the United States to change the units from the English system to the SI system. Despite their simplicity, all but two of these formulas have faded away with history because of their limitations. The two survived are the rational and the Burkli-Ziegler formulas which have been applied to different geographic regions with the coefficients evaluated over a wide range of conditions. Both formulas can provide reliable estimate of peak runoff if the coefficients are correctly chosen. Because of its simplicity, the rational formula is still used as a standard method in urban drainage design (ASCE, 1969; Wright-McLaughlin Engrs., 1969), despite the fact that its drawbacks are well known (Chow, 1964; Schaake et al, 1967; McPherson, 1969). A variation of the rainfall-intensity coefficient formulas is the drainage-area coefficient formulas which became popular at the turn of the century. These

formulas were developed for rural areas, subject to restricted regional and size limitations, and are not applicable to urban settings.

The frequency formulas or graphs based on past flood records have been proposed by many, including the USGS, for small as well as large watersheds. However, this method has yet to be successfully adapted to urban environment. First, there are usually lack of data for small urban areas to perform a flow frequency analysis. Secondly, such a frequency analysis requires the physical characteristics of the drainage area being stationary, i.e., not changing with time, which rarely happens in urban settings.

The monograph methods include the U.S. Soil Conservation Service (1971), BPR (Potter, 1961), California (1953), Chow (1962), and Cook (Hamilton and Jepson, 1940) methods. All of these methods were developed primarily for and have been widely used in rural areas, although some may be modified for urban areas. Because the monographs of these methods for urban areas have not been developed, they are seldom used in urban settings.

The hydrograph methods, which give not only the values of Q_p but also the entire runoff hydrograph, are understandably more sophisticated than the previously discussed methods and require more data. The basic concept behind this approach is to establish a reference hydrograph or hydrographs for a given drainage basin which can be used repeatedly for different rainfall conditions. Typical of this reference hydrograph is the unit hydrograph. Consequently this approach is subject to a similar restriction imposed on the frequency formulas; that is, requiring no appreciable changes in the physical nature of the drainage area that might alter the reference hydrograph. Examples of this approach proposed for urban runoff determination are the methods by Espey, Morgan, and Masch (1965) and by Rao, Delleur, and Sarma (1972). None of these methods has been sufficiently tested for urban drainage areas,

nor have they been accepted in engineering design or for operational purposes.

The hydraulic routing (distributed system) approach for the evaluation of overland runoff provides not only the runoff hydrograph but also some information on the flow within the drainage area. Two of these methods, the Izzard (1946) and the Horton (1938) methods, have long been accepted by hydraulic and sanitary engineers for urban, highway, and airport drainage designs. The kinematic wave method, which is supposedly better than the Izzard and Horton methods because it includes some flow unsteadiness effects, has been recently proposed (e.g., Henderson and Wooding, 1964; Grace and Eagleson, 1966; Eagleson, 1970, 1972; Harley et al, 1970) to engineers for practical applications. More sophisticated but accurate models such as solving the St. Venant equations in one-space dimension (e.g., Iwagaki, 1951, 1955; Behlke, 1957; Liggett and Woolhiser, 1967; Morgali and Linsley, 1965; Ragan, 1967; Abdel-Razaq et al, 1967; Chen and Chow, 1968; Kareliotis and Chow, 1971) and two-space dimensions (Ben-Zvi, 1970) have also been developed but have not yet verified by actual data.

II-2. Sewer Flow Models

Almost all of the existing sewer flow routing models consider the sewer flows independently from sewer to sewer disregarding the junction losses and backwater effects, and the flows in the sewers are related to one another only in a sequential manner by considering only the continuity relationship. In other words, the hydrographs from the upstream sewers at a junction are added linearly to produce hydrographs for the downstream sewer and the procedure is repeated in sequence without considering the mutual dynamic effects among the sewers and junctions.

Most of the commonly adopted methods to estimate sewer flows use the Manning, Chezy or similar formulas (e.g., ASCE, 1969; Wright-McLaughlin Engrs.,

1969) which implicitly assume the flow to be steady and uniform although in reality the contrary is true. The time variation of runoff is accounted for only indirectly through the continuity consideration. The flood waves in the sewers are not attenuated, usually the only delay time considered is the computed travel time of the flow in the sewers. From the hydraulics viewpoint, this is a linear kinematic wave approach.

With the advent of high speed computers and recent development in numerical techniques, improved methods by using more sophiscated hyraulic equations have been proposed for application to sewer flows. The conventionally used unsteady open-channel flow equation which is applicable to sewer flows is the momentum equation

$$\frac{\partial V_1}{\partial t} + V_1 \frac{\partial V_1}{\partial x} + g \cos\theta \frac{\partial h}{\partial x} = g(S_o - S_f) \qquad (1)$$

in which x is the longitudinal direction of the sewer; V_1 is the cross sectional average flow velocity along the x direction; t is time, g is the gravitational acceleration; h is the depth of flow measured perpendicular to x, θ is the angle between the channel bed and a horizontal plane; $S_o = \sin\theta$ is the sewer slope; and S_f is the friction slope. The corresponding equation of continuity is

$$\frac{\partial h}{\partial t} + D \frac{\partial V_1}{\partial x} + V_1 \frac{\partial h}{\partial x} = 0 \qquad (2)$$

in which D = A/b is the hydraulic depth of the flow where b is the width of the free surface.

Equations 1 and 2, known as the St. Venant equations, are first-order quasi-linear hyperbolic partial differential equations. They can be solved numerically with two initial and two boundary conditions known. However, in addition to the difficulties often encountered in defining the boundary con-

ditions, the numerical solution requires considerable amount of computation. Hence, various simplifications have been proposed to give simple approximate solutions. Routing models using only the continuity equation (Eq. 2), often rewritten in the form I-Q = dS/dt, where I and Q are respectively the rates of inflow into and outflow from the control volume considered and S is the storage within it, are known as hydrology routings. The hydrologic routing techniques, including the various coefficient routing methods such as the Muskinghum technique, and the reservoir routing, can be found in most standard references (Gilcrest, 1950; Chow, 1959, 1964).

The continuity equation (Eq. 2) can be solved together with various simplifications of the momentum equation (Eq. 1) to form the various approximate simulation models as show in Table 1. A discussion of these approximations

TABLE 1. - HYDRAULIC ROUTING MODELS

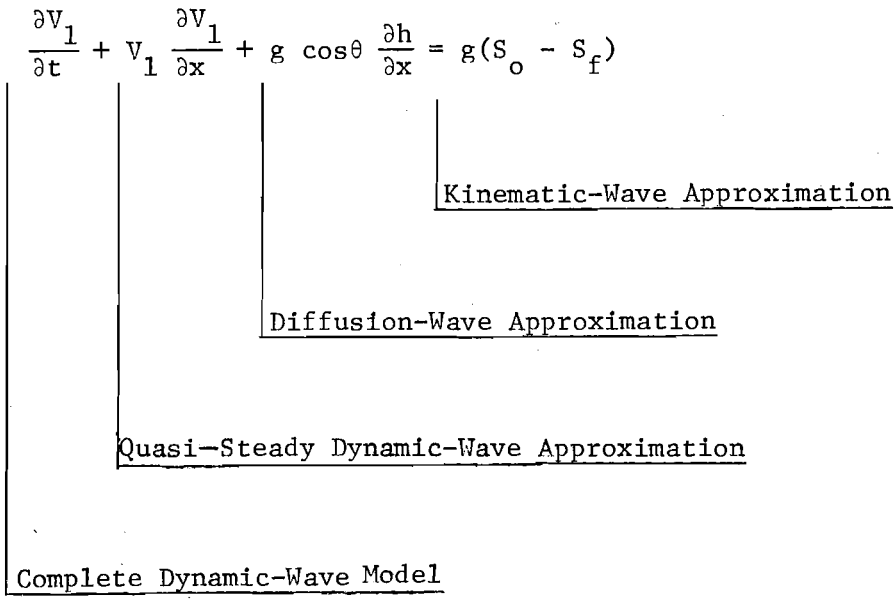

can be found elsewhere (Sevuk, 1973). Among the approximate nonlinear models, the simplest and widely discussed is the nonlinear kinematic-wave model (Harley et al, 1970) which has been applied to selected urban sewers. Neither the nonlinear diffusion-wave model nor the nonlinear quasi-steady dynamic-wave model has been adequately studies, nor have they been applied to sewer flows, although the former model has been discussed by Harley et al (1970). The most sophisticated model is the complete nonlinear dynamic wave model involving the solution of the St. Venant equations with different numerical techniques (Harris, 1970a; Yevjevich and Barnes, 1970). Because this model is so sophisticated, at present it has been used only by certain researchers for specific problems and has yet to be thoroughly investigated before introduction to practical engineers for adoption. It should be mentioned here that attempts have been made to linearize the diffusion-wave model for solutions such as the one developed by Harley et al (1970) and by Van de Nes and Hendriks (1971) for two-dimensional flows; but it does not seem to be promising for use in sewers because of the difficulty involved in linearization of the flow equations due to the geometry of the sewers.

All the aforementioned previously developed sewer flow routing models are applicable to a single sewer. For these models when applied to a network the sewers or channels are simply treated individually in sequence with the flows cascading from one channel to another towards downstream. However, in a sewer network in the field condition, considerations must be given to the mutual dynamic effects such as backwater and energy losses among the sewers and junctions. Several analyses have been developed for water supply distribution networks of completely pressurized pipes, yet they cannot be applied to sewer networks which are usually of tree type and with free surface flows. For a channel system composed of a main channel and a single

tributary, solutions based on the complete nonlinear flow equations have been obtained by Isaacson et al (1956), Larson et al (1971), Pinkayan (1972), and Fread (1972). They all recognized the continuity of water surface at the junction.

II-3. Integrated System Models

In these models the overland and sewer components described in the preceding two subsections are integrated together to give the runoff from a drainage system. All these models require rainfall and other inflows, if any, as the input, and give the runoff hydrograph at the point of interest in the drainage system as the output. Almost all the existing integrated models are sequential or cascade models by evaluating the runoff from upstream towards downstream in sequence without considering the mutual effects among the joining sewers or channels. This procedure simplifies the computation but sacrifices the reliability in estimating the runoff from a sewer network.

The Los Angeles hydrograph method proposed by Hicks (1944), the Chicago method (Keifer and Chu, 1957; Tholin and Keifer, 1960), the inlet method (Horn and Dee, 1967; Kaltenbach, 1963), and the British Road Research Laboratory (RRL) method (Watkins, 1962; Terstriep and Stall, 1969; Stall and Terstriep, 1972) adopted either the rational method or linear kinematic-wave model for overland flows and linear kinematic-wave approximation for sewer flows. These four methods have been adopted by engineers in practice in various places. The Texas Tech model (Wells, Austin, and Cook, 1971) is essentially an extension of the RRL model considering the stochastic nature of rainfall and water quality. The inlet method has been improved by Schaake (1965) to incorporate the dynamic wave routing. A similar routing model has been developed and used in the computer controlled routing of storm runoff in a Minneapolis-St. Paul storm sewer system (Bowers et al, 1968).

The Stanford Watershed Model (Crawford and Linsley, 1966), which was developed primarily for rural basins, has been modified at Hydrocomp (1969) to incorporate nonlinear kinematic-wave model in the hydraulic routing of the flow and can be used for urban settings. It was also modified as the Kentucky Watershed Model (James, 1970) applicable to urban areas.

The FWQA model (Chen and Shubinski, 1971) developed for urban areas assumes a series of rectangular overland sub-basins and adopts a linear kinematic-wave routing method by using the Manning and continuity equations. The Metcalf and Eddy, Inc., University of Florida and Water Resources Engineers, Inc. model (1971, SWM model) adopted a linear kinematic-wave approximation for both overland (Chen and Shubinski, 1971) and sewer flow routings. No special considerations were given to the junction effects. Recently the SWM model has been modified (Shubinski and Roesner, 1973) by considering the surface and total head compatibility conditions at the junctions. The discharge into the junction is computed by assuming constant discharge within the sewers and applying a modified form of the St. Venant equations only to the exit of the sewers. In other words, it is a quasi-steady approach.

The University of Cincinnati model (1970; Papadakis and Preul, 1972) adopts the linear kinematic-wave model for the overland and gutter flows by using the continuity equation together with the Manning formula, and the Chicago method is used for the sewers. The MIT model (Harley et al, 1970; Eagleson, 1972) routes the flow through the drainage system by using the nonlinear kinematic-wave model. Linear diffusion and dynamic-wave schemes are also discussed (Harley et al, 1970). The Utah model (Narayana et al, 1969; Evelyn et al, 1970) is an analog simulation model using a coefficient method derived on the basis of the Manning formula to route the runoff.

It should be mentioned here that for the similar but not identical situation of routing floods through river basins, Larson and his associates at the University of Minnesota (Wei and Larson, 1971; Golany and Larson, 1971)

proposed a model for two specified Minnesota watersheds by using the kinematic wave equations for the overland flows and the St. Venant equations with Manning's roughness factor for channel flows, and considering the junction effect by using the continuity relationships and assuming only limited effect of back-water.

III. RE-EXAMINATION OF FLOW EQUATIONS USED IN SOLVING URBAN STORM DRAINAGE PROBLEMS

Until the Nineteen Sixties, the commonly used flow equations in solving urban drainage problems are steady uniform flow equations. Recently with the demand for more accurate computational results for flow in drainage systems and river networks, attempts have been made by using more sophisticated flow equations such as the St. Venant Equations which, as complicated as they appear, were derived based on a number of assumptions.

With the rapid improvement in computer capabilities and numerical techniques, the commonly used approximate flow equations may not match the computational accuracy that can be achieved. Consequently, a re-examination on the reliability and assumptions involved in the flow equations is needed so that guidelines can be established on the appropriate flow equations to be used to match the required accuracy in solving storm drainage problems. This would on one hand prevent wasting of effort in obtaining results which are unnecessarily accurate and on the other hand provide reliable equations together with large computer capabilities and numerical techniques to give high accuracy solutions when required.

Sewer flows are usually free-surface flows, although occasionally pressurized conduit flows do occur. However, presureized sewers often cause problems such as pollution through leaking joints. Hence, in design practice sewers are assumed not pressurized. As stated in a report by ASCE Urban Water Resources Research Program (1968, p. H-54), transition from free-surface flow to pressurized flow contradicts the basic criterion of successful performance of a storm sewer. Therefore only free-surface flows are considered in this report. The research results from this project on re-examination of the open-channel flow equations have been presented in two publications (Yen, 1971, 1973). Thus, only a partial summary is given in this chapter.

To avoid the assumptions and approximations commonly made in deriving the flow equations, a rigorous approach is adopted by integrating over the flow cross section the equations of continuity, momentum, and energy for a point for a Newtonian fluid. The resulted equations are then transformed into one-dimensional form by using cross sectional averaged values of the flow and by introducing appropriate correction coefficients. This approach of derivation was first applied to almost homogeneous incompressible fluid as presented in a project research report (Yen, 1971). Later, because of the possible future use of the equations for water pollution problems, the derivation was extended to nonhomogeneous fluids (Yen, 1973). The derived general one-dimensional flow equations are applicable to channels of arbitrary cross sectional shape and alignment with fixed or erodible and impervious or pervious bed. The fluid can be homogeneous or nonhomogeneous, compressible or incompressible, and viscous or inviscid. The flow can be turbulent or liminar, rotational or irrotational, steady or unsteady, uniform or nonuniform, supercritical or subcritical, gradually or rapidly varied, and with or without spatially and temporally variable continuous or intermittent lateral discharges. The result for incompressible fluids is summarized in Tables 2, 3, and 4. A sketch of the flow reach and cross section considered is shown in Fig. 1.

In Tables 2, 3, and 4, the symbols used are defined in Notation. For the energy equations, in addition to the symbols defined in Table 4, the unsteady pressure correction factor is

$$\zeta = \frac{\int_A (\partial \bar{p}/\partial t)\, dA}{\gamma_a A\, (\partial h/\partial t)} \tag{3}$$

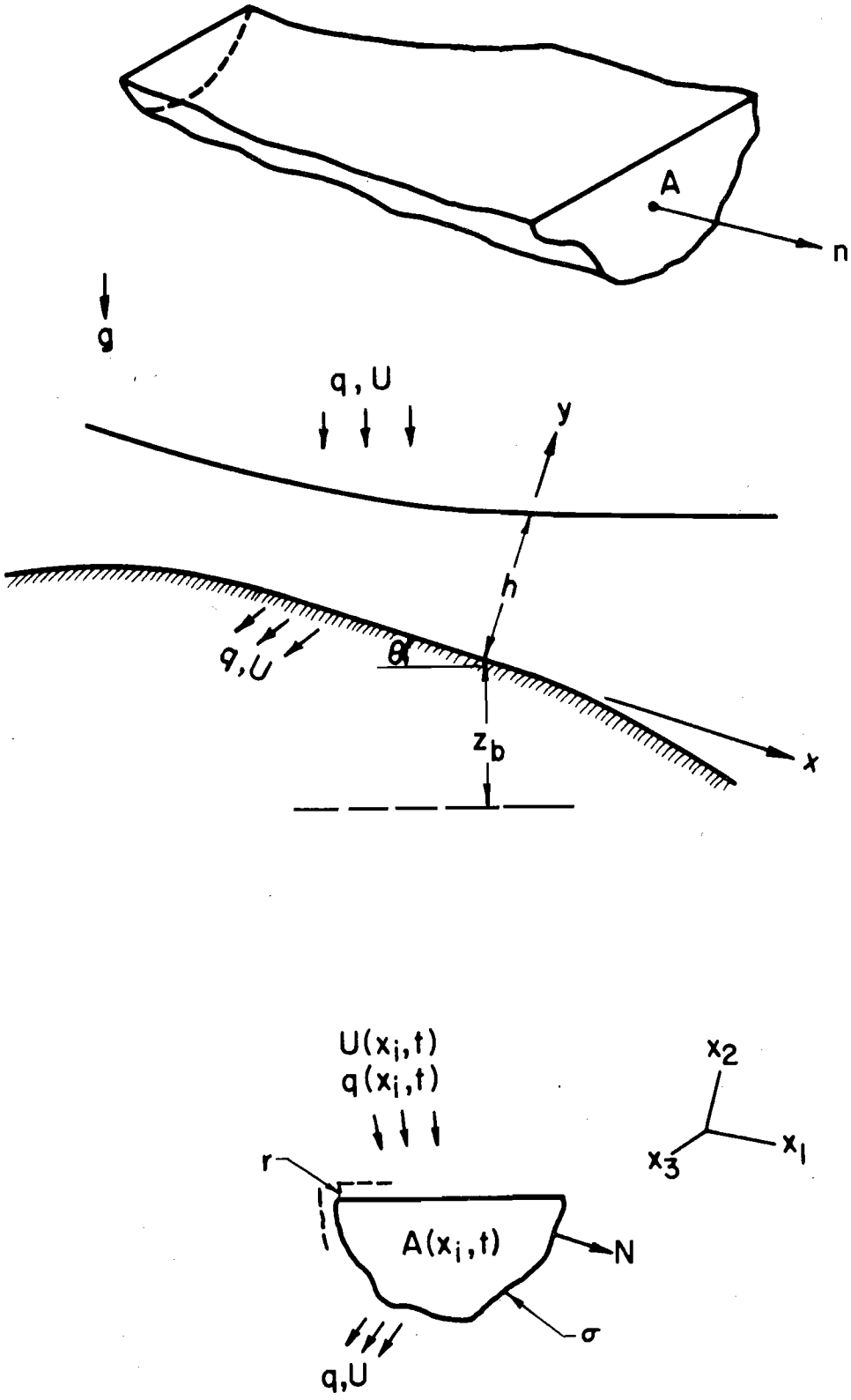

FIG. 1. SCHEMATIC DRAWING OF OPEN CHANNEL

TABLE 2. - ONE-DIMENSIONAL CONTINUITY EQUATION FOR SPECIAL CASES

	Incompressible Fluid (homogeneous or nonhomogeneous)	Compressible Fluid (homogeneous or nonhomogeneous)
Unsteady with lateral flow	$\frac{\partial A}{\partial t} + \frac{\partial}{\partial x}(AV_1) = \int_\sigma \overline{q}\, d\sigma$	$\frac{\partial}{\partial t}(\rho_a A) + \frac{\partial}{\partial x}[(\lambda + \lambda')\rho_a AV_1] = \int_\sigma (\overline{\rho}_L \overline{q} + \overline{\rho_L' q'})d\sigma$
Unsteady, no lateral flow	$\frac{\partial A}{\partial t} + \frac{\partial}{\partial x}(AV_1) = 0$	$\frac{\partial}{\partial t}(\rho_a A) + \frac{\partial}{\partial x}[(\lambda + \lambda')\rho_a AV_1] = 0$
Steady, with lateral flow	$\frac{d}{dx}(AV_1) = \int_\sigma \overline{q}\, d\sigma$	$\frac{d}{dx}[(\lambda + \lambda')\rho_a AV_1] = \int_\sigma (\overline{\rho}_L \overline{q} + \overline{\rho_L' q'})d\sigma$
Steady, no lateral flow	$\frac{d}{dx}(AV_1) = 0$	$\frac{d}{dx}[(\lambda + \lambda')\rho_a AV_1] = 0$

Note: $\lambda = \frac{1}{\rho_a AV_1}\int_A \overline{\rho}\,\overline{u}_1 dA$ $\quad \lambda' = \frac{1}{\rho_a AV_1}\int_A \overline{\rho' u_1'} dA$ $\quad \rho_a = \frac{1}{A}\int_A \overline{\rho}\, dA$ $\quad V_1 = \frac{1}{A}\int_A \overline{u}_1 dA$

TABLE 3. - ONE-DIMENSIONAL MOMENTUM EQUATION FOR INCOMPRESSIBLE FLUIDS

	Homogeneous Fluid	Nonhomogeneous Fluid
Unsteady flow	$\frac{1}{g}\frac{\partial V_1}{\partial t} + \frac{V_1^2}{g}\frac{\partial \beta}{\partial x} + (2\beta-1)\frac{V_1}{g}\frac{\partial V_1}{\partial x}$ $+ [(\beta-1)\frac{V_1^2}{g} + (K-K')h\cos\theta]\frac{1}{A}\frac{\partial A}{\partial x}$ $+ \frac{\partial}{\partial x}(Kh\cos\theta) = S_o - S_f + \frac{1}{\gamma A}\frac{\partial T}{\partial x}$ $+ \frac{1}{gA}\int_\sigma (\bar{U}_1 - V_1)\bar{q}\, d\sigma$	$\frac{1}{g}\frac{\partial}{\partial t}[(\lambda+\lambda')V_1] + [\beta+\beta'-(\lambda+\lambda')^2]V_1\frac{1}{\gamma_a A}\frac{\partial}{\partial x}(\rho_a A V_1) + \frac{V_1}{g}\frac{\partial}{\partial x}[(\beta+\beta')V_1]$ $- \frac{V_1^2}{2g}\frac{\partial}{\partial x}(\lambda+\lambda')^2 + \frac{\partial}{\partial x}(Kh\cos\theta) + (K-K')\frac{h\cos\theta}{A}\frac{\partial A}{\partial x}$ $= S_o - S_f + \frac{1}{\gamma_a A}\frac{\partial T}{\partial x} + \frac{1}{\gamma_a A}\int_\sigma [\bar{U}_1 - (\lambda+\lambda')V_1]\,(\bar{\rho}_L\bar{q} + \overline{\rho'_L q'})\,d\sigma$ $- \frac{Kh\cos\theta}{\rho_a}\frac{\partial \rho_a}{\partial x} + \frac{\cos\theta}{\rho_a A}\int_A y\frac{\partial \bar{\rho}}{\partial x}\, dA$
Steady flow (Nonuniform)	$\frac{V_1^2}{g}\frac{d\beta}{dx} + [(K-K')h\cos\theta - \beta\frac{V_1^2}{g}]\frac{1}{A}\frac{dA}{dx}$ $+ \frac{d}{dx}(Kh\cos\theta) = S_o - S_f$ $+ \frac{1}{\gamma A}\frac{dT}{dx} + \frac{1}{gA}\int_\sigma (\bar{U}_1 - 2\beta V_1)\bar{q}\, d\sigma$	$\frac{V_1^2}{g}\frac{d}{dx}(\beta+\beta') + [(K-K')h\cos\theta - (\beta+\beta')\frac{V_1^2}{g}]\frac{1}{A}\frac{dA}{dx} + \frac{d}{dx}(Kh\cos\theta)$ $= S_o - S_f + \frac{1}{\gamma_a A}\frac{dT}{dx} + \frac{1}{\gamma_a A}\int_\sigma [\bar{U}_1(\bar{\rho}_L\bar{q} + \overline{\rho'_L q'}) - 2(\beta+\beta')V_1\rho_a\bar{q}]d\sigma$ $- [Kh\cos\theta + (\beta+\beta')\frac{V_1^2}{g}]\frac{1}{\rho_a}\frac{d\rho_a}{dx} + \frac{\cos\theta}{\rho_a A}\int_A y\frac{\partial \bar{\rho}}{\partial x}\, dA$
T	$\int_A (2\mu\frac{\partial \bar{u}_1}{\partial x} - \rho\overline{u_1'^2})\, dA$	$\int_A [2\bar{\mu}\frac{\partial \bar{u}_1}{\partial x} + 2\overline{\mu'\frac{\partial u_1'}{\partial x}} - (\bar{\rho}\,\overline{u_1'^2} + \overline{\rho' u_1'}\,\bar{u}_1 + \overline{\rho' u_1'^2})]dA$

Note: $\beta = \frac{1}{\rho_a V_1^2 A}\int_A \bar{\rho}\bar{u}_1^2 dA$ $\qquad K' = (\gamma_a h\cos\theta\frac{\partial A}{\partial x})^{-1}\int_\sigma (\bar{P}\frac{\partial \bar{r}}{\partial x} + \overline{P'\frac{\partial r'}{\partial x}})d\sigma$

$\beta' = \frac{1}{\rho_a V_1^2 A}\int_A \overline{\rho' u_1'}\,\bar{u}_1\, dA$ $\qquad S_f = \frac{-1}{\gamma_a A}\int_\sigma [\bar{\tau}_{1j}]_\sigma N_j d\sigma$ $\qquad K = (\gamma_a A h\cos\theta)^{-1}\int_A \bar{P}\, dA$

TABLE 4. - ONE-DIMENSIONAL ENERGY EQUATION FOR MEAN MOTION OF INCOMPRESSIBLE FLUIDS

	Homogeneous fluid	Nonhomogeneous fluid
Unsteady flow	$\frac{\partial H_B}{\partial t} + (H_c - H_B)\frac{1}{A}\frac{\partial}{\partial x}(AV_1) + V_1\frac{\partial H_c}{\partial x}$ $- \frac{1}{A}\int_\sigma (H_L - H_B)\,\bar{q}\,d\sigma$ $= \zeta\frac{\partial h}{\partial t} - V_1 S_e + W$	$\frac{\partial H_B}{\partial t} + \frac{H_B}{\rho_a A}\frac{\partial \rho_a A}{\partial t} + V_1\frac{\partial}{\partial x}(H_c + H'_v) + \frac{H_c + H'_v}{\rho_a A}\frac{\partial}{\partial x}(\rho_a A V_1)$ $- \frac{1}{\rho_a A}\int_\sigma (H_L + H'_L)\,\bar{\rho}_L\bar{q}\,d\sigma$ $= \zeta\frac{\partial h}{\partial t} - V_1 S_e + W + E_f + E_u$
Steady flow (Nonuniform)	$V_1\frac{dH_c}{dx} - \frac{1}{A}\int_\sigma (H_L - H_c)\,\bar{q}\,d\sigma$ $= - V_1 S_e + W$	$V_1\frac{d}{dx}(H_c + H'_v) - \frac{1}{\rho_a A}\int_\sigma [(H_L + H'_L)\,\bar{\rho}_L - (H_c + H'_v)\,\rho_a]\,\bar{q}\,d\sigma$ $= - V_1 S_e - (H_c + H'_v)\frac{V_1}{\rho_a}\frac{d\rho_a}{dx} + W + E_f$
$\bar{\tau}_{ij}$	$\mu\left(\frac{\partial \bar{u}_i}{\partial x_j} + \frac{\partial \bar{u}_j}{\partial x_i}\right) - \rho\,\overline{u'_i u'_j}$	$\bar{\mu}\left(\frac{\partial \bar{u}_i}{\partial x_j} + \frac{\partial \bar{u}_j}{\partial x_i}\right) + \left(\overline{\mu'\frac{\partial u'_i}{\partial x_j}} + \overline{\mu'\frac{\partial u'_j}{\partial x_i}}\right) - \left(\bar{\rho}\,\overline{u'_i u'_j} + \overline{\rho' u'_i}\,\bar{u}_j + \overline{\rho' u'_j}\,\bar{u}_i\right)$

Note: $H_c = \alpha\frac{V_i V_i}{2g} + \eta h\cos\theta + \lambda z_b$ $\qquad \alpha = (\rho_a V_i V_i V_1 A)^{-1}\int_A \bar{\rho}\,\bar{V}^2\,\bar{u}_1 dA$ $\qquad \eta = (\gamma_a A V_1 h\cos\theta)^{-1}\int_A \bar{P}\,\bar{u}_1 dA$

$H'_v = \frac{1}{\gamma_a A V_1}\int_A \frac{\bar{V}^2}{2}\,\overline{\rho' u'_1}\,dA$ $\qquad W = \frac{1}{\gamma_a A}\left(\frac{\partial}{\partial x}\int_A \bar{u}_i\bar{\tau}_{i1}dA + \int_\sigma [\bar{u}_i\bar{\tau}_{ij}]_\sigma N_j d\sigma\right)$ $\qquad \bar{V}^2 = \bar{u}_i\,\bar{u}_i$

The work done due to fluctuating nonhomogeneous fluid are

$$E_f = \frac{1}{\rho_a A} \int_A (z_b + y \cos\theta) \frac{\partial \overline{\rho' u_i'}}{\partial x_i} dA \tag{4}$$

$$E_u = - \frac{1}{\gamma_a A} \int_A \overline{u}_i \frac{\partial \overline{\rho' u_i'}}{\partial t} dA \tag{5}$$

The dissipated energy gradient is

$$S_e = \frac{1}{\gamma_a A V_1} \int_A \overline{\tau}_{ij} \frac{\partial \overline{u}_i}{\partial x_j} dA \tag{6}$$

The true cross sectional total head of flow measured from the horizontal reference datum in terms of γ_a is

$$H_B = \frac{1}{\rho_a A} \int_A \overline{\rho} \frac{\overline{V}^2}{2} dA + Kh \cos\theta + z_b \tag{7}$$

The piezometric head of the lateral flow when it joins the channel flow and measured in terms of $\overline{\gamma}_L$ from the horizontal reference datum is

$$H_L = \frac{\overline{U}^2}{2g} + \frac{\overline{P}_L}{\overline{\gamma}_L} + z_b \tag{8}$$

and the local fluctuation or turbulence velocity head of the lateral flow when joining the channel flow is

$$H_L' = \frac{\overline{\rho' q'}}{\overline{\rho}_L \overline{q}} \frac{\overline{U}^2}{2g} \tag{9}$$

The subscript L represents the quantity for the lateral flow. The bar represents temporal averaging over fluctuations such as turbulence, and a primed term represents the fluctuation with respect to its temporal mean value. Repetition of the subscripts i or j in a term, except those for the one-dimensional correction coefficients, implies summation over the three possible orthogonal coordinate directions.

Examination of the derived flow equations reveals several significant points related to routing of runoff in drainage systems. First, the St. Venant equations (Eqs. 1 and 2) are approximations of the momentum and continuity equations applied to homogeneous incompressible fluids. In Eq. 1, the following assumptions are involved (Yen, 1973):

a) The velocity $\bar{u}_1$ is uniformly distributed over the cross sectional area A so that $\beta = 1$.

b) The pressure distribution is hydrostatic so that $K = K' = 1$.

c) The channel slope, S_o, and hence θ, is constant and independent of x.

d) The variation with respect to x of the internal normal stresses acting on the cross section, $\partial T/\partial x$, is relatively negligible.

e) There is no lateral flow.

These assumptions essentially require that there should be no rapid changes in flow cross section or direction.

In Eq. 2, the assumptions involved are that the channel bed is non-erodible or the time rate of change of bed profile is slow and the channel is straight and prismatic so that $\partial A/\partial x$ for a given h is equal to zero; or, alternatively, the channel is sufficiently wide so that $D \approx h$ and there is no rapid change or discontinuity of the width of the free surface with respect to x so that the $\partial b/\partial x$ term is relatively negligible. Again, there is no lateral flow.

At present there is no thorough study made to reveal quantitatively the significance of these assumptions involved in the St. Venant equations. However, some preliminary investigations made in this project indicate that with the exception of a few extreme cases the St. Venant equations can be used satisfactorily in solving storm drainage flow problems.

Second, the derived equations indicate that the dynamic equation derived based on the energy concept is inherently different from that based on the momentum concept. Consequently, the dissipated energy gradient, S_e (Eq. 6), is different from the friction slope, S_f, and they are different from the channel slope, S_o, the free surface slope, $\partial h/\partial x$, the hydraulic gradient or hydraulic grade line referred to a horizontal plane, $(\partial H_p/\partial x)-S_o$ where H_p is the cross-sectional average piezometric head of the channel flow with respect to the channel bottom, and the gradient $S_H = -\partial H/\partial x$ of the often used approximated total head H,

$$H = H_p + z_b + (V_1^2/2g) \tag{10}$$

Third, even if the approximations involved in the St. Venant equations are considered acceptable, numerical solutions for these equations cannot be proceeded because the exact mathematical expression for S_f for unsteady flow is unknown. The expressions for S_f have been established only for steady uniform flow with no lateral discharges, such as the Chezy, Manning, or Weisbach formulas. However, reliable estimation of S_f is important for storm runoff computations, particularly for sheet flows such as those on the streets. Manning's and Chezy's resistance factors were derived from steady, uniform, fully-developed turbulent flows with rough boundary and hence are often unsuitable for use in urban surface runoff problems.

Although at present there is a lack of knowledge on unsteady open-channel flow which would be useful in estimating the friction slope, some information can be obtained by studies on steady nonuniform flows. In order to determine the effect of lateral flows, particularly rainfalls, on surface runoffs, a study has been conducted on the resistance to steady spatially varied flow (Yen et al, 1972). It has been found that the lateral discharges, particularly rainfalls, indeed play an important role in determining the friction

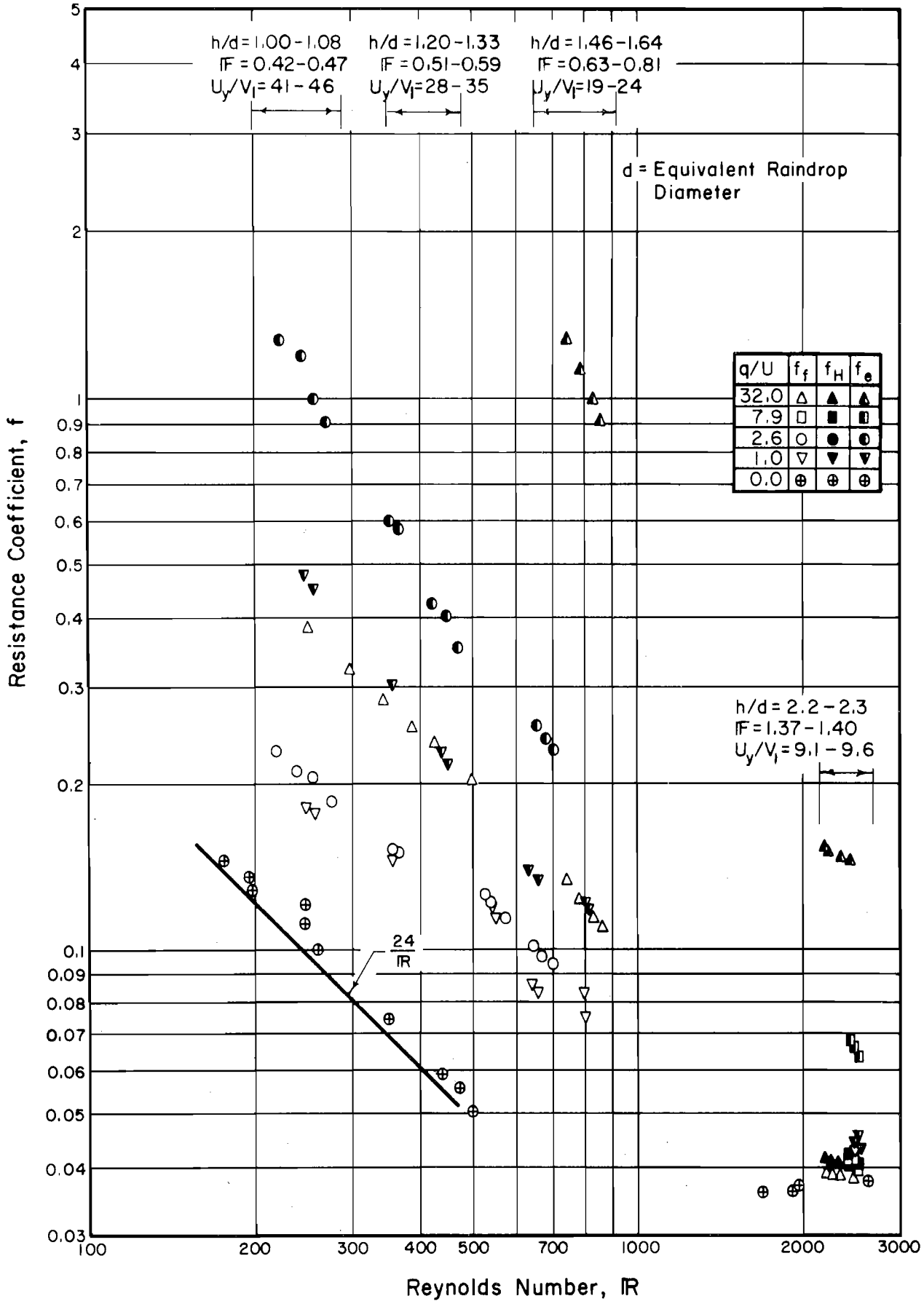

FIG. 2. RESISTANCE COEFFICIENTS FOR STEADY SHEET FLOW UNDER RAINFALL

slope in sheet flows. A result showing the variations of the friction resistance coefficient, f_f, energy dissipation coefficient, f_e, and total-head loss coefficient, f_H, all in the Weisbach resistance coefficient form, is reproduced as Fig. 2, in which the Froude number $\mathbb{F} = V_1/\sqrt{gD}$ and the Reynolds number $\mathbb{R} = V_1 R/\nu$, where R is the hydraulic radius.

Since the St. Venant equations are by themselves approximation of the complete momentum and continuity equations, there is a possibility that simpler flow equations may also be adequately applicable in solving urban storm runoff problems. As discussed in Chapter 2, various approximations, or models, by dropping terms in the St. Venant equations have been proposed by previous investigators. For the linear approximations, the linear kinematic-wave model has been proven unsatisfactory. The accuracies of the linear diffusion-wave model and the linearized St. Venant equations have not been investigated or calibrated, and often it is not easy to select properly the reference flow conditions for the linearization of the equations.

The nonlinear approximate models, however, can be compared for their solutions with the solutions of the St. Venant equations which in turn have been calibrated against existing experimental results (Sevuk, 1973). To illustrate the relative accuracies of the nonlinear models, a comparison is made by considering a rather critical condition of a flood wave routed through a long (4000 ft) sewer. A four-point noncentral implicit finite difference numerical scheme is adopted and identical time and space increments are used in the computation for all the models. A typical result for an inflow hydrograph having a duration t_i = 40 min routed through the sewer with a diameter D = 6 ft and slope S_o = 0.0006 over a constant baseflow Q_b = 20 cfs is shown in Fig. 3. The computed results show that the nonlinear kinematic-wave model is the least accurate one and in fact it can account for neither the backwater effect nor the attenuation of the unsteady flow. The computer time

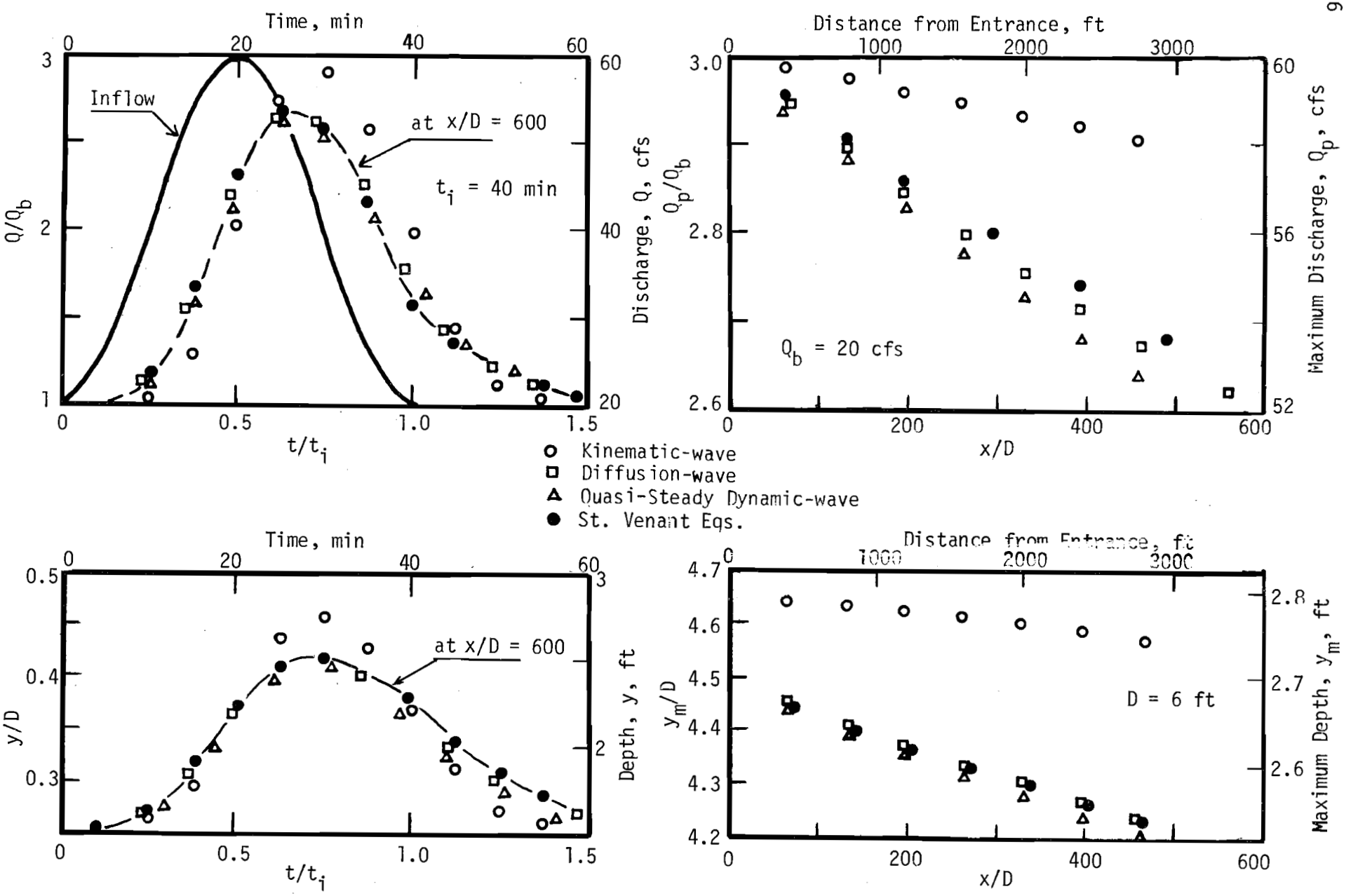

FIG. 3. COMPARISON OF NONLINEAR MODELS

required for the kinematic-wave model is approximately one-half of that for the St. Venant equations.

The solution of the nonlinear diffusion-wave model has been found to agree closely with that of the St. Venant equations. The former, unfortunately, requires only slightly shorter computer time, 20% or less for the conditions tested, as compared to the later solution. The nonlinear quasi-steady dynamic-wave model gives slightly less accurate solutions while requiring more computer time as compared to the nonlinear diffusion-wave model.

Selection of the most desirable model for routing of unsteady flows in urban storm drainage systems depends on the objective of and the accuracy required for the routing. Since the objective of this research project is to develop a reliable routing model for flow through urban storm drainage systems, and because the nonlinear diffusion-wave model offers no great savings in computer time, nor in simplicity in programming, the choice is obvious: The complete nonlinear form of the St. Venant equations are adopted as much as possible and practical in this project to develop the improved mathematical model for routing of storm runoff through storm drainage systems.

IV. SOLUTION METHODS FOR SAINT VENANT EQUATIONS

As discussed in the preceding chapter, in view of the objective of this research project and the present knowledge on the flow equations and hydraulic resistance, it has been decided the St. Venant equations be adopted herewith as the basis in solving storm runoff problems. Nevertheless, a quantitative study in the future on the reliability and approximations involved in these equations would be desirable.

Since the St. Venant equations (Eqs. 1 and 2) are first-order quasi-linear hyperbolic partial differential equations, no explicit solution exists and they can be solved only numerically with two initial and two boundary conditions specified. In view of the possible large number of gutters and sewers in a drainage system, the selection of an appropriate solution method is most important. A study has been conducted in this project on different solution methods for the St. Venant equations applied to a single channel in order to reveal a suitable solution method that can be adopted for the analysis of drainage systems, particularly the sewer networks. The results of this part of research have been reported in a paper (Sevuk and Yen, 1973a) and a theses (Sevuk, 1973).

Numerical solutions of the St. Venant equations can be attempted by using various finite difference techniques which can be classified into the following three major categories:

a) Explicit finite difference schemes, in which Eqs. 1 and 2 are written in finite difference form, usually linear algebraic equations, from which the unknowns are evaluated explicitly.

b) Implicit finite difference schemes, in which Eqs. 1 and 2 are written in finite difference form as a set of nonlinear algebraic equations, from which the unknowns are solved simultaneously.

c) Method of characteristics, in which Eqs. 1 and 2 are transformed into characteristics equations, then written in finite difference form for solutions.

Within each category different computational schemes have been proposed. Studies pertaining to the convergence, stability, computational speed and simplicity concerning these methods have been made by various investigators (Amein and Fang, 1969; Baltzer and Lai, 1968; Gunaratnam and Perkins, 1970; Liggett and Woolhiser, 1967; Strelkoff, 1970; Yevjevich and Barnes, 1970). In this research project, additional information concerning the method of characteristics and implicit schemes are provided.

The explicit schemes have been popular and explored extensively by previous investigators because of their directness in expressing the unknowns. Various computational procedures, including the diffusion scheme, staggered scheme, leap-frog scheme, and the Lax-Wendroff scheme have been proposed. The computational space and time intervals are usually chosen based on the Courant criterion which does not necessarily guarantee computational stability. Limitation on the computational intervals to satisfy the stability problem often results in lengthy computation, particularly for long duration unsteady flows. Furthermore, for short duration rapidly varying transient flows, Yevjevich and Barnes (1970) have shown that the explicit schemes are less accurate than the Courant scheme applied to the method of characteristics. Therefore,it was decided that the explicit schemes are not suitable for routing storm runoff in this research.

Various implicit finite difference schemes such as the four-point central or noncentral and six-point central or noncentral schemes have been proposed. The six-point central scheme has been reported (Liggett and Woolhiser, 1967) in solving overland flow problems to exhibit inaccuracy at the boundaries which may lead to computational instability for time steps greater than twice the value given by the Courant criterion. The six-point noncentral

and the four-point central schemes have been found losing liquid through the process of computation and also exhibit oscillation in the solutions (Fread, 1973; Gunaratnam and Perkins, 1970). None of these problems have been observed for the four-point noncentral scheme provided the Courant criterion is not violated excessively and hence it is chosen for further investigation in this project. The finite difference formulation of this scheme has been reported previously (Sevuk and Yen, 1973a). A generalized Newton iteration method has been adopted for the solutions.

Four schemes applied to the method of characteristics are investigated in this study; namely, the Courant scheme which is an explicit scheme, the first order scheme which is a pseudo-explicit scheme, the second order scheme which is a pseudo-implicit scheme solved by a predictor-corrector method, and the four-point noncentral implicit scheme applied to the canonical form of the characteristics equation. For a comparison of these four schemes as well as the direct four-point noncentral implicit

TABLE 5. - EXPERIMENTAL DATA ADOPTED FOR COMPARISON WITH THEORETICAL SOLUTION FOR SINGLE SEWERS

Sewer and Inflow Properties	CSU Run No. 19	HRS Run No. 115
Diameter, D, ft	3.0	0.25
Length, L, ft	822	300
Slope, S_o	0.00099	0.0010
Roughness	f = 0.012	k = 0.00004 ft
Base Flow, Q_b, cfs	2.60	0.0189
Peak Inflow, $Q_p(0)$, cfs	26.17	0.0532
Duration of Inflow Hydrograph, t_i, sec	89.0	36.7
Shape of Inflow Hydrograph	Symmetric, triangular	Symmetric, trapezoidal with peak inflow for 3.3 sec

scheme, and to test the reliability of using the St. Venant equations in sewers and channels, flow conditions for experiments performed by Ackers and Harrison (1964) at British Hydraulic Research Station at Wallingford (HRS) and by Yevjevich and Barnes (1970) at Colorado State University (CSU) are reproduced theoretically by using each of these schemes. The computed and experimental results for two flow conditions given in Table 5 are shown in Figs. 4 and 5 and they indicate that the solutions for all the five schemes are in good agreement with the experimental maximum depth, Y_m. Therefore, these schemes are further tested for more critical condition by routing hypothetical flood waves through a long (8000 ft) 6-ft diameter sewer having a small slope (0.0006) and a Manning's roughness factor, n, equal to 0.015. The use of n instead of Weisbach's f here is because of the relative constancy and hence simplicity of n for the range of flow considered. A typical result is shown in Fig. 6. The error in flood volume conservation, ε, is defined as the ratio of the difference between the storage increment and the cumulative net inflow to the cumulative flood volume. All the computer programs developed in this research project for the comparative study of single sewer solution methods are written in Fortran IV language and filed in the Hydrosystems Laboratory of the University of Illinois at Urbana-Champaign.

Comparison of the relative merit of the computational schemes to approximate the continuous differential equations by discrete finite difference formulations is usually made based on the computational stability, convergence or some kind of accuracy, and the computational time or speed of the schemes. Details of this comparative study have been reported elsewhere (Sevuk and Yen, 1973a). From a practical view point one should keep in mind that it is unnecessary and not worthwhile to carry out a computational scheme beyond the required accuracy, particularly in view of the approximations involved in the St. Venant equations.

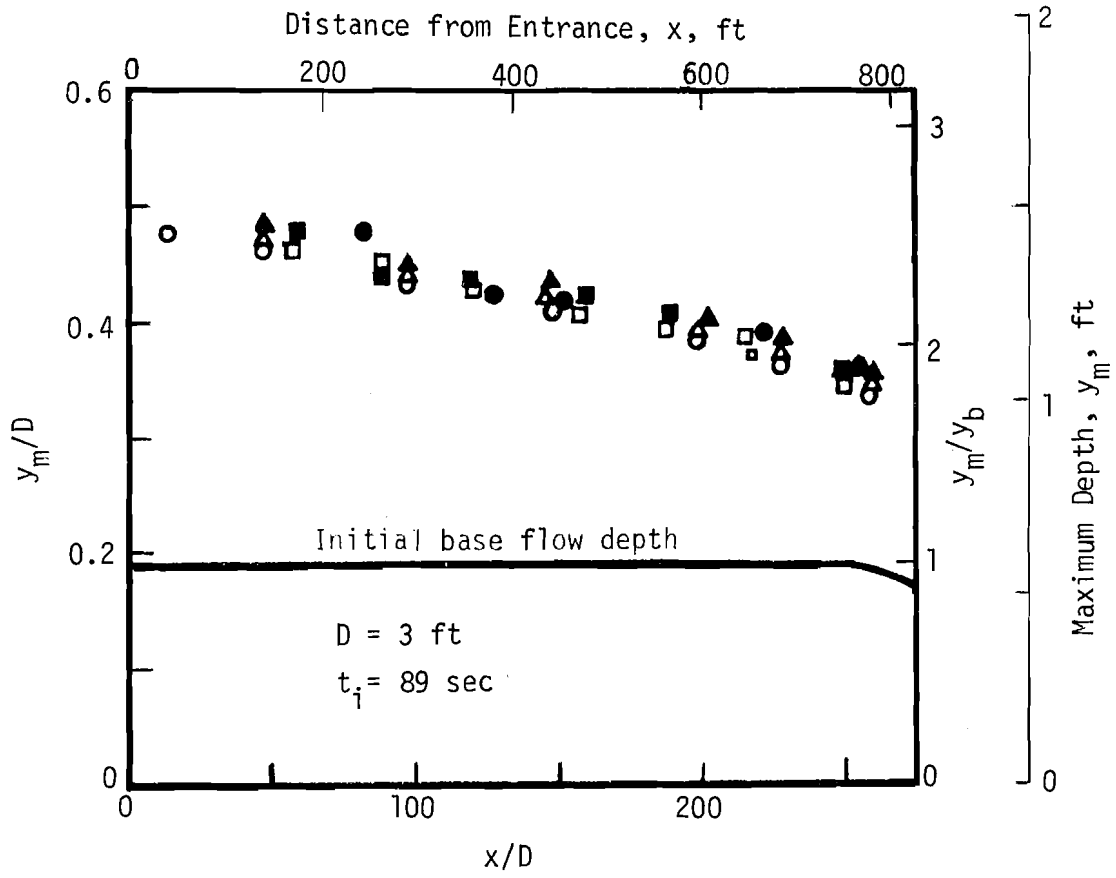

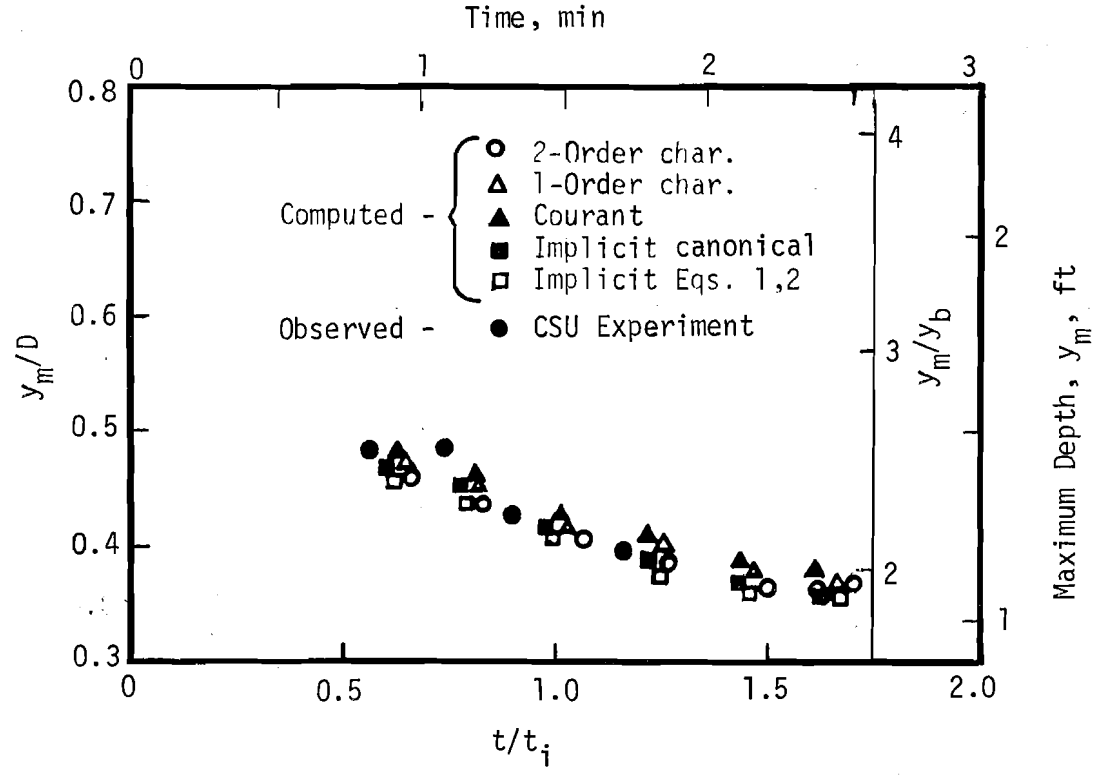

FIG. 4. COMPARISON OF THEORETICAL SOLUTIONS WITH CSU EXPERIMENTAL DATA

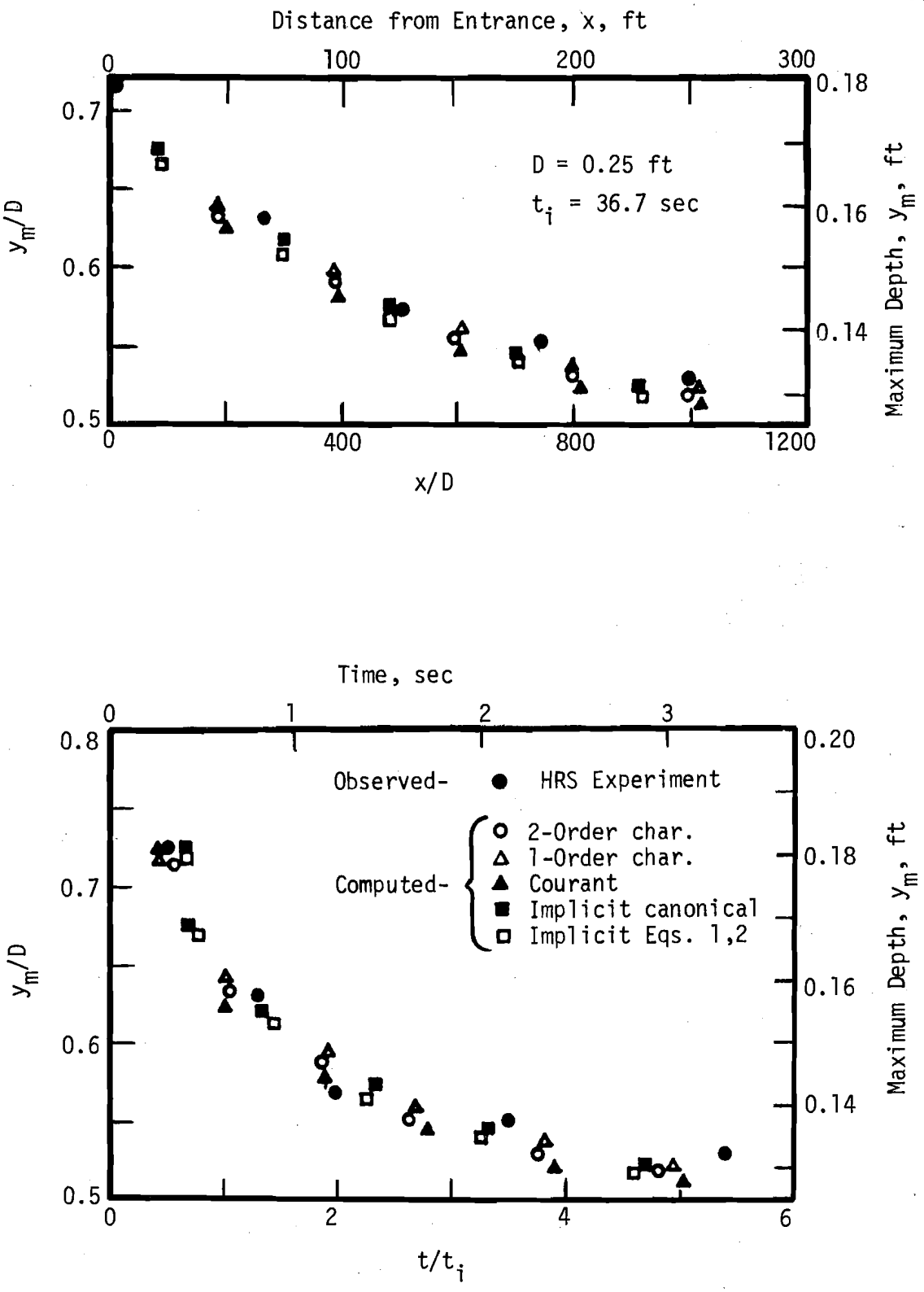

FIG. 5. COMPARISON OF THEORETICAL SOLUTIONS WITH HRS EXPERIMENTAL DATA

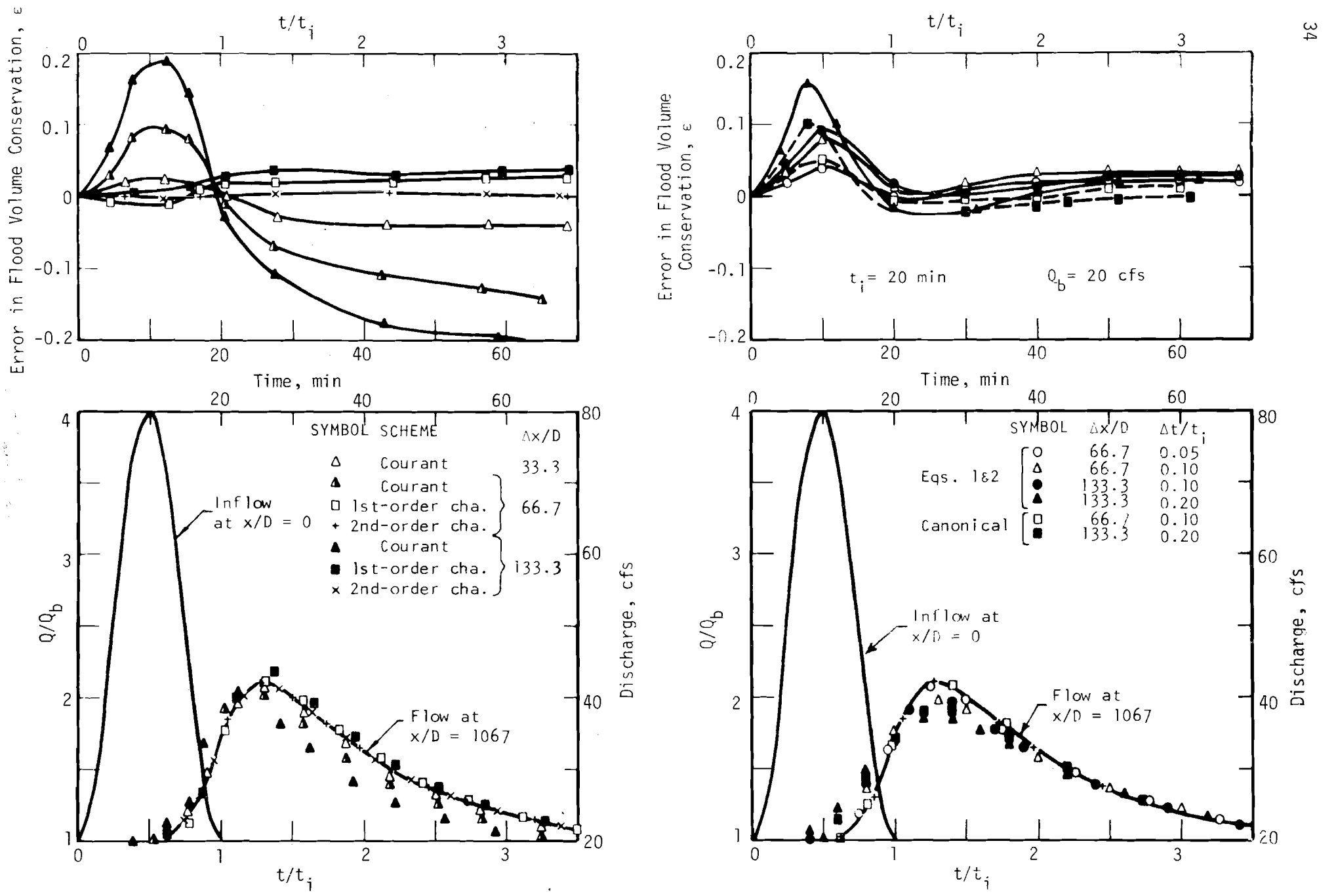

FIG. 6. COMPARISON OF PREDICTED HYDROGRAPHS AND CORRESPONDING ERRORS FOR 20-MIN FLOOD WAVE THROUGH 6-FT SEWER

By using the error in flood volume conservation, ε, as an indirect indication of the convergence of the finite difference solution to approach the true solution of the differential equations, it can be seen from Fig. 6 that the second order characteristic scheme appears to be the most satisfactory whereas the Courant scheme is the least. The first-order characteristic scheme is good at the relatively early period or with a small space increment. Contrarily, the direct implicit scheme and the implicit scheme applied to the canonical characteristics equations are good only for the later period, and the latter appears to be the better. It has also been found that among the schemes tested, Courant's is the one most sensitive to the change of computational space interval, whereas the second-order characteristic scheme the least. For the implicit scheme applied to the canonical or direct forms, an increase in computational space interval tends to cause a small numerical dumping. Contrarily, the first-order characteristic schemes appears to cause a numerical amplification.

As to the computational stability, based on previous investigations, the following conclusions can be drawn. The four-point noncentral implicit scheme, whether applied to canonical characteristic form or direct form, is unconditionally stable, and hence the computational space and time intervals can be selected independently (Amien and Fang, 1969; Fread, 1973). The second-order characteristic scheme is always stable provided that the Courant criterion is satisfied (Wylie, 1970). The first-order characteristic scheme, the Courant scheme, as well as the explicit schemes are usually stable if the Courant criterion is satisfied (Gunaratnam and Perkins, 1970; Liggett and Woolhiser, 1967; Richtmyer, 1962; Sevuk, 1973).

Two factors which should also be considered in comparing different computational methods are the computer time required and the difficulties in programming. No generally agreed yardsticks have been established concerning this aspect. However, loosely it may be stated that in programming explicit

schemes are easier than implicit schemes, and the direct form (Eqs. 1 and 2) is slightly simpler than the characteristic form. However, the precise comparison depends on the particular scheme and equations used and the logic in programming.

As to the computer time, for explicit schemes it depends mainly on the time increment Δt used which is determined by some stability criteria for given space increments. However, the maximum value of Δx that can be used is often limited by the channel geometry, and consequently resulted in small Δt and long computer time. For the implicit schemes, for which Δt and Δx can be selected independently, subject to the convergence constraint, the computer time depends mainly on the number of iterations required which in turn depends on the values of Δt and to a lesser degree Δx used. Therefore, for long-duration slowly-varying transient flows implicit schemes, which usually require shorter computer time because the value of Δt can be selected well in excess of those given by the Courant criterion without sacrificing the accuracy, are preferred to the explicit schemes. However, for short-duration rapidly-varying flows, the advantage on computer time of the implicit schemes over the explicit schemes diminishes because of the Δt limitation imposed by the convergence consideration. Usually the computer time required for the explicit schemes can be estimated approximately by that for the Courant scheme.

Selection of the most suitable numerical solution schemes for urban drainage problems depends on the flow and channel conditions in addition to the required accuracy and size of the computer available. For the same storm drainage system, the optimum solution scheme for the sewer network is not necessary the best for the gutters or the overland flows and no simple general rules can be established. Nevertheless, the information summarized in this chapter would help considerably in selecting the most suitable models for different components of a storm drainage system.

As a further test on the second-order characteristic scheme, and to present the results of this part of investigation in an alternative manner which may be useful for certain applications, numerical solutions have been made to develop nondimensional relationships to describe the peak discharge and peak flow depth, as well as their times of travel, as functions of inflow and sewer characteristics. The friction slope is approximated by using the Darcy-Weisbach formula. As shown in Fig. 7, the nondimensional peak discharge, $Q_p^* = Q_p(x)/Q_p(0)$, at any cross section along the sewer is a function of the nondimensional inflow and sewer characteristics parameter π_1 where

$$\pi_1 = \left(\frac{x}{D}\right) \left(\frac{R_b}{D}\right)^{-0.25} \left[\frac{t_p Q_p(0)}{D^3}\right]^{-0.41} \left[\frac{Q_p(0)}{t_p D^2 g}\right]^{0.25} \left(\frac{k}{R_b}\right)^{0.17} \left(\frac{t_p}{t_g - t_p}\right)^{0.25} \quad (11)$$

in which $Q_p(0)$ and $Q_p(x)$ are the peak discharges above the base flow at the entrance $x = 0$ and at a distance x from entrance, respectively; t_p is the time of occurrence of peak discharge of inflow; t_g is the time to the center of gravity of the inflow hydrograph; D is the diameter of sewer; R_b is the hydraulic radius at base flow rate; and k is the surface roughness of sewer. Shown in Fig. 8 is the nondimensional plot representing the time of occurrence of the peak discharge in which the dimensionless time parameter π_2 is

$$\pi_2 = \left[\frac{(t-t_p)V_W}{D}\right] \left(\frac{R_b}{D}\right)^{-0.57} \left[\frac{t_p Q_p(0)}{D^3}\right]^{-0.44} \left(\frac{t_p}{t_g - t_p}\right)^{0.50} \left(\frac{k}{R_b}\right)^{0.11} \left[\frac{Q_b}{t_p D^2 g}\right]^{0.40} \quad (12)$$

in which $V_W = V_1 + \sqrt{gA/b}$ is the wave celerity for a discharge equal to the base flow rate Q_b.

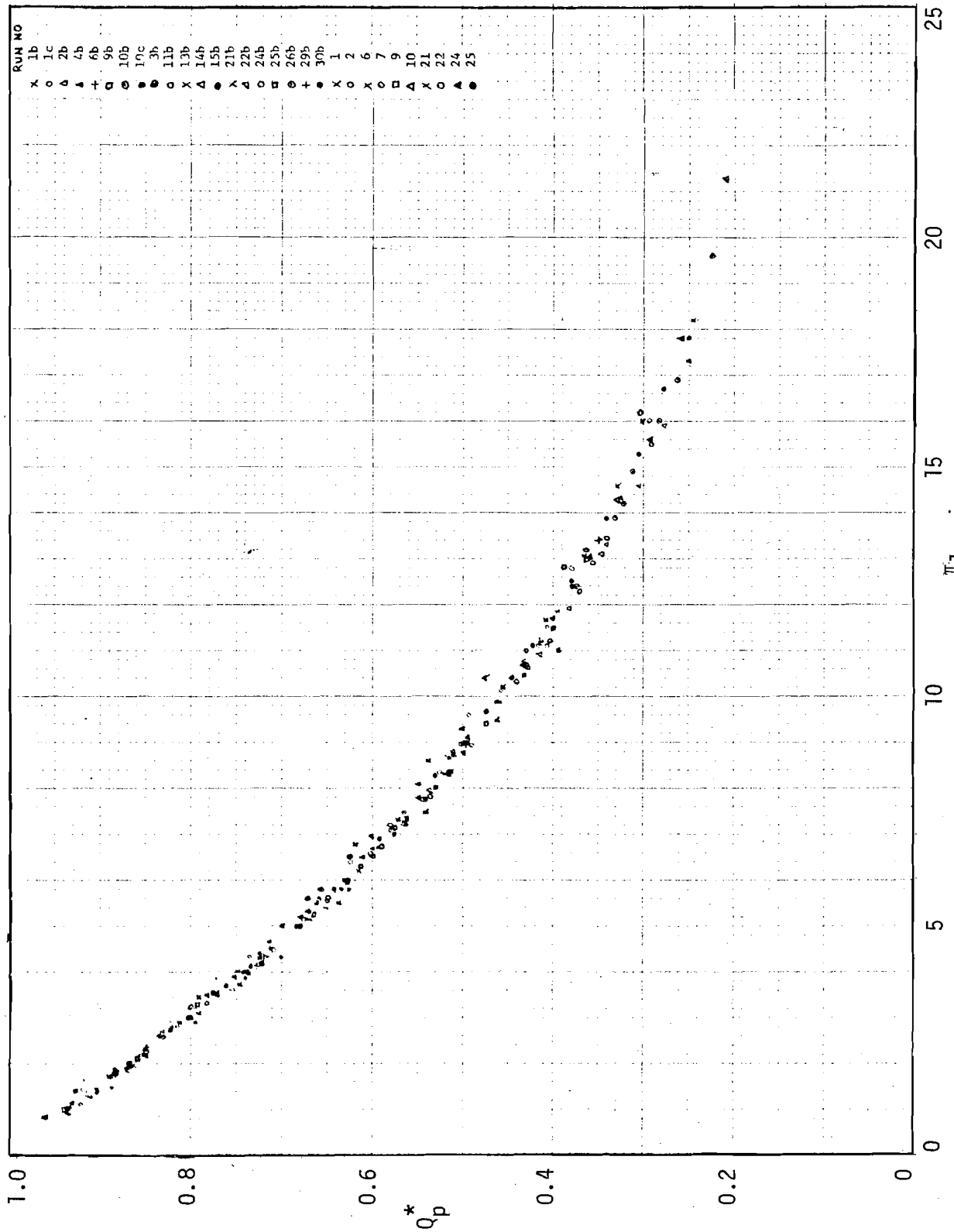

FIG. 7. ATTENUATION OF PEAK DISCHARGE ALONG SEWER AS FUNCTION OF INFLOW AND SEWER CHARACTERISTICS

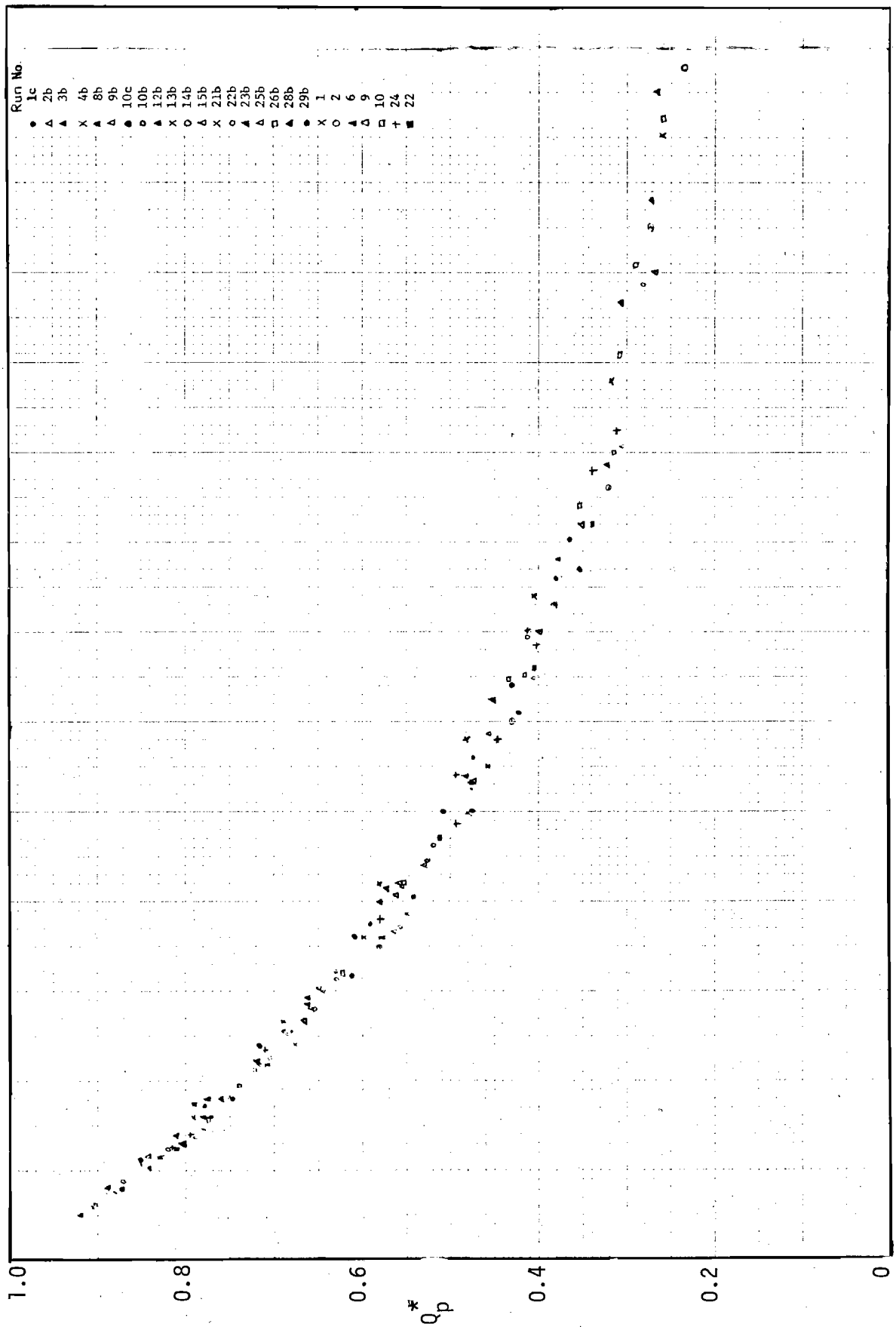

FIG. 8. TIME OF TRAVEL OF PEAK DISCHARGE IN SINGLE SEWERS

V. SURFACE RUNOFF INTO INLET CATCH BASINS

As discussed in Chapter I, from the hydraulic view point an urban storm drainage system can be divided into two major parts; namely, the part upstream from the inlet catch basins, and the part downstream of them. The former transfers the water from rainfall on roofs, lawns, pavement and other land surfaces through gutters, ditches or other devices into inlet catch basins. In the present study the surface runoff part upstream from the inlets is simplified as the overland and gutter flows. The overland flow is considered as from pavement or similar land surface. However, it should be mentioned here that the methodology used in this study is sufficiently general and can easily be adopted to other types of land surface conditions.

Traditionally, in practice, the overland and gutter runoffs are calculated by using steady uniform flow equations such as Manning's formula. In reality, natural rainfalls are never steady nor uniformly distributed over the land surface. Consequently, the surface runoffs are unsteady and non-uniform. It will be shown later that the unsteady surface runoff differs considerably from the steady flow conventionally assumed.

V-1. Dimensional Analysis

The flow from a gutter depends on the physical characteristics of the gutter, pavement, inflow, properties of the fluid, and the downstream flow condition if the flow is subcritical. There are various types of gutters and street pavement crown shapes. The most popular ones are the triangular gutters and straight pavement cross slopes (Fig. 9). For such gutters and pavements, the physical characteristics of the gutter consists of its longitudinal slope S_o which is usually equal to the street slope, its length L_g, its width B, the transverse angle, ϕ, of the gutter made with the horizontal, and a measure of the roughness of the gutter surface, k. The curb side of the gutter

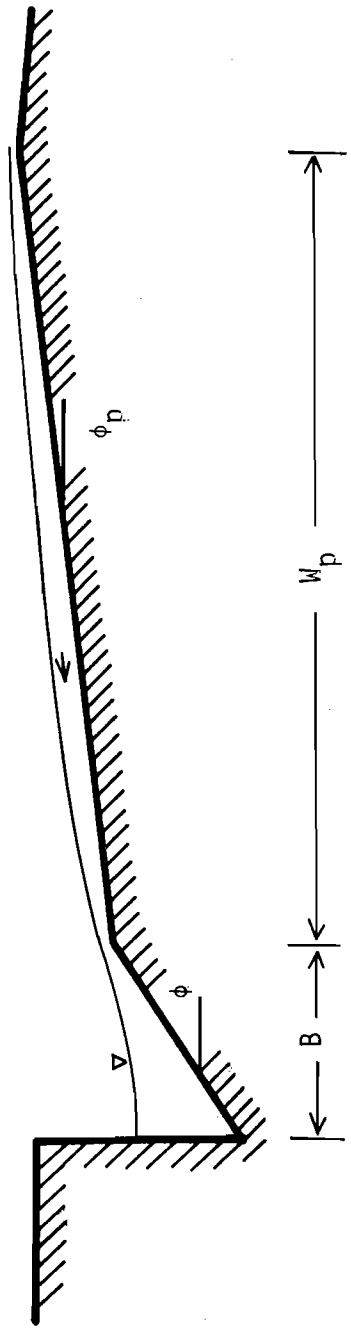

FIG. 9. CROSS SECTION OF GUTTER AND PAVEMENT

is assumed to be vertical. The pavement characteristics include its cross slope or sometimes called crown slope, expressed in terms of the angle made between the pavement and the horizontal, ϕ_p, its length along the transverse direction of the street, W_p, and its surface roughness, k_p.

The inflow consists of rainfall and the inflow at the upstream of the gutter. The rain which falls on the pavement as well as directly over the gutter has an average intensity i over its duration t_i. For the area on a street contributing to an inlet the areal variation of i is usually small and hence assumed uniform. This assumption on uniform areal and temporal distributions of rainfall intensity is made simply for the sake of simplicity in presenting the results and can easily be removed. For simplicity, i considered here is assumed to be rainfall excess, i.e., rainfall minus infiltration and other losses. This again can easily be modified and improved by including infiltration and other abstractions.

The gutter upstream inflow can be the spill-over from the previous inlet, the flow from street washing or hydrant, the water from melted snow, or, simply only a portion of the entire gutter is considered in the analysis to save computational time and cost and hence the flow from the upstream portion is estimated as the inflow. The inflow through the upstream cross section of the gutter can be described by the peak discharge Q_{pu} and duration t_u of the inflow hydrograph together with nondimensional parameters J_t, representing the time distribution of the inflow, and J_p, J_d, and J_v for the pressure, depth, and velocity distributions, over the upstream entrance cross section of the gutter. If the length of the gutter, L_g, considered is not very short, say greater than 50 times the hydraulic radius of the gutter flow at peak discharge, then the influence of the backwater effect due to the velocity, depth, and pressure distributions at the entrance section of the gutter on the flow at the gutter exit is insignificant. In other words, as far as the flow through

the exit section of the gutter is concerned, the flow at the entrance section behaves like a source and hence the characteristics of the inflow hydrograph is important but the effects due to J_p, J_d, and J_v can be neglected. The parameter J_t describes the shape of the hydrograph and here for the sake of simplicity without losing generality the gutter inflow hydrographs are assumed to be sine curves.

The fluid properties include its density ρ, specific weight γ, kinematic viscosity ν, and surface tension σ. Although surface runoffs are often sheet flow with depth smaller than one inch, the roughness of the surface texture of the gutters and streets together with infiltrations would make the effect of surface tension negligible.

Thus, the discharge Q_o at the exit section of the gutter can be expressed as a function of the influential factors as

$$Q_o = F_1 (t,B,S_o,L_g,\phi,k,k_p,\phi_p,W_p,t_i,i,Q_{pu},t_u,\rho,\gamma,\nu,\delta) \tag{13}$$

in which t is time, δ is a dimensionless parameter representing the downstream conditions of the gutter, and F represents a function.

The downstream condition of the gutter flow depends on the physical properties of the inlet. If the flow is supercritical, the flow in the gutter is independent of the downstream condition as long as a one-dimensional analysis is applied. Contrarily, if the gutter flow is subcritical, the backwater effect due to the downstream condition would affect the flow in the gutter. There are two major types of inlets, namely, the grate inlets and the curb inlets. Many variations exist for each type and they are used individually as well as mixed and combined. Even within the U.S., none of the states has standardized the inlets. It is not possible in this study to investigate at present the different effects of the numerous various types of inlets, nor is

it desirable because it is postulated that when more information is known about the inlets in the near future there will be fewer types of inlets used. It is the conventional design logic that the inlet should be designed to handle all the water from the gutter and pavement it covers. Accordingly, this concept is adopted here and a unique downstream condition, such as critical depth if the flow is subcritical, is assumed for δ.

Hence, through dimensional analysis, for a constant δ,

$$\frac{Q_o}{iA} \text{ or } \frac{Q_o}{Q_s} = F_{2,3}\left(\frac{t}{t_i}, S_o, \frac{L_g}{B}, \phi, \frac{k}{B}, \frac{k_p}{B}, \phi_p, \frac{W_p}{B}, \frac{t_i}{B}, \frac{Q_{pu}t_i}{B^3}, \frac{t_u}{t_i}, \frac{B}{gt_i^2}, \frac{B^2}{\nu t_i}\right) \qquad (14)$$

in which $A = L_g (B + W_p \cos\phi_p)$ is the horizontally projected area receiving rainfall i; $Q_s = (iA + Q_{pu})$ is the corresponding maximum steady flow discharge; and g is the gravitational acceleration.

The physical meanings of the terms in Eq. 14 are as follows. To the left of the equality sign is the relative gutter discharge at its exit measured in terms of the rainfall inflow rate and the possible maximum total inflow rate, respectively. To the right the first term indicates the time distribution of the nondimensional hydrograph. The second term accounts for the effect of the street slope on both the gutter and pavement flows. The third term is the relative length of the gutter, and as discussed previously, only when the gutter is relatively long that the effects of the velocity, depth, and pressure distributions of the gutter upstream inflow can be neglected. The fourth represents the transverse slope of the gutter, usually ranging from 1 to 10 degrees for triangular cross sections; and for more general cases of non-triangular cross section it will be replaced by the terms representing the cross sectional

shape of the gutter. The fifth and sixth terms are the relative surface roughnesses of the gutter and pavement, respectively. The seventh term is simply the cross slope of the pavement usually ranging from 1/8 to 1/2 in. per ft, i.e., 1 to 4 percent, or approximately 0.6 to 2.4 degrees. The eighth term represents the relative size of the overland surface and the ninth the amount of rainfall, and these two terms together is an indication of the relative importance of the lateral flow. The tenth term is an indirect measure of the volume of the upstream inflow into the gutter relative to the volume of the gutter. The eleventh term is the relative duration of gutter upstream inflow as compared to that for the rainfall and is an indication of their relative importance in determining the runoff hydrograph. The twelfth term represents the effect of gravity and the last term represents the effect of viscosity, and they replace respectively the representative Froude and Reynolds numbers of the surface runoff.

Because the flow is unsteady and nonuniform, even for a given inflow, it may vary between turbulent and laminar and between subcritical and supercritical, depending on the time and location . Consequently it is difficult, if not impossible, to define a representative Froude or Reynolds number for the flow over the entire area and duration. Likewise, from the fluid mechanics viewpoint, the relative surface roughness should be measured in terms of the hydraulic radius of the flow instead of B because it is the former ratio together with the Reynolds number, and to some degree with the Froude number, that the flow resistance is determined. Again, because the hydraulic radius varies from time to time and from location to location for an unsteady nonuniform flow, a physically significant hydraulic radius cannot be found to be used in the dimensional analysis.

V-2. Mathematical Modeling of Flow from Pavement and Gutter into Inlet

The factors affecting runoff from gutters into inlets have been discussed in the preceding section. The mathematical expressions describing the flow have been presented in Chapter III and the methods of solution in the preceding chapter. The St. Venant equations are modified to include the lateral flow and expressed in terms of discharge as

$$\frac{1}{Ag}\frac{\partial Q}{\partial t} + \frac{2V_1}{Ag}\frac{\partial Q}{\partial x} + \left(1 - \frac{Q^2}{gA^3}\frac{dA}{dh}\right)\frac{\partial h}{\partial x} = S_o - S_f \qquad (15)$$

$$\frac{\partial A}{\partial t} + \frac{\partial Q}{\partial x} = \int_\sigma \bar{q}\, d\sigma \qquad (16)$$

Equations 15 and 16, nondimensionalized by using the gutter width B and rainfall duration t_i, are first applied to gutter flow with constant steady lateral discharge from the pavement. The first order method of characteristics is adopted for the numerical solutions. The effects of the gutter slope, upstream gutter inflow, and lateral flow are studied. Details of this phase of study can be found in Akan's (1973) thesis.

The investigation is then extended to include unsteady pavement flows. Strictly from a theoretical viewpoint, it is more interesting and accurate to apply the St. Venant equations to the pavement flow as well. However, this approach would require a scheme to account for the ever changing internal boundary between the gutter and pavement flows and hence necessitates a trial-and-error computational scheme requiring large amount of computations. Contrarily, the nonlinear kinematic-wave model would require no downstream boundary condition for the pavement flow whether it is subcritical or supercritical and hence only simple computations are needed, particularly if the pavement conditions are identical along the

street, although the results are understandably less accurate. Nonetheless, it is considerably more reliable than the results of linear kinematic-wave models such as the Manning formula or the Izzard or Horton methods.

Because of its shallow depth, pavement flow resistance are subject to much greater influence of the rainfall than the gutter flow. In view of the considerable savings in computational time and cost for the nonlinear kinematic-wave model and the lack of accurate information on unsteady flow resistance under rainfall, it is judget that from a practical viewpoint the accuracy gained by using the St. Venant equations for the pavement flow does not offset their disadvantages at this stage of research, and hence the nonlinear kinematic-wave model is adopted as the mathematical simulation for the pavement flows.

The numerical analysis has been performed by using the nondimensional St. Venant equations for the gutter flows and nondimensionalized nonlinear kinematic-wave equations for the pavement flows. The nondimensional parameters considered are guided by Eq. 14. The flow conditions analyzed are summarized in Table 6 and they cover a sufficient range of the field conditions. The results of the analysis are presented in nondimensional forms for general uses. The runoff hydrographs at the exit section of the gutter are shown in Figs. 10 to 16 for the parameters S_o, k/B, W_p/B, $Q_{pu}t_i/B^3$, t_u/t_i, $t_i i/B$, and B/gt_i^2. The variations of the relative peak discharge from the gutter, Q_{op}/Q_s, which is of practical importance from a design viewpoint, are shown in Figs. 17 to 20. The hydrographs for the parameter k_p/B are not presented because the effect of this parameter is relatively small as can be seen from Fig. 18 and Table 6.

TABLE 6. - CONDITIONS FOR SURFACE RUNOFFS ANALYZED

S_o (%)	$\frac{k}{B}$ (10^{-3})	$\frac{k_p}{B}$ (10^{-3})	$\frac{W_p}{B}$	$\frac{t_u}{t_i}$	$\frac{Q_{pu}t_i}{B^3}$	$\frac{t_i i}{B}$ (10^{-3})	$\frac{B}{gt_i^2}$ (10^{-5})	$\frac{Q_s}{iA}$	$\frac{Q_{op}}{iA}$	$\frac{Q_{op}}{Q_s}$	$\frac{t_{op}}{t_i}$
1.06	6.0	6.0	4.22	1.57	0.227	0.87	6.94	2.00	0.99	0.49	3.15
0.20	6.0	6.0	4.22	1.57	0.227	0.87	6.94	2.00	0.26	0.13	6.30
0.30	6.0	6.0	4.22	1.57	0.227	0.87	6.94	2.00	0.36	0.18	5.55
0.50	6.0	6.0	4.22	1.57	0.227	0.87	6.94	2.00	0.53	0.26	4.56
0.70	6.0	6.0	4.22	1.57	0.227	0.87	6.94	2.00	0.66	0.33	3.81
0.80	6.0	6.0	4.22	1.57	0.227	0.87	6.94	2.00	0.71	0.36	3.65
0.90	6.0	6.0	4.22	1.57	0.227	0.87	6.94	2.00	0.79	0.40	3.45
1.20	6.0	6.0	4.22	1.57	0.227	0.87	6.94	2.00	1.04	0.52	3.00
1.06	1.0	6.0	4.22	1.57	0.227	0.87	6.94	2.00	1.73	0.87	2.30
1.06	2.0	6.0	4.22	1.57	0.227	0.87	6.94	2.00	1.45	0.73	2.55
1.06	3.0	6.0	4.22	1.57	0.227	0.87	6.94	2.00	1.30	0.65	2.75
1.06	4.0	6.0	4.22	1.57	0.227	0.87	6.94	2.00	1.17	0.58	2.90
1.06	5.0	6.0	4.22	1.57	0.227	0.87	6.94	2.00	1.06	0.53	3.05
1.06	10.0	6.0	4.22	1.57	0.227	0.87	6.94	2.00	0.86	0.43	3.50
1.06	6.0	6.5	4.22	1.57	0.227	0.87	6.94	2.00	0.98	0.49	3.15
1.06	6.0	7.0	4.22	1.57	0.227	0.87	6.94	2.00	0.98	0.49	3.15
1.06	6.0	8.0	4.22	1.57	0.227	0.87	6.94	2.00	0.97	0.48	3.15
1.06	6.0	9.0	4.22	1.57	0.227	0.87	6.94	2.00	0.95	0.48	3.15
1.06	6.0	10.0	4.22	1.57	0.227	0.87	6.94	2.00	0.94	0.47	3.15
1.06	6.0	6.0	6.0	1.57	0.227	0.87	6.94	1.745	0.77	0.44	3.15
1.06	6.0	6.0	9.0	1.57	0.227	0.87	6.94	1.522	0.56	0.37	3.15
1.06	6.0	6.0	12.0	1.57	0.227	0.87	6.94	1.403	0.43	0.31	3.15
1.06	6.0	6.0	15.0	1.57	0.227	0.87	6.94	1.326	0.35	0.29	3.15

TABLE 6. - (Cont'd)

S_o (%)	$\frac{k}{B}$ (10^{-3})	$\frac{k_p}{B}$ (10^{-3})	$\frac{W_p}{B}$	$\frac{t_u}{t_i}$	$\frac{Q_{pu}t_i}{B^3}$	$\frac{t_i i}{B}$ (10^{-3})	$\frac{B}{gt_i^2}$ (10^{-5})	$\frac{Q_s}{iA}$	$\frac{Q_{op}}{iA}$	$\frac{Q_{op}}{Q_s}$	$\frac{t_{op}}{t_i}$
1.06	6.0	6.0	4.22	0.75	0.227	0.87	6.94	2.00	0.46	0.23	3.15
1.06	6.0	6.0	4.22	1.00	0.227	0.87	6.94	2.00	0.64	0.37	3.15
1.06	6.0	6.0	4.22	2.00	0.227	0.87	6.94	2.00	1.10	0.55	3.30
1.06	6.0	6.0	4.22	3.00	0.227	0.87	6.94	2.00	1.25	0.63	3.64
1.06	6.0	6.0	4.22	4.00	0.227	0.87	6.94	2.00	1.29	0.65	3.97
1.06	6.0	6.0	4.22	1.57	0.100	0.87	6.94	1.44	0.44	0.30	3.67
1.06	6.0	6.0	4.22	1.57	0.150	0.87	6.94	1.66	0.61	0.37	3.45
1.06	6.0	6.0	4.22	1.57	0.300	0.87	6.94	2.32	1.04	0.45	3.11
1.06	6.0	6.0	4.22	1.57	0.350	0.87	6.94	2.54	1.26	0.49	3.04
1.06	6.0	6.0	4.22	1.57	0.450	0.87	6.94	2.98	1.33	0.45	2.96
1.06	6.0	6.0	4.22	1.57	0.600	0.87	6.94	3.65	1.70	0.47	2.81
1.06	6.0	6.0	4.22	1.57	0.750	0.87	6.94	4.30	2.05	0.48	2.61
1.06	6.0	6.0	4.22	1.57	0.227	0.174	6.94	6.00	2.94	0.49	3.50
1.06	6.0	6.0	4.22	1.57	0.227	0.435	6.94	3.00	1.45	0.48	3.35
1.06	6.0	6.0	4.22	1.57	0.227	1.740	6.94	1.50	0.70	0.47	2.85
1.06	6.0	6.0	4.22	1.57	0.227	2.610	6.94	1.33	0.60	0.45	2.65
1.06	6.0	6.0	4.22	1.57	0.227	4.000	6.94	1.22	0.57	0.46	2.17
1.06	6.0	6.0	4.22	1.57	0.227	6.000	6.94	1.14	0.62	0.54	1.79
1.06	6.0	6.0	4.22	1.57	0.227	0.87	9.71	2.00	0.50	0.25	3.90
1.06	6.0	6.0	4.22	1.57	0.227	0.87	8.77	2.00	0.62	0.31	3.65
1.06	6.0	6.0	4.22	1.57	0.227	0.87	7.77	2.00	0.89	0.44	3.35
1.06	6.0	6.0	4.22	1.57	0.227	0.87	5.83	2.00	1.08	0.54	2.95
1.06	6.0	6.0	4.22	1.57	0.227	0.87	2.50	2.00	1.50	0.75	2.14
1.06	6.0	6.0	4.22	1.57	0.227	0.87	1.66	2.00	1.64	0.82	1.91
1.06	6.0	6.0	4.22	1.57	0.227	0.87	0.50	2.00	1.90	0.95	1.43
1.06	6.0	6.0	4.22	1.57	0.227	0.87	0.20	2.00	1.90	0.95	1.18

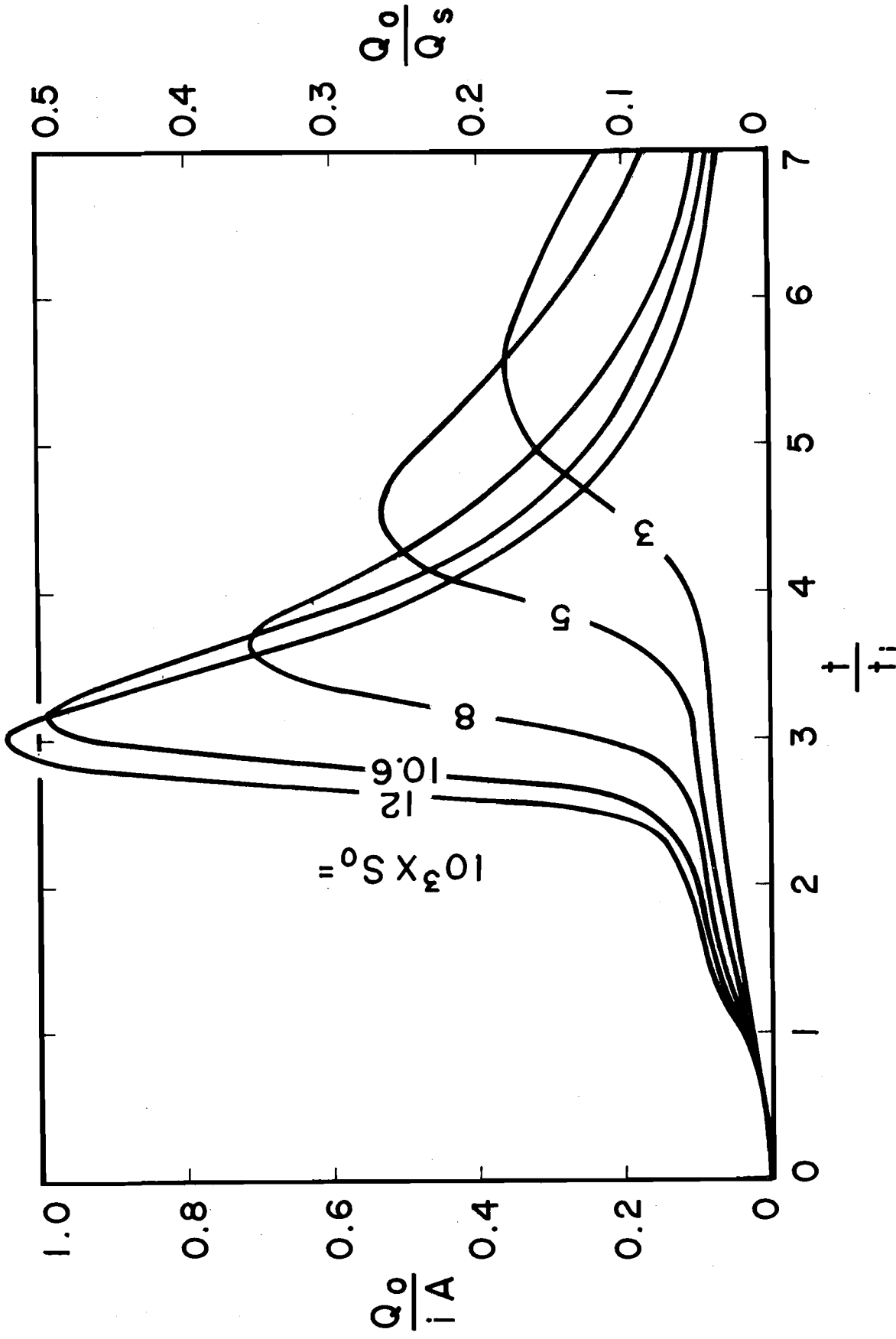

FIG. 10. HYDROGRAPHS AT GUTTER EXIT FOR DIFFERENT STREET SLOPES

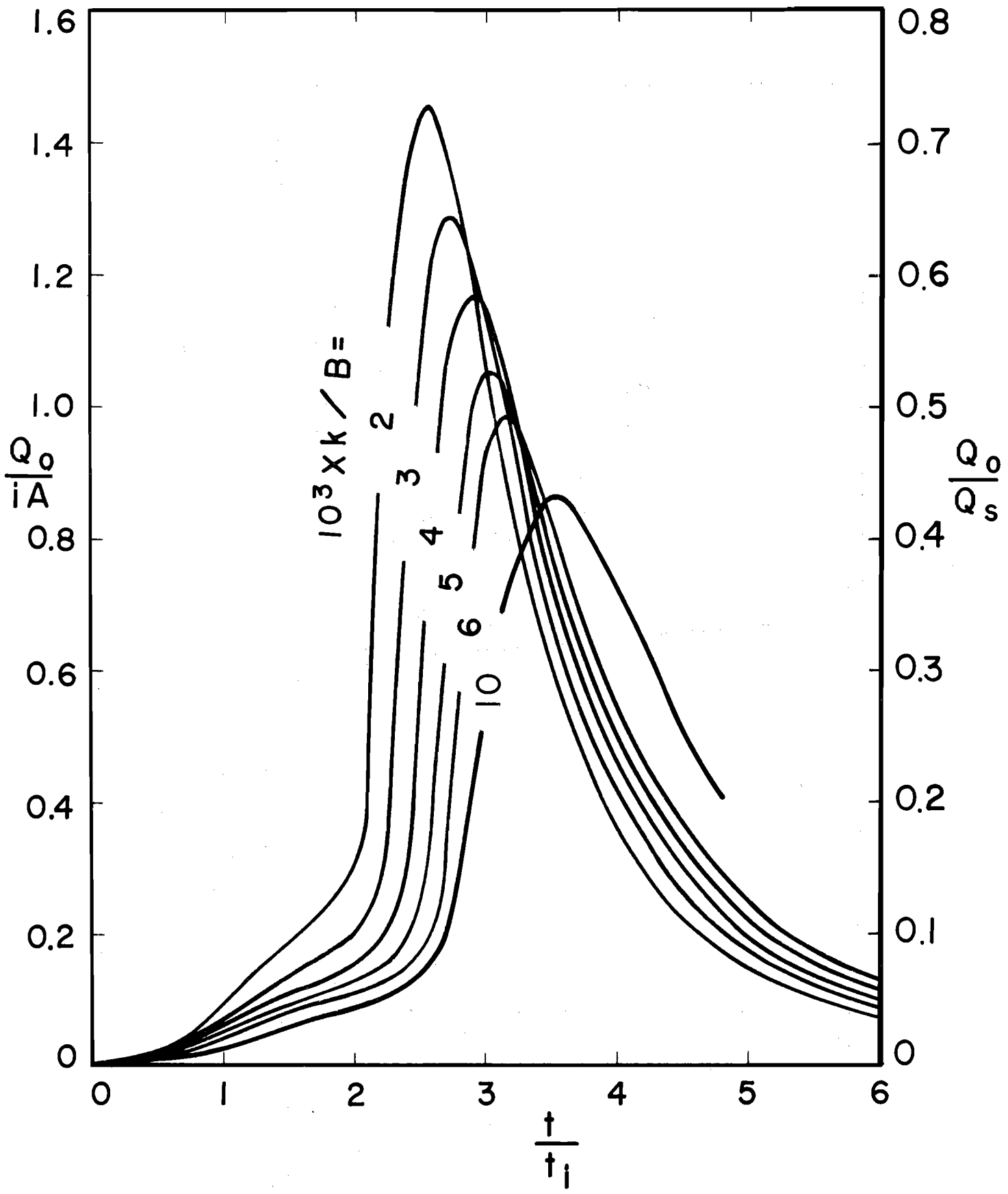

FIG. 11. HYDROGRAPHS AT GUTTER EXIT FOR DIFFERENT GUTTER SURFACE ROUGHNESSES

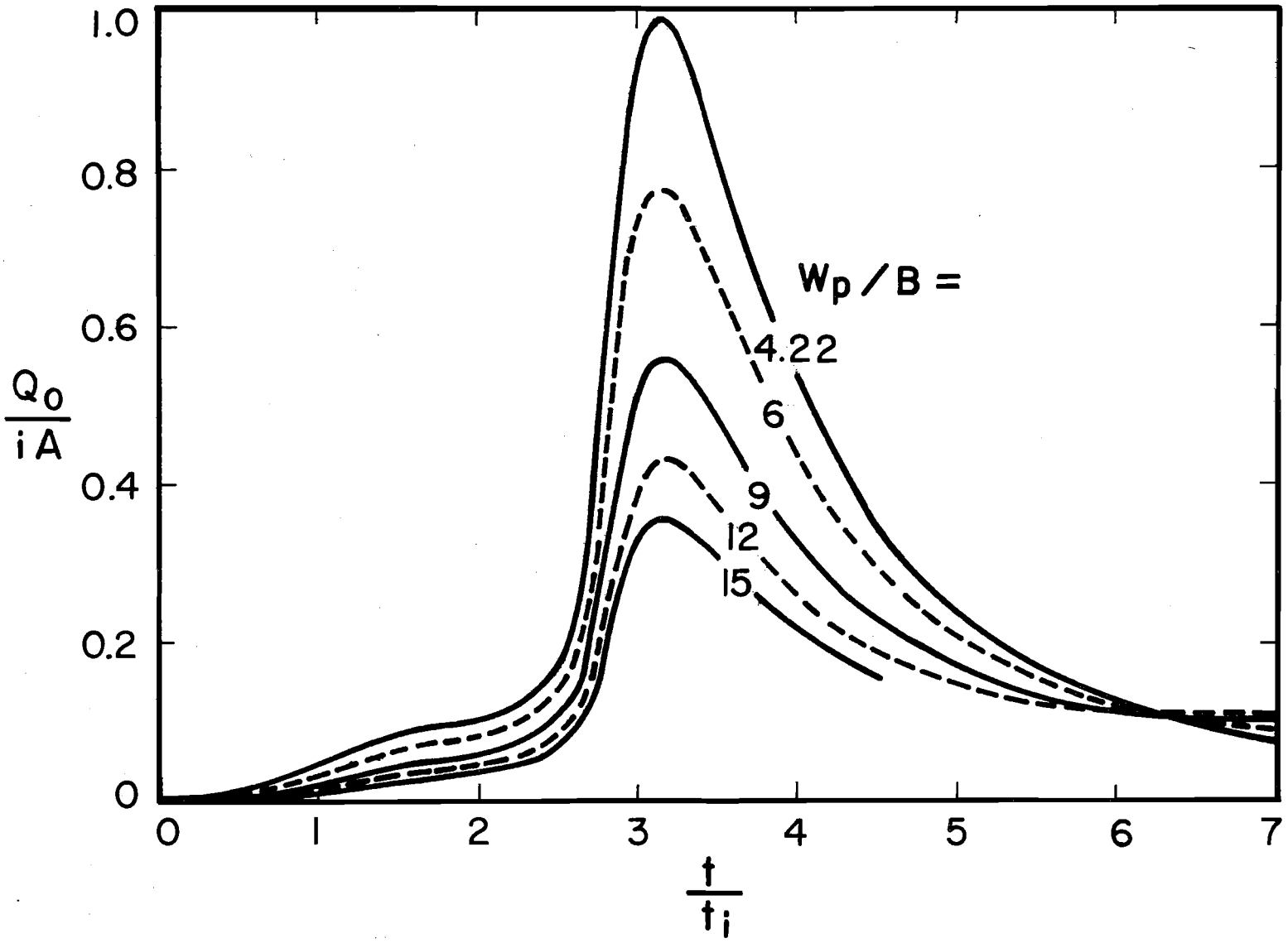

FIG. 12. HYDROGRAPHS AT GUTTER EXIT FOR DIFFERENT PAVEMENT WIDTHS (a) Q_o/iA vs. t/t_i

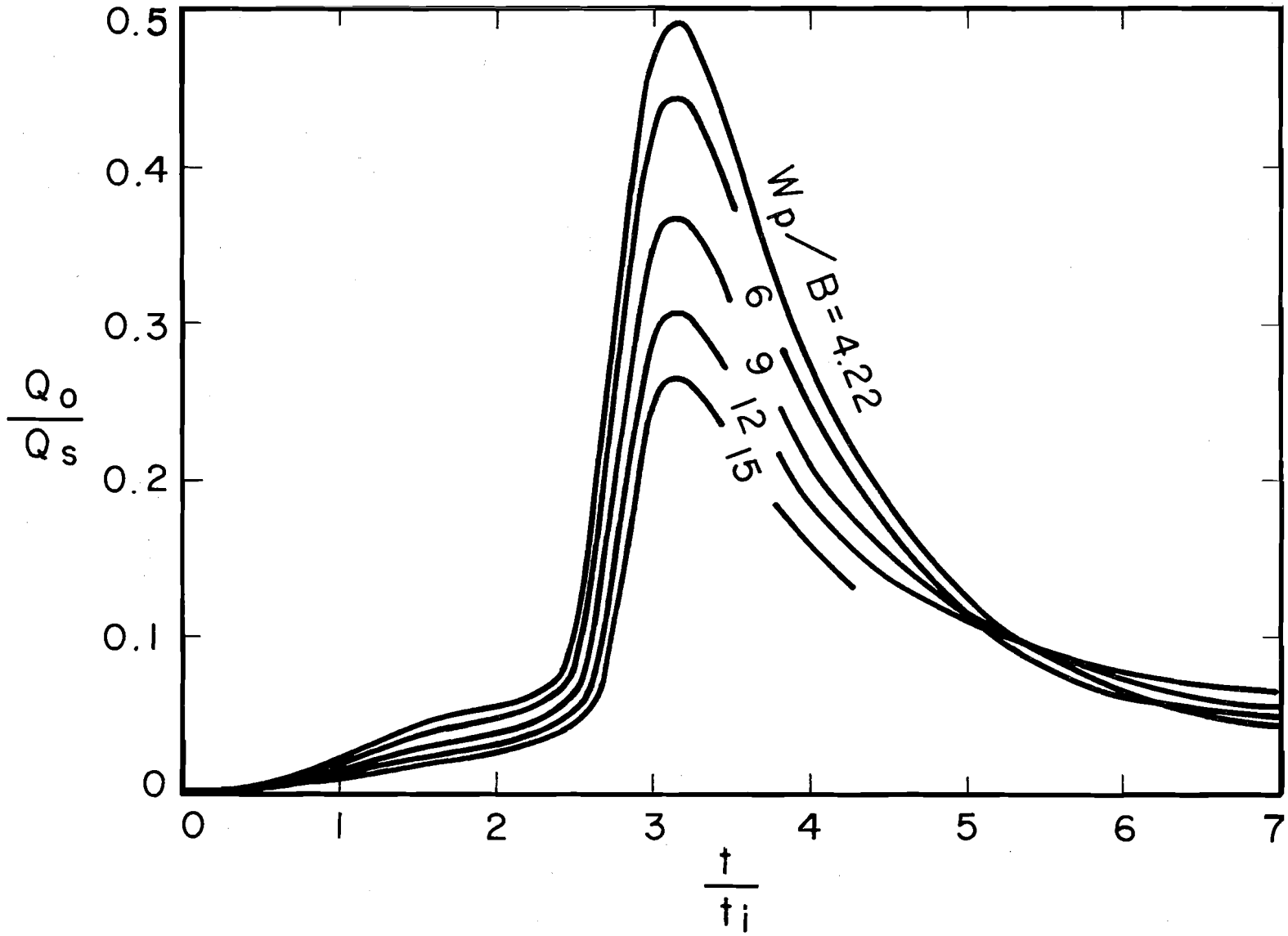

FIG. 12. (b) Q_o/Q_s vs. t/t_i

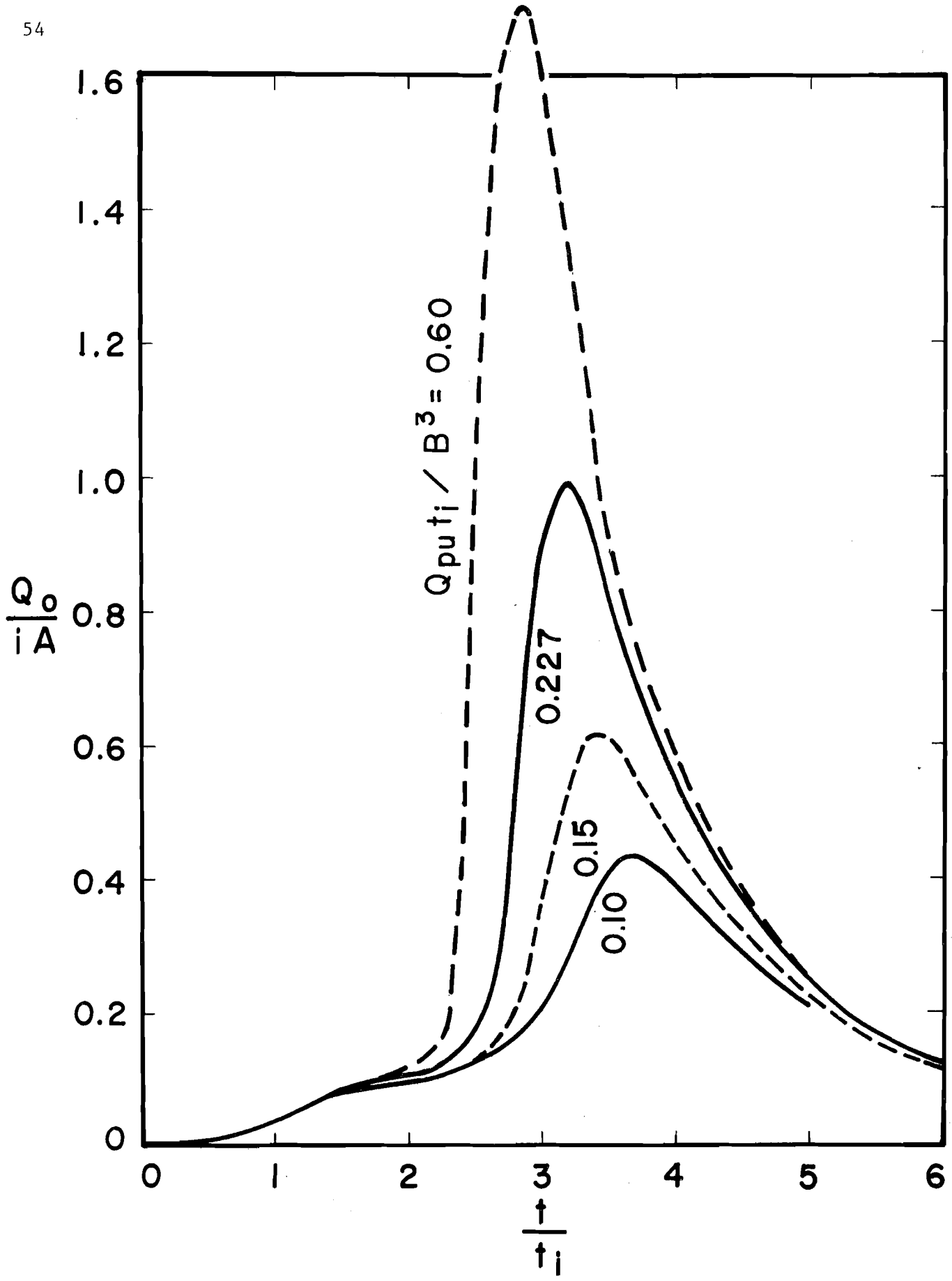

FIG. 13. HYDROGRAPHS AT GUTTER EXIT FOR DIFFERENT UPSTREAM INFLOW RATES
(a) Q_o/iA vs. t/t_i

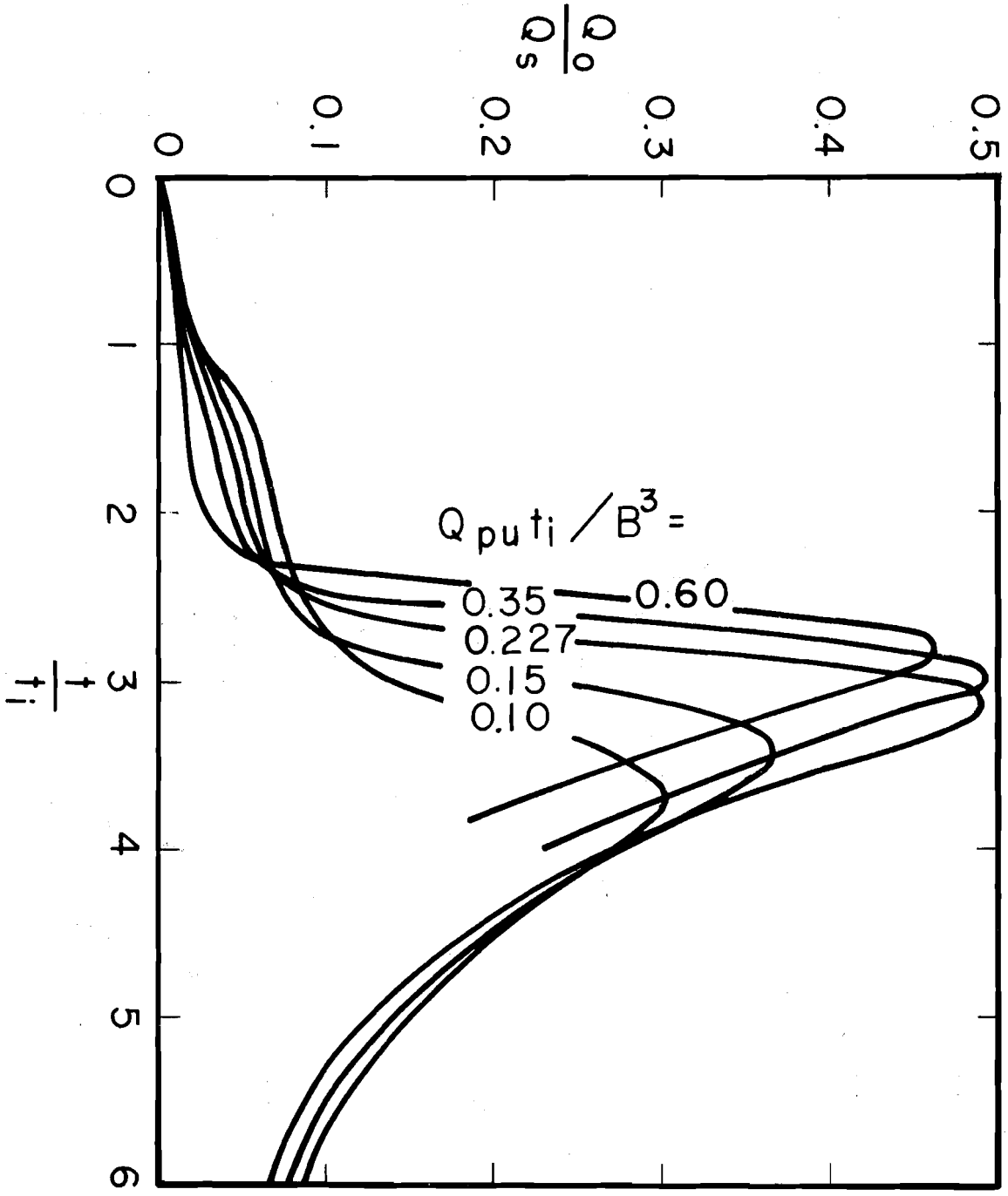

FIG. 13. (b) Q_o/Q_s vs. t/t_i

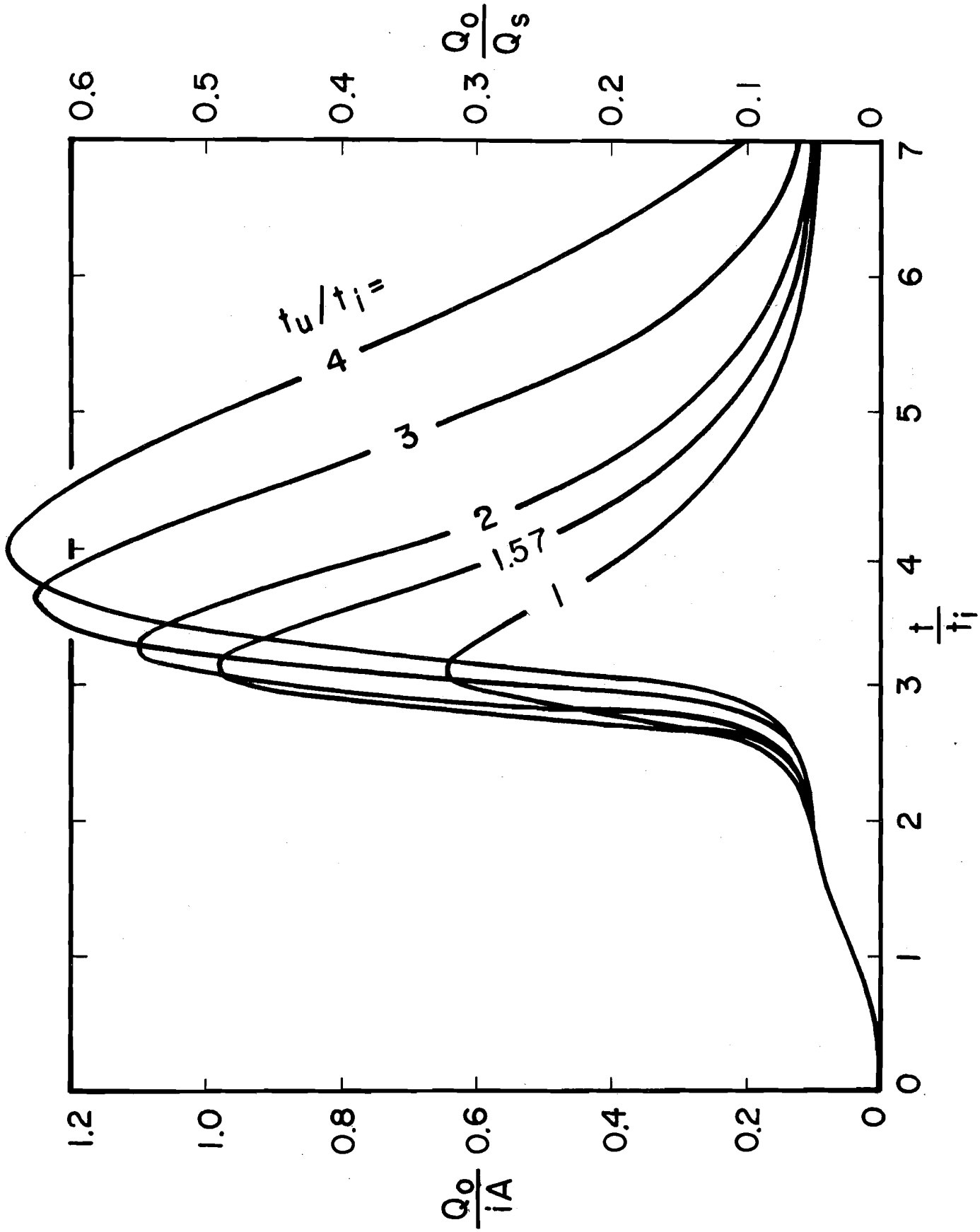

FIG. 14. HYDROGRAPHS AT GUTTER EXIT FOR DIFFERENT UPSTREAM INFLOW DURATIONS

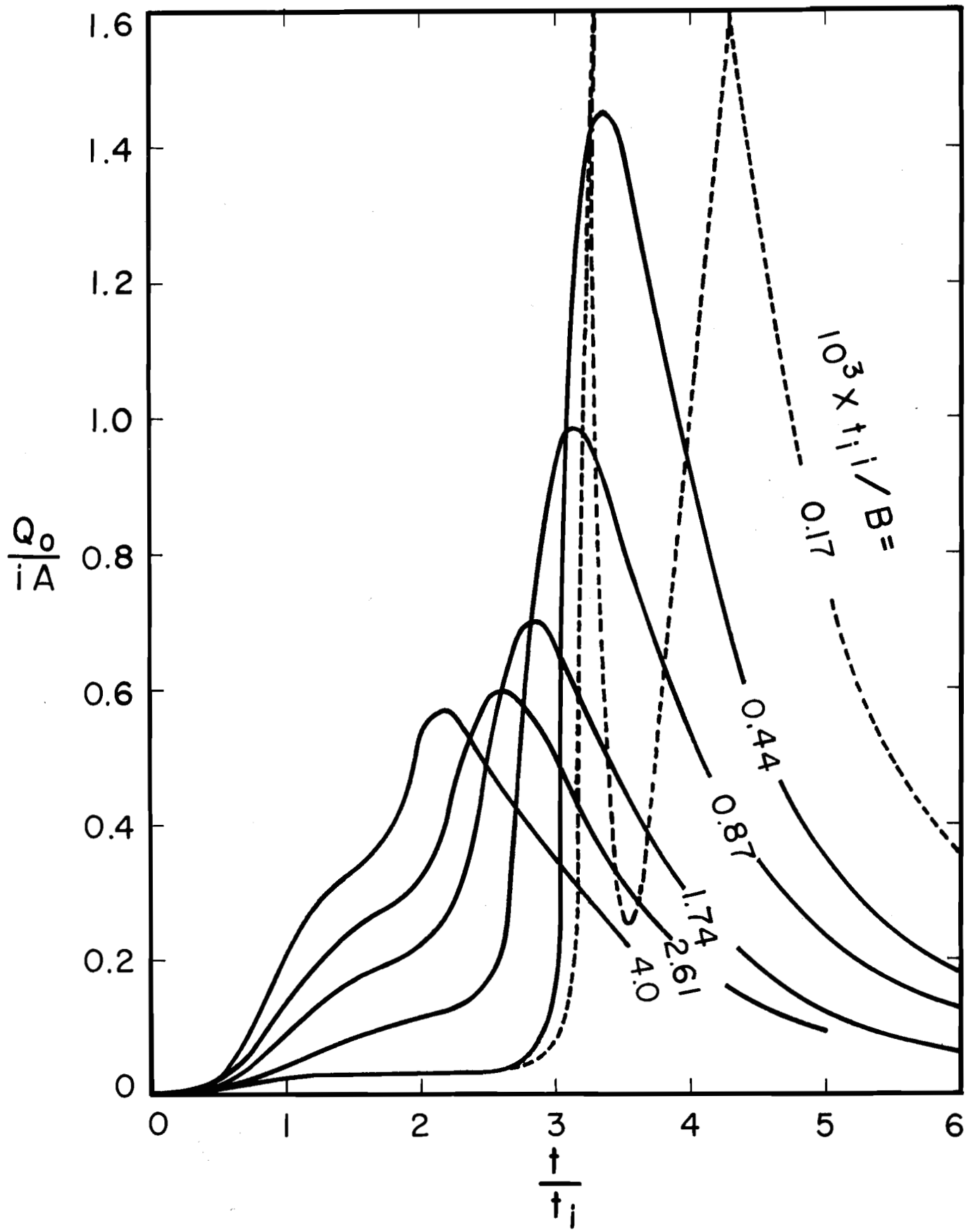

FIG. 15. HYDROGRAPHS AT GUTTER EXIT FOR DIFFERENT RAINFALL INTENSITIES
(a) Q_o/iA vs. t/t_i

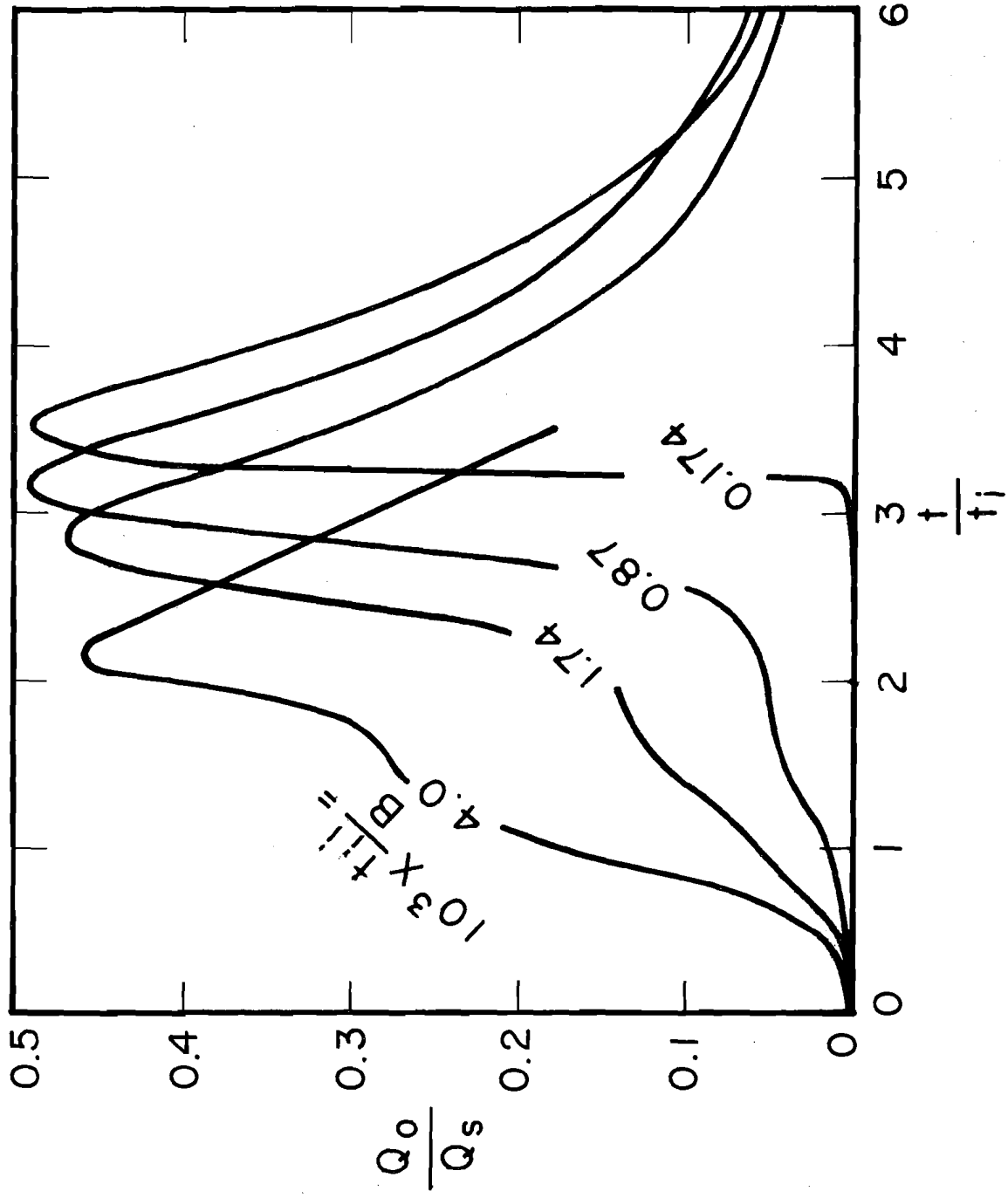

FIG. 15. (b) Q_o/Q_s vs. t/t_i

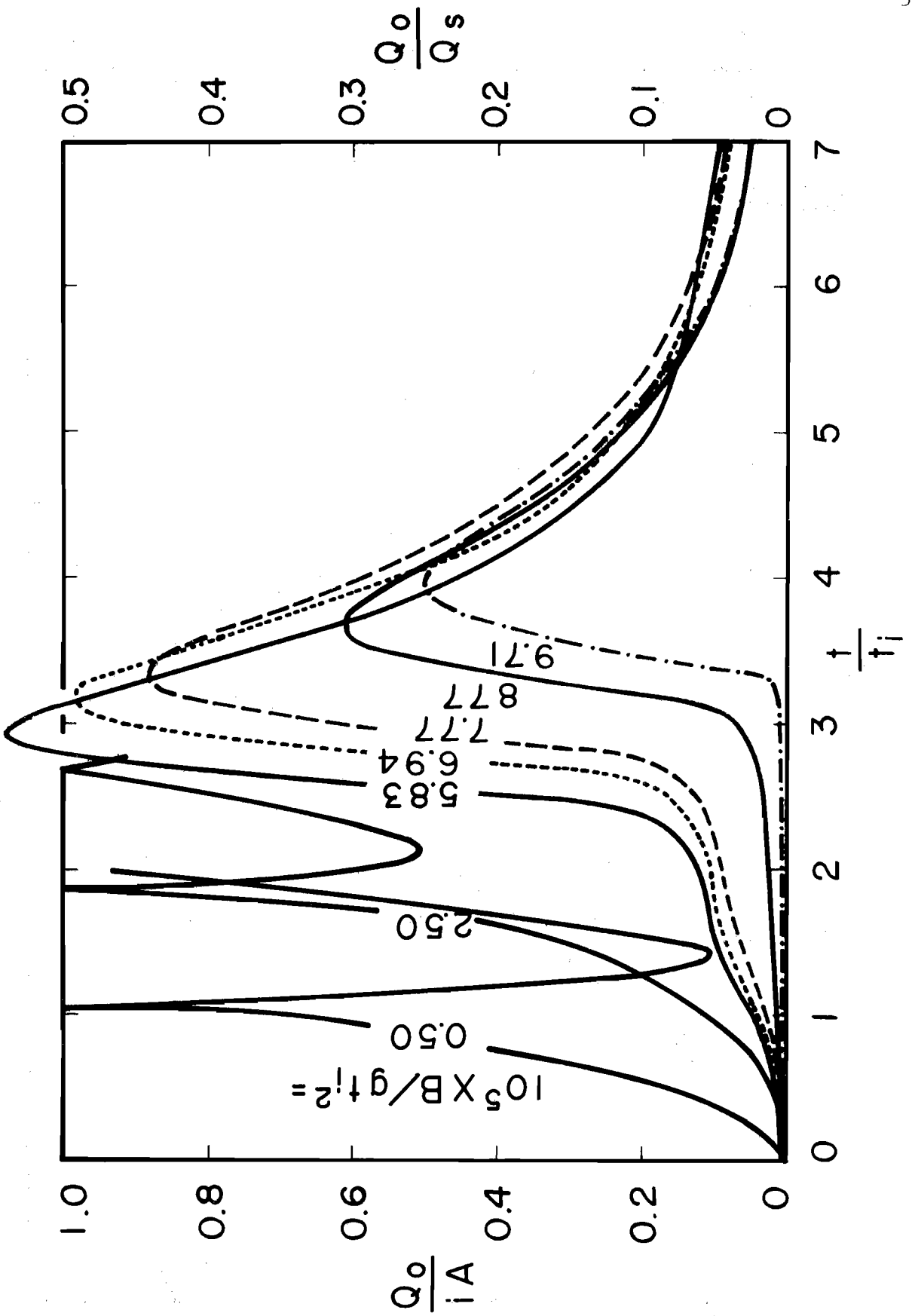

FIG. 16. HYDROGRAPHS AT GUTTER EXIT FOR DIFFERENT GRAVITATIONAL EFFECTS

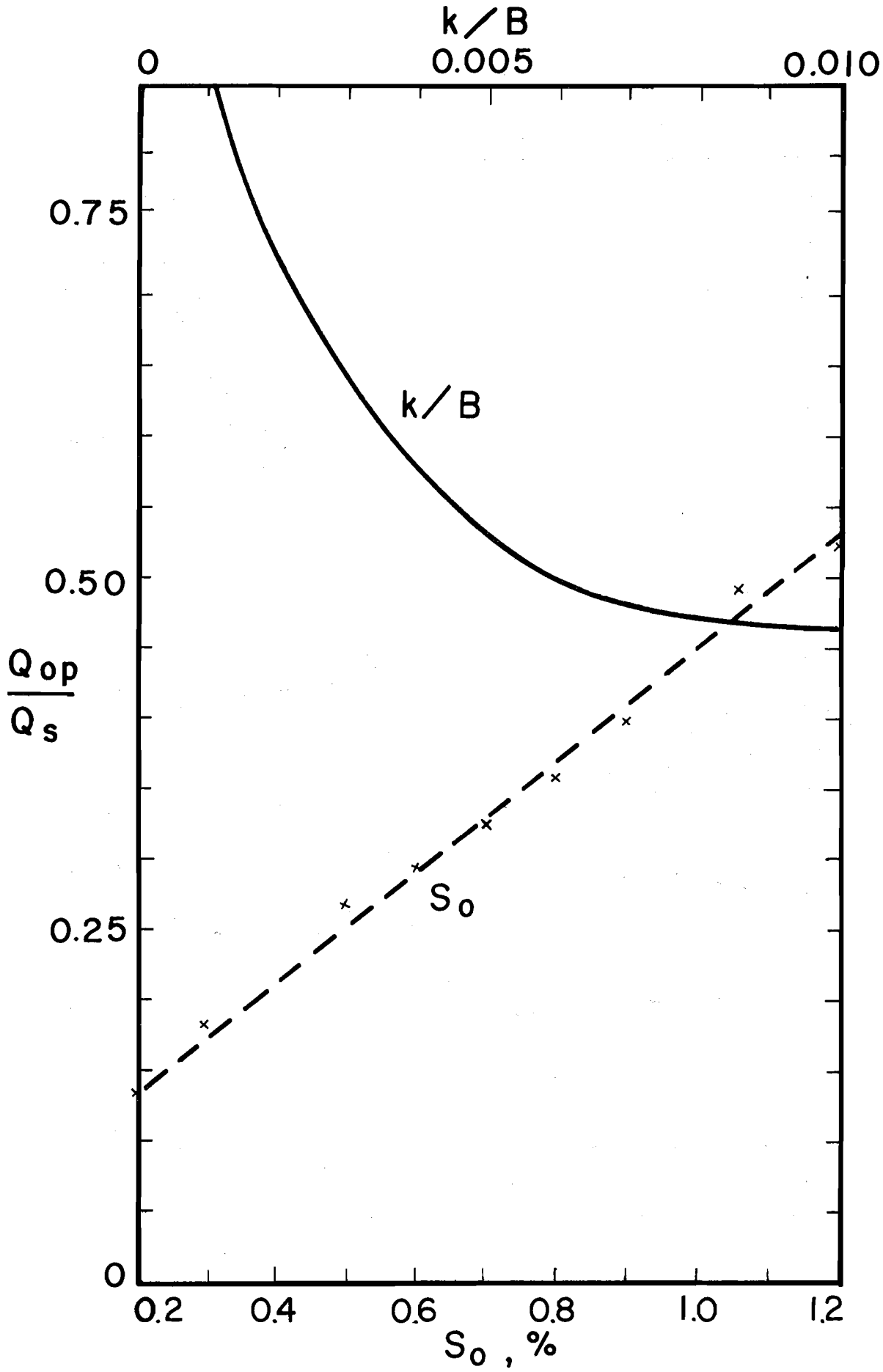

FIG. 17. VARIATIONS OF PEAK DISCHARGE FROM GUTTER WITH GUTTER

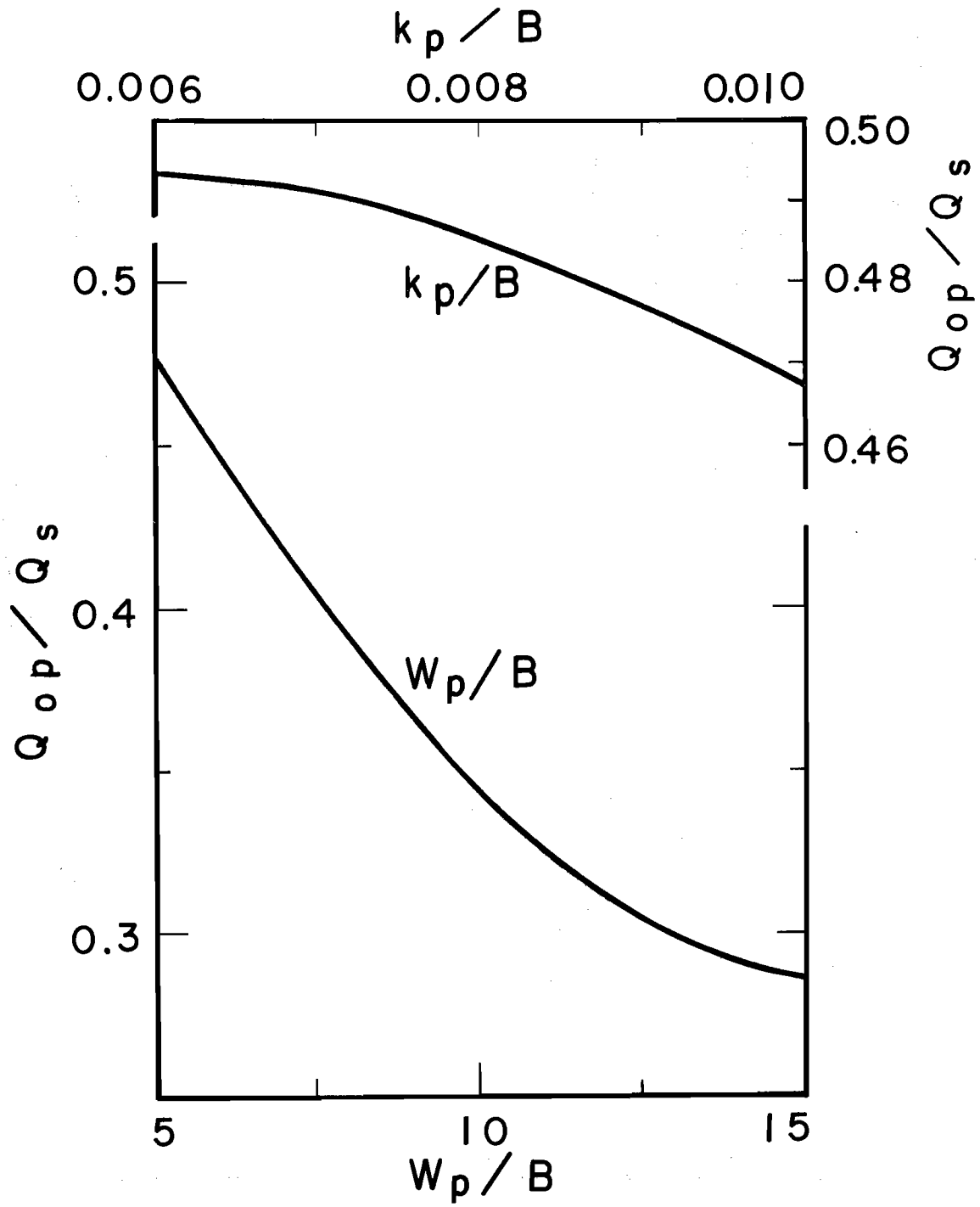

FIG. 18. VARIATIONS OF PEAK DISCHARGE FROM GUTTER WITH PAVEMENT CHARACTERISTICS

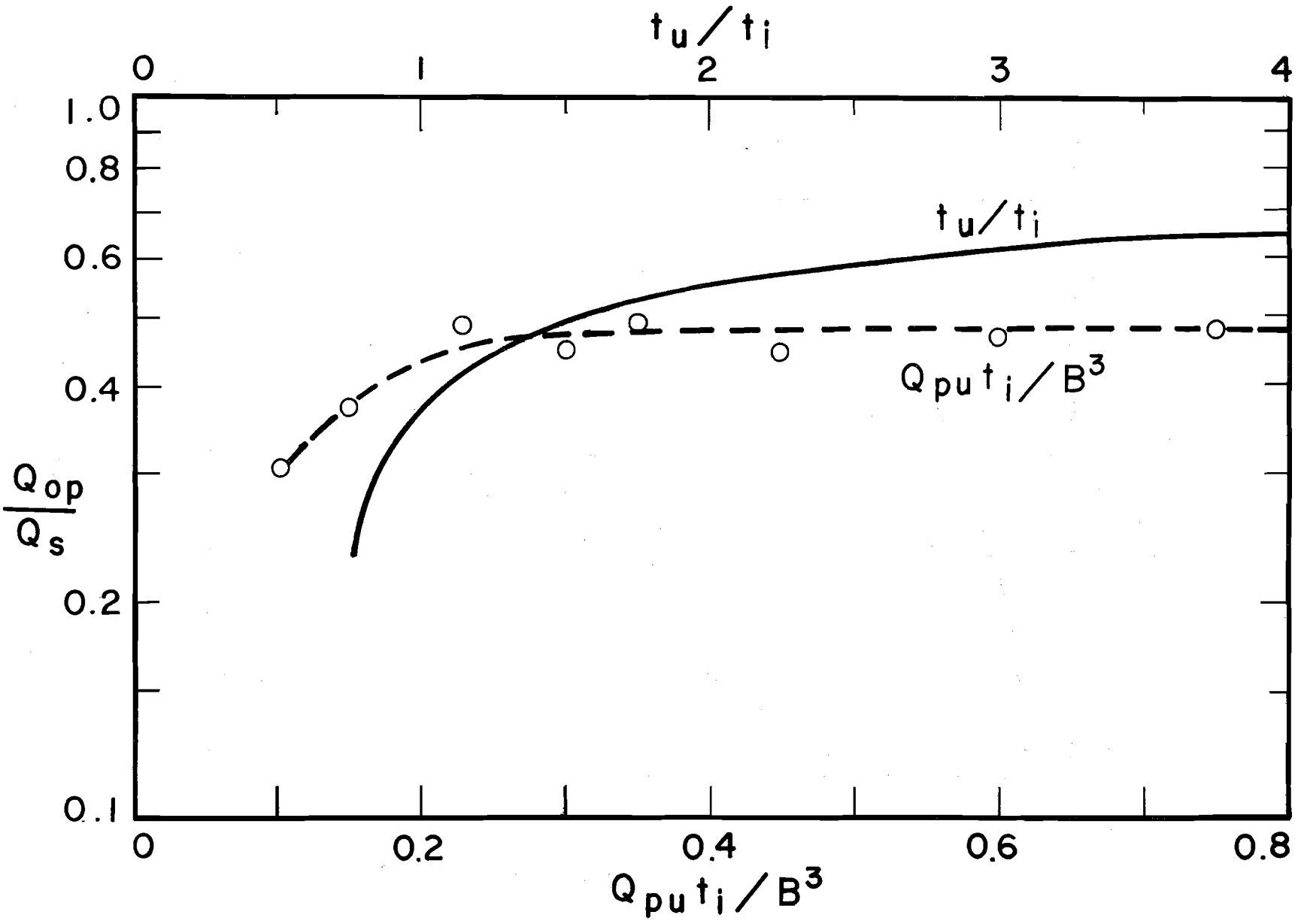

FIG. 19. VARIATIONS OF PEAK DISCHARGE FROM GUTTER WITH UPSTREAM INFLOW CHARACTERISTICS

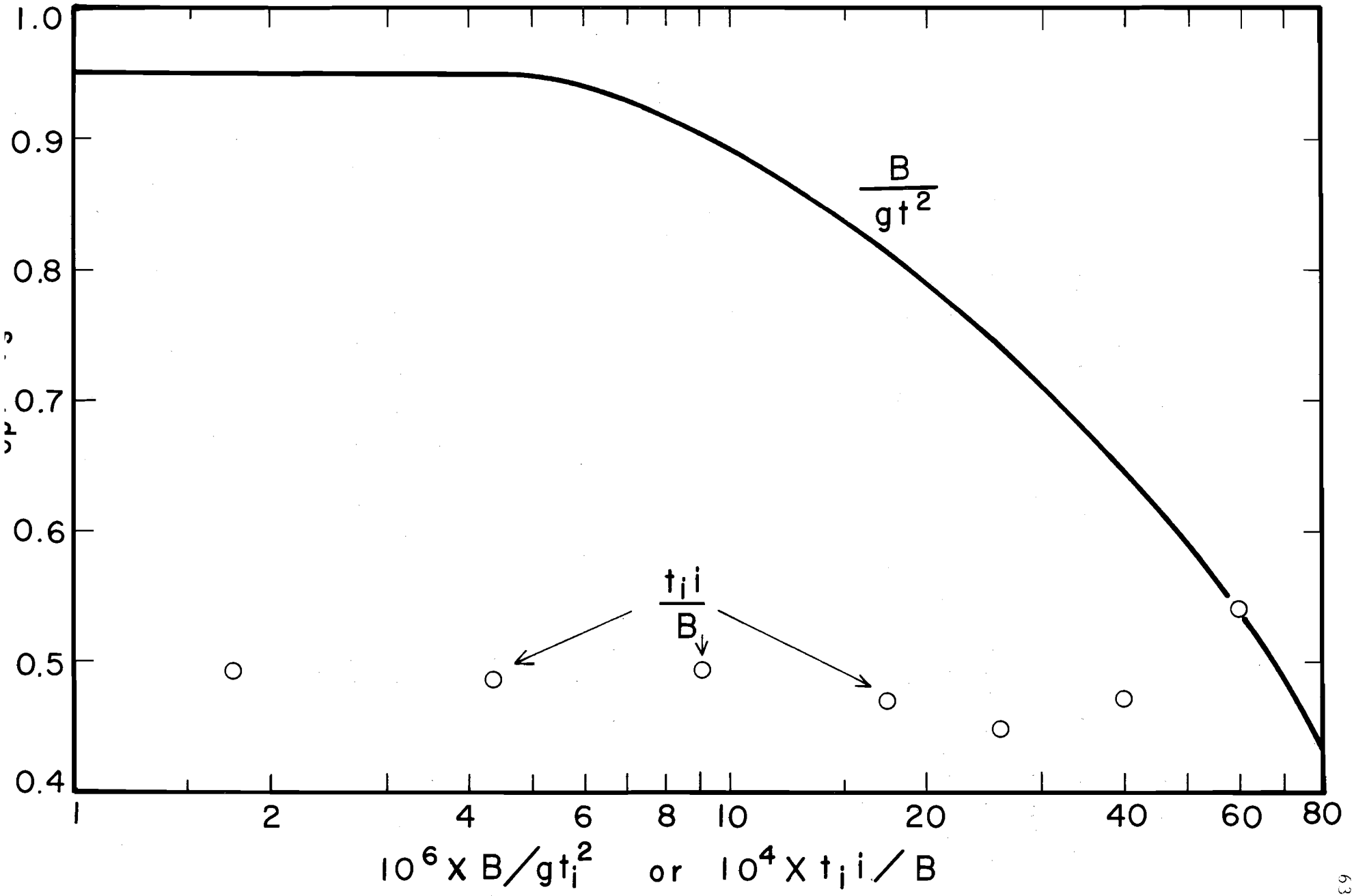

FIG. 20. VARIATIONS OF PEAK DISCHARGE FROM GUTTER WITH RELATIVE RAINFALL INTENSITY AND GRAVITATIONAL EFFECT

V-3. Evaluation of Friction Slope

In the momentum equation (Eq. 1 or 15) the magnitude of the friction slope term is usually larger than any of the other terms, except the term containing S_o. Therefore, the method adopted to determine the value of S_f is particularly important. Inasmuch as the effects of unsteadiness and nonuniformity on the frictional resistance are not yet known quantitatively, one has to rely on the steady uniform flow formulas such as the Manning, Chezy, or Darcy-Weisbach formulas to approximate the value of S_f.

The friction slope can be expressed in the form of the Darcy-Weisbach formula as

$$S_f = \frac{f_f V_1^2}{8gR} \tag{17}$$

in which f_f is the frictional resistance coefficient. Following the suggestion by Chen and Chow (1968), Kareliotis and Chow (1971) proposed to approximate f_f by the Weisbach resistance coefficient f given in the well known Moody diagram for steady uniform flow. Thus, for laminar flow,

$$f = C_f/\mathbb{R} \tag{18}$$

where C_f is a constant and the Reynolds number $\mathbb{R} = V_1 R/\nu$. For sheet flow under rainfall, the value of C_f depends on the rainfall intensity as shown in Fig. 2. For turbulent flow over hydraulically smooth surface, f is given by the Blasius formula

$$f = \frac{0.223}{\mathbb{R}^{0.25}} \tag{19}$$

and for fully developed turbulent flow over hydraulically rough surface,

$$\frac{1}{\sqrt{f}} = 2 \log \frac{2R}{k} + 1.74 \tag{20}$$

in which k is a length measure of the surface roughness.

Actually, as can be seen from the Moody diagram, there is a continuous transition between the laminar flow region (Eq. 18) and the hydraulically smooth turbulent flow region (Eq. 19); and again between the latter (Eq. 19) and the fully developed turbulent flow region (Eq. 20). Furthermore, the Blasius formula (Eq. 19) is valid only for Reynolds number smaller than 4×10^5. For turbulent flow over hydraulically smooth boundary with $\mathbb{R} > 4 \times 10^5$, the Karman-Prandtl equation

$$\frac{1}{\sqrt{f}} = 2 \log \mathbb{R} \sqrt{f} + 0.404 \qquad (21)$$

applies. Nevertheless, hydraulically smooth boundary turbulent flow rarely occurs in sewers and on surface runoffs because of the roughness of the boundaries. Inclusion of the transitions and Eq. 21 in the storm runoff analysis would make the computations and programming lengthy and inefficient. Therefore, for the sake of simplicity without significant effect on accuracy, they are not

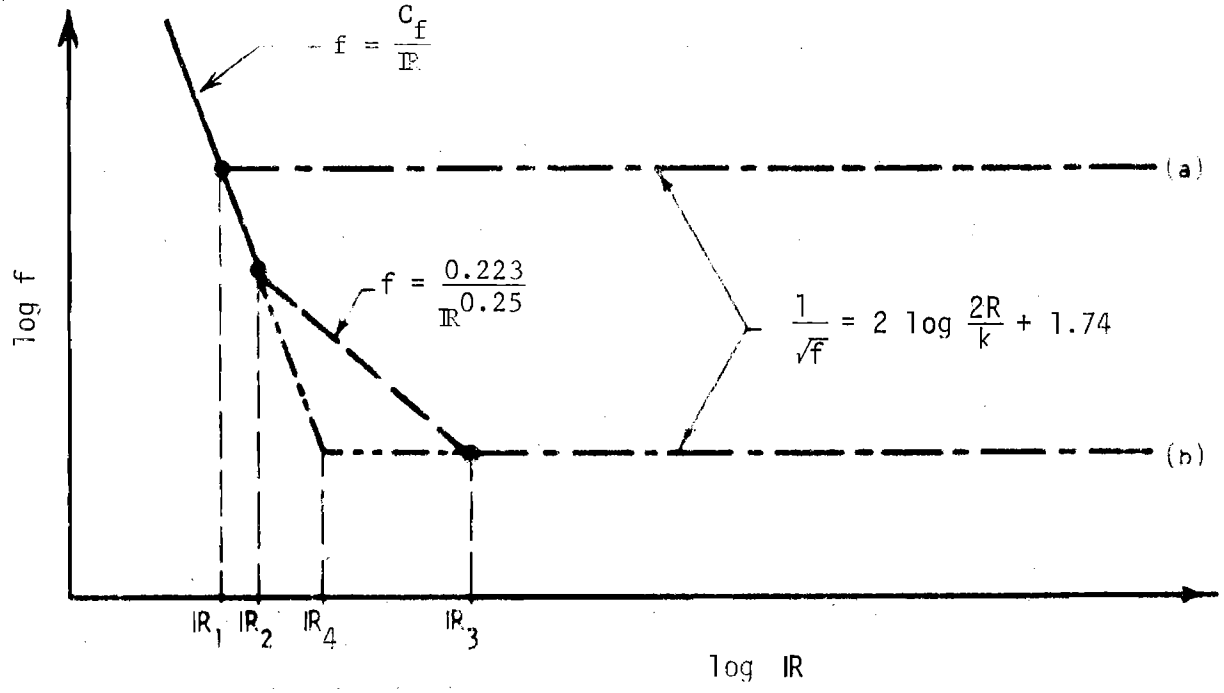

FIG. 21. EVALUATION OF WEISBACH FRICTION COEFFICIENT

considered in this study. As by Kareliotis and Chow (1971) the resistance coefficient is approximate by using Eqs. 18, 19, and 20 as illustrated in Fig. 21.

In solving the St. Venant equations the Reynolds number of the flow at the cross section considered is computed and then compared with the values of the reference threshold Reynolds numbers to determine the proper resistance coefficient equation that should be used. The reference Reynolds number, $\mathbb{R}_1$, between Eqs. 18 and 20 for large surface roughness can be obtained by solving these two equations simultaneously. Thus,

$$\mathbb{R}_1 = C_f \left(2 \log \frac{2R}{k} + 1.74\right)^2 \tag{22}$$

Likewise, between Eqs. 18 and 19,

$$\mathbb{R}_2 = (C_f/0.223)^{4/3} \tag{23}$$

and between Eqs. 19 and 20,

$$\mathbb{R}_3 = 0.633 \left(\log \frac{2R}{k} + 0.87\right)^8 \tag{24}$$

Note that $\mathbb{R}_4$ in Fig. 21 is a special case of $\mathbb{R}_1$ and hence Eq. 22 applies.

The critical value of k/R to determine which equations should be used can be found by equating Eqs. 22 and 23 to yield

$$\left(\frac{k}{R}\right)_c = 2 \times 10^{\left(0.87 - \frac{C_f^{1/6}}{0.736}\right)} \tag{25}$$

For $k/R > (k/R)_c$, if the Reynolds number of the flow $\mathbb{R} < \mathbb{R}_1$, Eq. 18 is used to give the value of f; otherwise, if $\mathbb{R} > \mathbb{R}_1$, Eq. 20 applies. For $k/R < (k/R)_c$, three cases exist: If $\mathbb{R} < \mathbb{R}_2$, Eq. 18 applies. If $\mathbb{R}_2 < \mathbb{R} < \mathbb{R}_3$, Eq. 19 gives the value of f. If $\mathbb{R} > \mathbb{R}_3$, Eq. 20 applies.

V-4. Discussion of Results

For the sake of comparison of the computed results a reference common condition is chosen and listed as the first one in Table 6. For the reference flow condition the sine-curve shape gutter upstream inflow hydrograph is so chosen that its peak discharge Q_{pu} is equal to one-half of the discharge for a steady uniform critical flow in the gutter which is flowing just full with the water surface width equal to B. The duration of the gutter inflow hydrograph, t_u, is chosen equal to 1.57 times the duration of rainfall, t_i, and the rainfall intensity i is equal to Q_{pu}/A so that the total volume of the gutter upstream inflow is equal to the total volume of the lateral inflow which in turn is equal to the volume of rainfall.

In Figs. 10 to 20 the values of the nondimensional parameters, except the one being considered, are the same as those for the reference condition given in Table 6. For the results shown the values of the parameters $L_g/B = 50$, $\phi = 0.048$ rad (approximately 2.7° or 5%), and $B^2/\nu t_i = 9090$. Of course, effects of these three parameters can also be evaluated numerically if desired. However, as discussed previously, the effect of L_g/B is indirect as long as it is not too small so that the upstream inflow behaves like a source. The value of ϕ is arbitrary chosen. As to $B^2/\nu t_i$, this parameter actually represents the effect of viscosity. In field conditions of unsteady flow on pavement and in gutters, particularly when under rainfall, turbulence effect is dominant in determining the runoff hydrographs. Laminar flows occur only at the very beginning and near the end of runoff when the velocity is slow and the depth is small. Consequently for field conditions the effect of $B^2/\nu t_i$ is insignificant and hence not presented herewith. Alternatively, by cross multiplying the last two terms in Eq. 14, either $B^2/\nu t_i$ or B^2/gt_i^2 can be replaced by ν^2/gB^2 which indicates the relative importance of viscous effect as compared to the gravity effect.

Because the nonlinear kinematic-wave approximation is used in evaluating the pavement flow, understandably some of the calculated results do not fall exactly on a smooth line as one would hope. For such cases the computed points are plotted as in Figs. 17, 19, and 20 to illustrate the deviations. However, it is believed that from a practical viewpoint these deviations are not significant and the computed results are perhaps at present the most reliable values available. Particularly, the method presented in this chapter is a considerable improvement from the Manning or Chezy formulas and the Izzard and Horton methods commonly used in estimating pavement and gutter flows.

From the computed results as shown in Figs. 10 to 20, it can be seen that the effect of flow unsteadiness is quite important. Should a steady-flow approach be adopted as in common practice, the design discharge would be $Q_s = Q_{pu} + iA$. As shown by the computed values of Q_{op}/Q_s (Figs. 17 to 20), the peak discharge from the gutter is always smaller than Q_s, and significantly, the reduction is more for smaller relative gutter upstream inflow. In other words, presumably the runoff coefficient in the rational formula commonly used should account for, among other things, the effect of detention storage on the surface. In engineering practice, the runoff coefficient is selected independent of the intensity and duration of the rainfall, whereas the computed results show the contrary.

However, as shown in Fig. 20, the effects of rainfall duration and intensity on the relative gutter peak outflow Q_{op}/Q_s are not as dominant as those by S_o, k/B, W_p/B, and t_u/t_i. Obviously, with increasing street slope, S_o, the surface detention storage decreases and the value of Q_{op}/Q_s increases, and the runoff hydrograph becomes steeper and with a shorter runoff time, as shown in Fig. 10. Increase in surface roughness of the gutter retards the flow and consequently reduces Q_{op}/Q_s as shown in Figs. 11 and 17. However,

as the value of k/B increases, its affect on changing the gutter flow decreases. The effect of W_p/B on Q_{op}/Q_s is somewhat similar to that of k/B in that increasing W_p/B results in decreasing Q_{op}/Q_s at a decreasing rate as shown in Figs. 12 and 18.

Ideally, an inlet should be designed to receive all the water from the gutter. However, for various reasons some water may pass by or spill over the inlet without being intercepted. For such a case the downstream condition of the gutter flow depends on the hydraulic characteristics of the inlet which need to be determined experimentally or theoretically. An approximate practical means to analyze the partial intercepted flow by using steady-flow experimental results for inlets has been described in Akan's thesis (1973). In addition, an engineering design example has also been presented by Akan and is omitted here.

VI. FLOW IN SEWER NETWORKS

VI-1. Sewer Network Simulation

The surface runoff collected by the inlet catch basins is delivered through the sewer network for disposal into channels, streams, lakes, ponds, reservoirs, treatment plants, oceans, or other natural or artificial water bodies or devices. As discussed previously, in most field cases, flow in storm sewers is open-channel flow. Consequently, the St. Venant equations (Eqs. 1 and 2) can be applied to the flow in sewers. In addition, the flow is also controlled by the compatibility conditions at the junctions of the sewers.

Most of the storm sewer networks are tree type systems as shown in Fig. 22. Because of the backwater effects of the junctions, the problem of sewer flow becomes extremely complicated. At present neither the configuration of a sewer network nor its flow conditions can be presented accurately in detail in a single mathematical simulation model because of the limitations in accessible computer software in handling arbitrary network topologies, requirements of excessive computational effort for the solution, and inadequate information on certain necessary input parameters such as the frictional resistance of the sewers and energy loss in the junctions. On the other hand, conventional approaches for sewer design or flow prediction by considering each sewer as an individual and independent unit of steady uniform flow have been found inadequate and unsatisfactory. The mathematical model proposed in this study, the Illinois Storm Sewer System Simulation Model (ISS Model) is developed with the intention to be an accurate practical tool for engineering applications.

Briefly, the ISS Model utilizes the St. Venant equations to describe mathematically the flow in sewers together with the compatibility

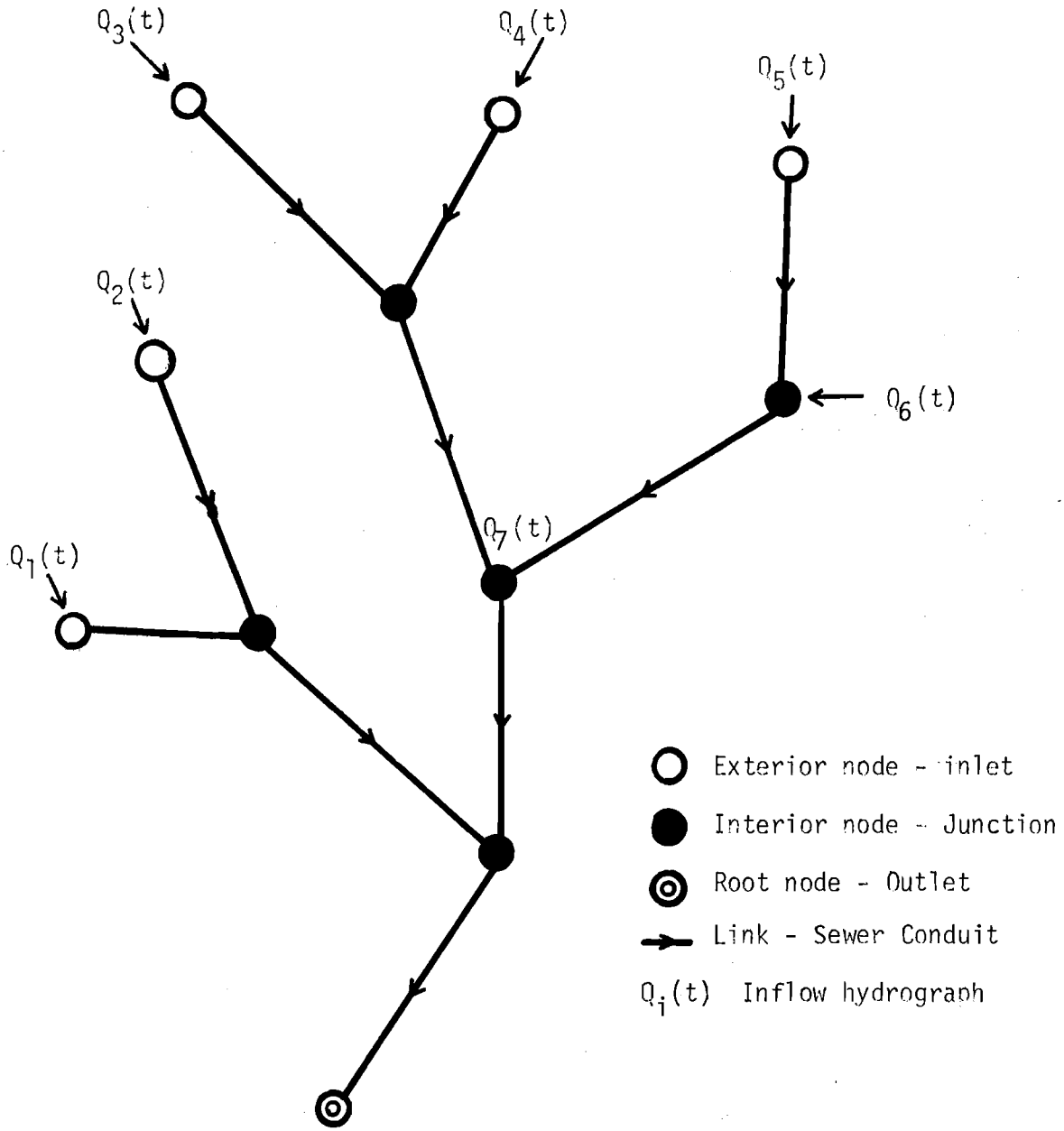

FIG. 22. TYPICAL TREE TYPE SEWER SYSTEM

conditions at the junctions which include the continuity of water surface at the junction and the conservation of mass

$$\Sigma Q_i = \frac{dS}{dt} \tag{26}$$

in which Q_i is the flow into the junction from the i-th sewer and S is the storage in the junction. The backwater effects are accounted for through an overlapping segment scheme which is essentially a single-step iteration process.

VI-2. Assumptions on Physiography of Network Components

An urban storm sewer system may consist of a large number of sewers, junctions, manholes and inlets, plus other regulating or operational devices such as gates, valves, weirs, overflows, regulators, and pumping stations. Some of these devices such as weirs and pumps provide flow controls dividing hydraulically a complex system into a number of subsystems interrelated by the hydrographs at the controls. Each of these subsystems can be applied individually to the proposed ISS Model and then integrated together following an appropriate sequence provided the hydraulic characteristics of the controls are known. For the sake of simplicity, these special devices are incorporated only indirectly into the mathematical simulation model for a specific sewer system by known functions representing their hydraulic characteristics. In addition, in the development of the ISS Model, the following assumptions are made regarding the physical characteristics of sewers and junctions:

a) The sewers are circular in cross section.

b) The diameter, slope, and surface roughness of each sewer remain constant along its entire length.

c) The inflow of storm water into the sewer system occurs only at discrete nodal points, viz., inlets, junctions, and manholes.

d) Manholes and junction boxes are open to atmospheric pressure. At both the manholes and junctions, invert lines of the upstream incoming sewers are at the same or higher elevation than that of the downstream outflowing sewer.

e) There are no more than three sewers joining together at a junction or manhole.

The first assumption is not too restrictive because most storm sewers are constructed by standard concrete, clay, iron, or steel pipes. Only when standard pipe is not available, or when the size is extremely large, or for other reasons that cast-in-place reinforced concrete sewers with horseshoe, trapezoidal, rectangular, or other shapes of cross section are employed (ASCE, 1969). Moreover, even if sewers with horseshoe or other cross-sectional shapes are used, they can be approximated by representative circular conduits without significant loss in accuracy, as it has been shown by Harris (1970b); or alternatively, their cross-sectional characteristics can be incorporated into the Model with minor modifications.

The second and third assumptions are likewise not too critical. Whenever a significant change in the geometrical features or an inflow along the course of a sewer occurs, it can be treated as an hypothetical junction point in the mathematical model.

Assumption (d) essentially restricts the application of the Model to those networks which do not include a lift or a pumping station. However, if it is assumed that the flow conditions in the sewers are not subject to direct backwater effects of pumping, then the pumping station can be treated as a drop junction box and the model can still be applied. In fact, as discussed earlier, such a pumping station with its hydraulic characteristics known may provide a handy location to divide the system into subsystems on each of which the Model can be applied separately.

Assumption (e) is not as restrictive as it appears. Additional sewers are allowed to join as long as they do not impose significant backwater effects. In other words, they behave like point sources (Eq. 26). In reality, for a junction or manhole with four or more joining sewers, the sewer invert elevations and other geometry considerations often make it possible to identify the sewers with insignificant backwater effects from the junction and other sewers.

It should be noted here that although most of the sewer systems are tree type in pattern, on rare occasions they may form closed-loop networks. However, the matrix-like structures used for digital manipulation of such looped networks are invariably very sparse (Harley et al, 1970), and they are inefficient in view of computation when applied to the tree type systems. Hence, the closed-loop networks are not incorporated into the ISS Model. Furthermore, many of such closed-loop networks are actually formed by sewer branches joining the main or intercepting sewers through overflows or drops and there are no direct mutual backwater effects between the branches and the mains. As described in the preceding paragraph, the ISS Model permits inflows or outflows directly at the junctions in addition to the flows from the joining branches as long as there is no need for backwater consideration for these direct flows.

VI-3. Assumptions on Flow Conditions

(A) Initial Conditions.

In solving the St. Venant equations numerically, it is necessary to know all the depths and velocities along the sewer network at a given initial time. For combined sewers, these initial depths and velocities can be estimated from dry-weather flow conditions. For storm sewers, generally the only known initial condition is that of zero depth and velocity throughout the network. This dry-bed initial condition, however, constitutes a singularity

and the numerical methods fail to advance the solution to the next immediate time level. Thus, it is assumed herein that initially a constant base flow, no matter how small and negligible from practical viewpoint, occurs along each sewer in the network.

It should be mentioned here that, while the manner the initial conditions specified has a significant effect on the solution of overland flow problems, it is not of a major concern in the solution of transient flow problems in rivers or sewer systems (Gunaratnam and Perkins, 1970). In the latter cases as the solution advances in time the effect of the initial conditions diminishes and the solution becomes totally controlled by the boundary conditions after a short time period, inasmuch as the magnitude of the initial base flow is small as compared to that of the flood flow (Yevjevich and Barnes, 1970).

(B) Flow Conditions at Junctions.

The use of one-dimensional flow equations of conservation of mass, energy and momentum is admittedly a simplified representation of the flow processes at a storm sewer junction, which involves rapid changes in depth, direction of flow, and velocity and pressure distributions. Nevertheless, even such a simplified one-dimensional formulation of the problem is extremely complicated. Use of the momentum equation is impractical because of the difficulties involved in evaluating the pressure and friction forces acting on the boundaries of the junction. In using the energy equation, loss at the junction is to be known for the flow conditions and junction geometry, experimentally or otherwise. Unfortunately, existing knowledge on the energy losses is again inadequate.

From a mathematical viewpoint, omitting the momentum equation reduces the number of compatibility conditions by one, and hence it requires additional assumptions on the boundary conditions. For example, at a Y-junction with

subcritical flow in all of its three joining sewers, the continuity and energy compatibility conditions alone cannot provide the necessary three boundary conditions, one for each of the three sewers. In view of this difficulty, some approximations have been made in this study. Two types of junctions, depending on whether the junction has a storage capacity or not, are considered.

a) Point-Type Junction

For the point-type junction the junction box is assumed to be represented by a single confluence point (more precisely, a section) without storage capacity. The net discharge into the junction is therefore zero at all times. Hence, from Eq. 26,

$$Q_1 + Q_2 + Q_j - Q_3 = 0 \tag{27}$$

in which the subscripts 1, 2 and 3 identify the joining sewers at the junction (Fig. 23); and Q_j represents the direct temporally variable water inflow into, or the pumpage or leakage out from the junction box, if any.

For subcritical flow in the inflowing sewers, the flow discharges freely into the junction only when a free-fall exists over a nonsubmerged drop at the end of the sewer. Otherwise the subcritical flow in the inflowing sewer is subject to backwater effect from the junction. Since the junction is considered as a point, the energy compatibility condition can be represented by a common water surface at the junction for all the joining sewers (Dronkers, 1964, 1969). Thus, by referring to Fig. 23,

$$y_i = y_{ic} \qquad \text{if } Z_i + y_{ic} > y_3 \tag{28}$$

$$y_i + Z_i = y_3 \qquad \text{otherwise} \tag{29}$$

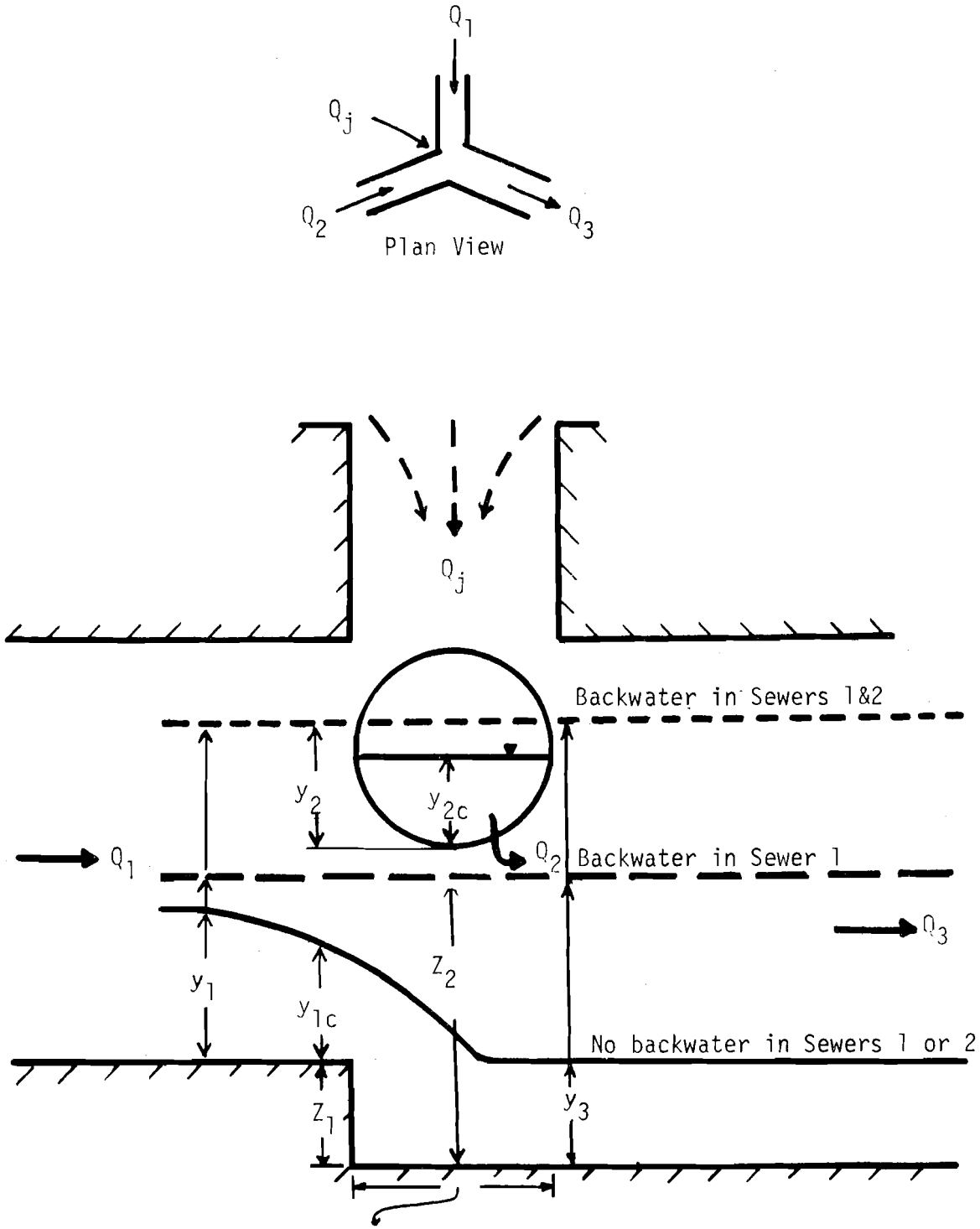

FIG. 23. SCHEMATIC OF POINT-TYPE JUNCTION

in which y_{ic} is the critical depth corresponding to the instantaneous flow rate Q_i, and Z_i is the height of the drop of the inflowing sewers, i = 1 or 2. Flow in the outflow sewer may be either subcritical or supercritical. In the latter case y_3 in Eqs. 28 and 29 is equal to the critical flow depth, y_{3c}, corresponding to the instantaneous flow rate Q_3.

Flow in the inflow sewers can also be supercritical discharging freely into the junction, provided the flow at the downstream end of the sewer is not submerged by the backwater in the junction. In this study, when supercritical flow occurs in Sewers 1 or 2 or both, it is assumed to discharge freely into the junction to avoid considering moving hydraulic jumps in the sewers. Thus, the discharge can be computed without considering the flow condition in the junction, i.e., without specified downstream condition. Subsequently, the discharge in the outflowing Sewer 3 can be computed by using Eq. 27 without iteration.

For a three-way junction there are 18 different possible combinations of flow conditions depending on whether the flows in the joining sewers are subcritical, critical, or supercritical. Different sets of nonlinear simultaneous equations are included in the ISS Model to handle these flow combinations in the computations.

Although three-way junctions are most common in sewer networks, there also exist two-way junctions at locations where a direct inflow or a significant change in dimension, slope, or horizontal alignment occurs along the course of a sewer. These two-way junctions can be considered as a special case of the three-way junctions by letting Sewers 1 and 3 represent the inflowing and outflowing sewers, respectively. Consequently, Eq. 27 with $Q_2 = 0$ and Eqs. 28 and 29 can again be used. Supercritical flow in Sewer 1 is once more assumed to be free from backwater effects of the junction.

b) Reservoir-Type Junction

The reservoir-type junction box has a relatively large storage capacity in comparison to the flow. Consequently, it can be assumed to behave like a reservoir with a horizontal water surface and capable to absorb and dissipate all the kinetic energy of the inflows. The net discharge into the junction is equal to the time rate of change of storage in the junction. Therefore, for a three-way junction (Fig. 24),

$$Q_1 + Q_2 + Q_j - Q_3 = \frac{dS}{dt} = A_j \frac{dh}{dt} \tag{30}$$

in which A_j is the constant horizontal cross-sectional area of the junction box and the depth of water h in the junction is assumed equal to the specific energy of the flow at the entrance of the outflowing sewer, i.e.,

$$h = y_3 + \frac{V_3^2}{2g} \tag{31}$$

Since the kinetic energy of the inflows is assumed lost at the junction, for the three-way junction shown in Fig. 24, for subcritical flow in the inflow sewers with i = 1 and 2,

$$Z_i + y_i = h \qquad \text{if } Z_i + y_{ic} < h \tag{32}$$

$$y_i = y_{ic} \qquad \text{otherwise} \tag{33}$$

If the flow in the outflow Sewer 3 is supercritical, critical flow condition exists at its entrance and hence h in Eq. 32 should be replaced by the minimum specific energy corresponding to the instantaneous flow rate Q_3.

As it has been discussed in the point junction, supercritical flows in Sewers 1 and 2 are assumed to be discharging freely into the reservoir.

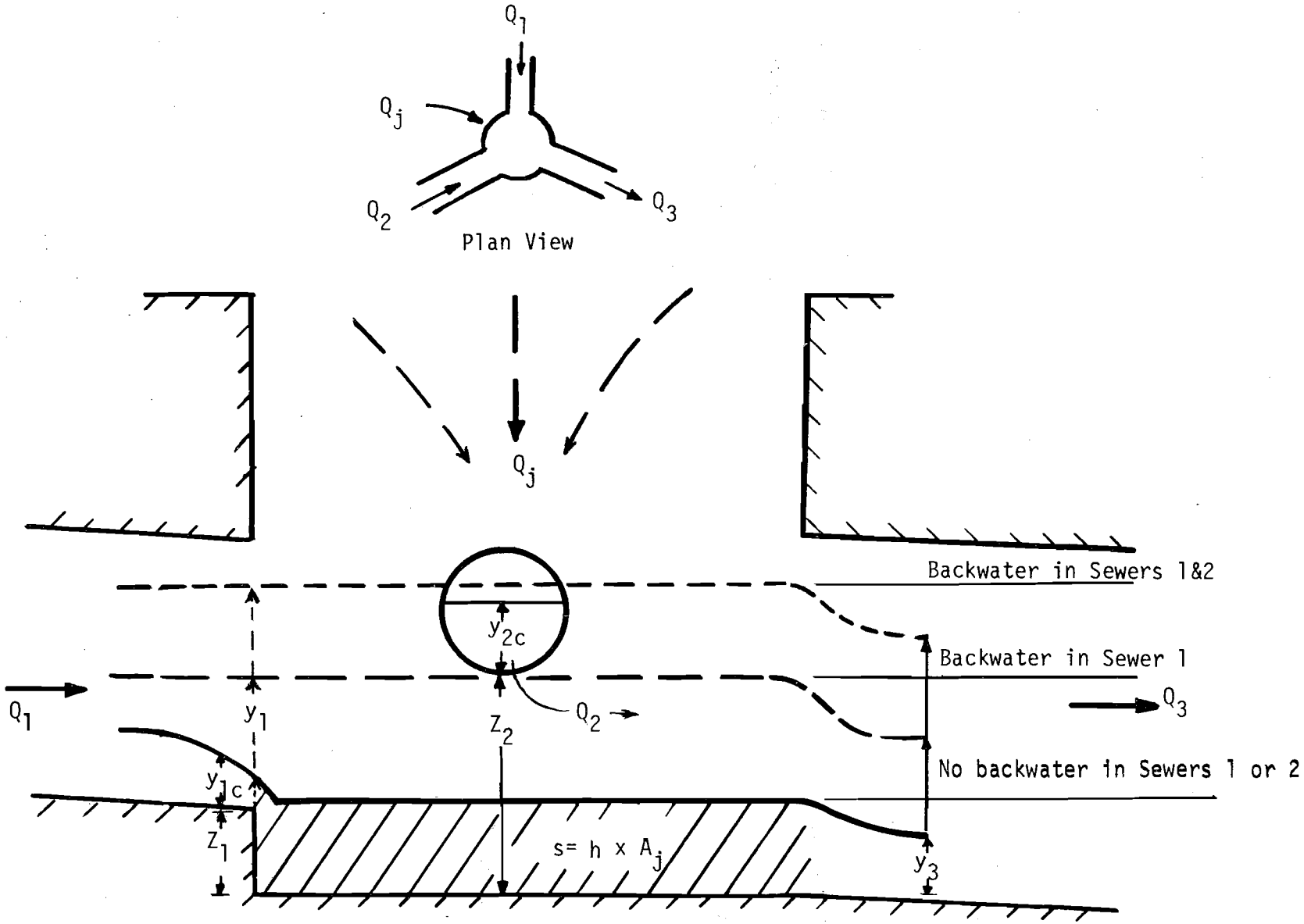

FIG. 24. SCHEMATIC OF RESERVOIR-TYPE JUNCTION

Thus for such cases the inflows Q_1 and Q_2 from these sewers are computed without considering the existing flow conditions in the junction or Sewer 3.

The 18 different flow combinations which have been described in the three-way point junction can also be observed in a three-way reservoir junction. Again, both of the inflowing sewers, or either one, or neither of them may be subjected to backwater effects, and one, two, or all three of these conditions may be observed during the passage of the flood waves through a particular junction (Fig. 24).

Like the two-way point-type junction, a two-way reservoir junction can be treated as a special case of a three-way junction with the joining Sewers 1 and 3, and Eq. 30 with $Q_2 = 0$ together with Eqs. 32 and 33 can be used as the compatibility conditions. Supercritical flow in the inflowing Sewer 1 is again assumed to be free from backwater effects from the reservoir junction. A two-way reservoir junction, besides representing an actual storage element with or without a direct inflow or outflow (i.e., Q_j), may approximately represent a concentrated energy loss along the course of a sewer.

(C) Evaluation of Friction Resistance.

As discussed in Sec. V-3, the Darcy-Weisbach resistance formula (Eq. 17) is adopted in this study to evaluate the friction slope S_f. The resistance coefficient f_f is approximated by Eqs. 18, 19, and 20 which strictly speaking are valid only for steady uniform flows. In reality, laminar flow rarely occurs in storm sewers. Therefore, for the sake of simplicity in programming and computation without significant effect on the accuracy, only the Blasius (Eq. 19) and the Karman-Prandtl (Eq. 20) equations are utilized in the ISS Model.

The threshold Reynolds number, $\mathbb{R}_3$, which separates the hydraulically smooth and rough regions is determined by Eq. 24. In the computational

process, at each cross section the values of the Reynolds number of the flow $\mathbb{R}$ is compared with $\mathbb{R}_3$. If the former is greater, Eq. 20 is used to give f. Otherwise, Eq. 19 is used.

(D) Surges and Hydraulic Jumps.

Surges and hydraulic jumps are rapidly varying flows for which the flow profiles change abruptly. The former is defined herein as a steep-front propagating wave which usually originate from the upstream of a sewer as a result of sudden rapid increase in inflow and propagates downstream. The formation of a surge is mathematically characterized by the crossing of the forward characteristics which emanate from the upstream boundary at different instants. A hydraulic jump which is a rapid change from supercritical to subcritical flow often originates at the downstream part of the sewer as a result of backwater effects and then propagates according to the instantaneous flow conditions. Strictly speaking, the St. Venant equations, being valid only for gradually varied unsteady flows, are not applicable in the vicinity of the rapidly varying flows of the surge front and hydraulic jump (Yen, 1971, 1973), although in practice they are commonly used as an approximation.

The use of a rectangular computational grid and linear spatial interpolations in the first-order characteristic scheme precludes the possibility of formation of a steep-front surge (Zovne, 1970). That is, the crossing of the forward characteristics is not allowed by the solution technique although the boundary conditions may indicate that such a crossing is likely to occur. Instead, the solution approximates the surge by a continuous smooth but rapidly varying profile in the vicinity of the surge which may be adequate for most engineering purposes. As stated by Zovne (1970), the profile behind the surge gradually attains the maximum anticipated depth which is often of primary interest to the engineer. It should be mentioned,

however, that if the surge takes the form of a moving hydraulic drop, i.e., transition from subcritical to supercritical flow, some computational problems may be encountered.

The formation and existence of hydraulic jumps should not be excluded in a mathematical simulation model unless the supercritical flow in a sewer is assumed to be free from the backwater effect of the junction at its downstream end. This assumption, unfortunately, is necessary in this study, because in an interconnected system of channels it is extremely difficult to keep track of the moving hydraulic jumps in the numerical computations, particularly in view of their possible eventual mutual interaction at the junctions. Furthermore, in the mathematical model a hydraulic jump must be treated as an internal boundary where the Rankine-Hogoniot shock conditions (Gunaratnam and Perkins, 1970) hold. This, however, leads to an iterative solution, (Zovne, 1970) and requires inordinately large amounts of computer time. Further studies on moving hydraulic jumps and surges are most desirable for future improvement of the ISS Model.

VI-4. Method of Overlapping Segments

For a tree-type network consisting of N sewers, the St. Venant equations together with two initial and two boundary conditions for each of the sewers represent N distinct propagation problems. Numerical solution for each of these propagation problems along the individual sewers can be obtained with the selected first-order characteristic scheme discussed in Chapter IV. The numerical solution must be advanced over all the sewers within the network because the propagation problems over the adjoining sewers are in most of the cases linked by common boundary conditions at their junctions. However, it is impractical to obtain solutions for all the sewers simultaneously (Sevuk, 1973). Therefore, an approximate iteration method of overlapping segments is adopted for solutions. In this

method the network is considered to be formed by a number of overlapping Y-segments. Each of these segments covers one junction to which two or three sewers are joined. Starting from the upstream inlets and following an appropriate sequence, these Y-segments are solved one at a time, as shown schematically in Fig. 25, and the solutions are then combined together to find the solution over the entire network:

a) The solutions are first obtained over those Y-segments whose inflowing sewers are connected to the inlet catch basins. The prescribed inflow hydrographs at the inlets given by, say from the method proposed in Chapter V, the compatibility conditions at the junction, and the known flow condition at the downstream end of the segment (or alternatively, if the downstream condition is unknown, the forward differences as a substitute) are used as the boundary conditions. For instance, for the network shown in Fig. 25a, the solutions are first obtained over the three Y-segments shown in Fig. 25b.

b) The use of forward differences as a substitute for the unknown downstream boundary condition which accounts for the backwater effect at the downstream end of a Y-segment is assumed to affect only the solutions obtained over the outflowing sewer of the segment. After the computation for the Y-segment is completed, this first approximation solution for the outflowing sewer is discarded, but the "true" solutions for the inflowing sewers of the segment are retained. The inflow hydrographs into the junction of the current Y-segments can then be obtained. For instance, the solutions for the inflowing Sewers 1 through 5 of the three Y-segments shown in Fig. 25b are retained, and hence the inflow hydrographs to the junctions upstream of the sewers 6, 7 and 9 are obtained.

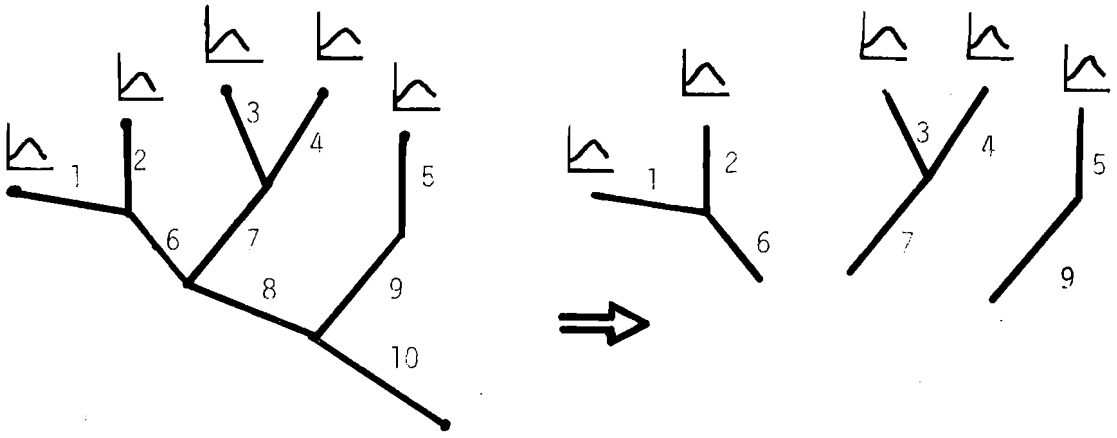

a. Complete solution domain

b. Solution domains for first-order sewers (1 through 5)

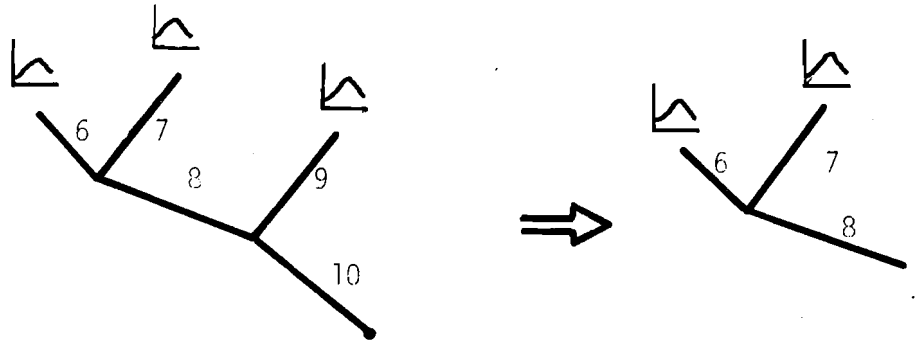

c. Reduced solution domain

d. Solution domain for second-order sewers (6 and 7)

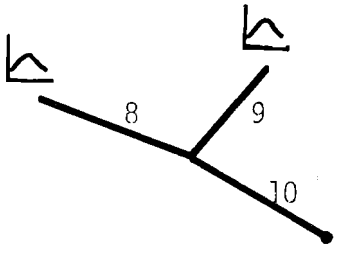

e. Final solution domain for the sewers 8, 9, and 10

FIG. 25. SCHEMATIC OF SOLUTION BY METHOD OF OVERLAPPING SEGMENTS

c) The inflowing sewers of the current Y-segments are trimmed in the computations. The junction of the current Y-segments are then treated as the inlets of the advanced segments of the pruned network. The numerical solution steps (a) and (b) just described are then applied to the new segments. This procedure is repeated in sequence over the network until it is reduced to the last Y-segment at the outlet of the network as shown in Fig. 25e.

d) For the last segment, the prescribed boundary condition at its downstream end (outlet of the network) is used, and thus the numerical solution over the entire network is completed.

Solution by the method of overlapping segments accounts for the backwater effect only for the immediate adjacent sewers and cannot reflect the backwater effect to sewers farther upstream if such a condition occurs. However, by considering the length to diameter ratio of storm sewers, the effect of backwater beyond the immediate adjacent sewers appears to be insignificant and hence it does not impose significant error in the proposed mathematical routing model.

The method requires computation to be performed twice over all the interior sewers of a network. Conversely, it permits the use of greater time steps in advancing the solutions because the maximum allowable time step over a particular segment is not constrained by that of any other segment. This latter capability more than offsets the required extra computations for the interior sewers, and makes the method more efficient as compared to the method of simultaneous solutions.

Efficiency of the method is particularly pronounced in applying the model for design of sewer networks, for it enables the formulation of an algorithm by which the appropriate sewer sizes can be computed with a minimum number of repeated routings, as will be described in the following section.

VI-5. Procedure for Design of Sewer Size

Depending on the constraints imposed, there are three possible approaches for the design of a storm sewer system with specified design inflows:

a) Select a layout, select the slopes and determine the sizes of the sewers.

b) Select a layout, and find the optimum slopes and diameters of the sewers which will ensure the minimum cost or satisfy other objective functions for the selected layout.

c) Find the optimum layout and the optimum slopes and diameters of the sewers which will ensure the minimum cost or satisfy other objective functions.

With the present computer capabilities and existing optimization algorithms, implementation of the second and third design procedures does not appear to be feasible, so long as the hydraulics of the system is simulated by using the St. Venant equations. Therefore, in this study the first design approach is adopted and is carried out as follows:

a) The diameters of the first-order* sewers which emanate from inlet catch basins (e.g., Sewers 1 through 5 in the network shown in Fig. 25a) are initially estimated by using the Darcy-Weisbach equation for steady full pipe flow

$$D = 0.48 \left(f \frac{Q_p^2}{S_o}\right)^{1/5} \tag{34}$$

in which D is the diameter, Q_p is the peak discharge of the prescribed design inflow hydrograph at the upstream end of the sewer, S_o is the bottom slope of the sewer, and f is the Weisbach resistance coefficient, determined as described in Sec. VI-3.

*The sewer ordering adopted in this study is the same as that proposed by Strahler for streams.

b) With the diameter of a sewer computed from Eq. 34, the maximum depth at the upstream end of the sewer would be approximately 0.8D due to the specific nature of the rating curve for circular pipes if the flow were steady and uniform. However, the unsteadiness and non-uniformity of the flow usually cause a further reduction of the maximum depth of the flow. Therefore, the diameter computed by using Eq. 34 is replaced by the nearest smaller commercially available pipe diameter rather than a larger one.

c) The design inflow hydrographs at the inlets are routed through the first-order sewers using linear kinematic-wave approximation by assuming a constant propagation velocity equal to that for the half-full, steady, uniform flow. Thus, the peak inflows entering into the junction at the downstream end of the first-order sewers are computed, and from the sum of these inflows estimate of the peak inflow into the outflowing sewer from the junction is obtained.

d) Using this estimated peak inflow for the outflowing sewer from the junction, a first approximation for its diameter can be calculated by using Eq. 34.

e) The Y-segment with its sewer sizes so determined is now ready for routing of the known inflow hydrographs.

f) The numerical solution of the St. Venant equations is obtained for the Y-segment with the known downstream boundary condition, or with the forward differences as a substitute if the downstream boundary condition is unknown. If the maximum depth of flow in the sewers of the Y-segment does not fall within the range between 0.8D and D, the next larger or smaller commercially available pipe diameter is selected, and the numerical solution in this step is repeated. If the maximum flow depth cannot be restricted within 0.8D to D because

of the discrete sizes of the commercially available pipes, then the available commercial size which gives a depth nearest but smaller than 0.8D is used.

g) Steps (a) to (f) are repeated for all other upstream segments (e.g., the three Y-segments shown in Fig. 25b).

h) With the sewer diameters and junction inflow hydrographs computed for all the upstream Y-segments, the method of overlapping segments is applied. The inflow sewers of the upstream Y-segments are trimmed. The junctions of these segments are treated as the inlets of the pruned network. The outflowing sewers of the previous upstream segments for which the diameter has been computed approximately in Step (f) become the inflowing sewers of the new Y-segment. The outflow hydrographs from the junctions of the previous Y-segments become the inflow hydrographs for the new segment.

i) Steps (d) to (h) are repeated until the diameters of all the sewers except the last one are computed.

j) The network is now reduced to the last Y-segment as shown in Fig. 25e. The diameters of the sewers in this last segment can then be determined by exactly the same procedure, Steps (d) to (f), except that in Step (f) the downstream boundary condition is known.

The computational details of the ISS Model have been presented elsewhere (Sevuk, 1973). A summary flow chart of the computational logic is shown in Fig. 26. The computer program is written in PL/1 language, consisting of about 3000 statements and it uses approximately 220K segment of the memory of the IBM 360/75 system at the University of Illinois at Urbana-Champaign. The computer system specific instructions of the program are kept to a minimum, and hence the program can be executed with minor modifications on any other

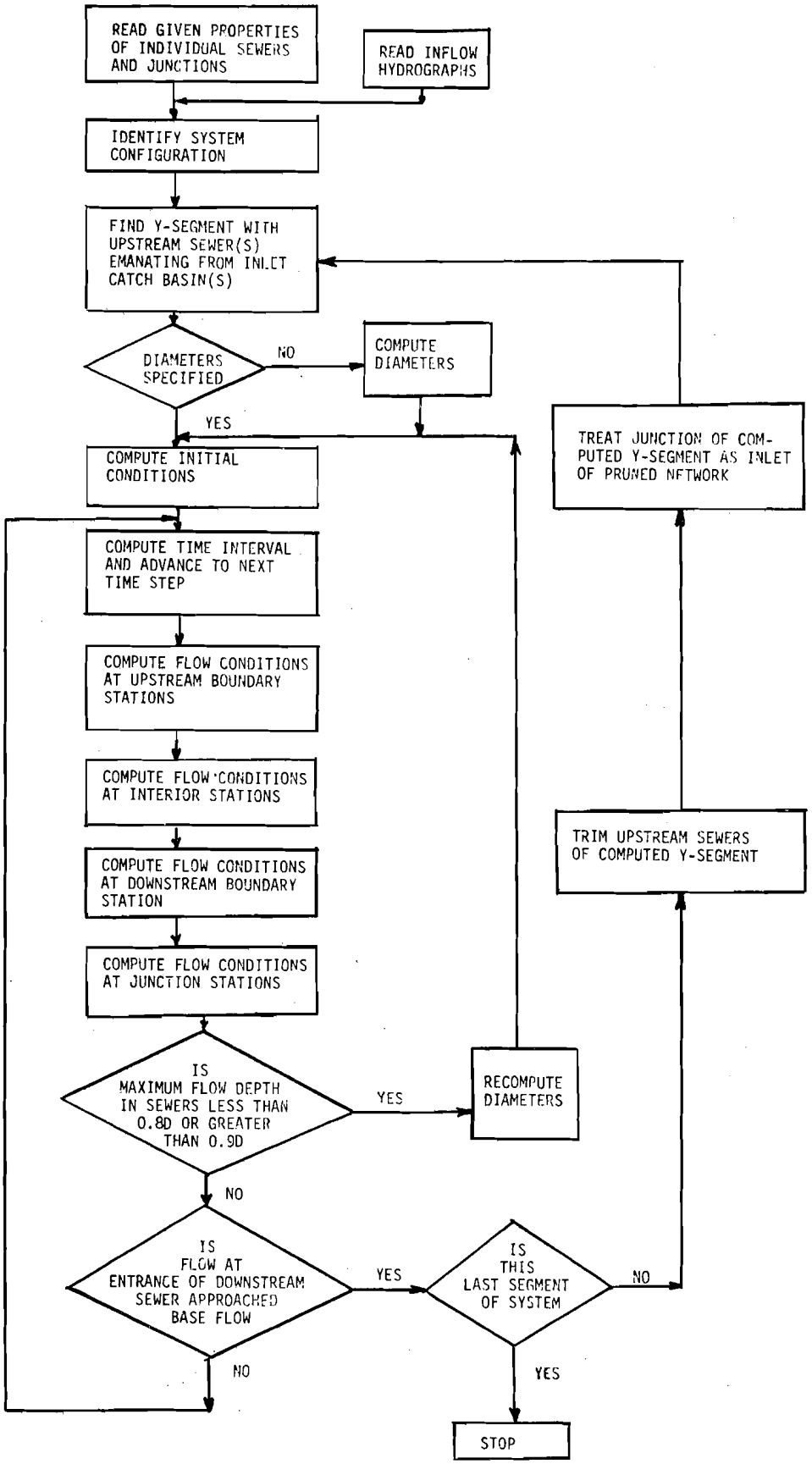

FIG. 26. SUMMARY FLOW CHART OF COMPUTER PROGRAM FOR ISS MODEL

large computer system having disk facilities. A user's manual for the ISS Model has been prepared for easy adoption in engineering practices (Sevuk et al, 1973).

VII. APPLICATION OF ISS MODEL TO EXAMPLE SEWER SYSTEM

VII-1. Description of Example Sewer System

The reliability of a mathematical simulation model to a physical phenomenon can be assessed, in an absolute sense, only through experimental verification. In this study such a verification is not possible at present due to lack of field data and the cost and instrumentation difficulties involved in laboratory modeling.. However, as discussed in Chapter III, it has been verified with experimental data that the mathematical model can reliably predict the unsteady flow in a single sewer. Therefore, an extension of the mathematical prediction of unsteady flow to a sewer network system is in the order to illustrate the effects of flow unsteadiness in sewers and junctions.

The sewer system adopted as an example in this chapter has known configuration and sewer sizes, and hence the example is typical for flow prediction and operation for existing systems. Since the size of the sewers are known, their diameters are not computed in the numerical processes. As discussed in Chapter VI, the ISS Model can also be used for design purpose in sizing the sewer diameters. The model has been applied to the design of a number of small hypothetical sewer systems. However, for the sake of brevity, the results are not presented here.

The layout of the sewer system adopted as an example in this chapter is shown schematically in Fig. 27. The system has a tree-type configuration consisting of seven networks each of which has four inlets and seven sewers with the exception of Network 7 which has only six sewers. The networks are of different physical characteristics in order to illustrate the differences in their respective responses to inflows. The flood inputs at the 28 inlets and directly at one junction are conveyed through the 48 sewers of the networks to the main line, and then through the 6 main sewers to the outlet of the system. The physical characteristics of the sewers are listed in Table 7.

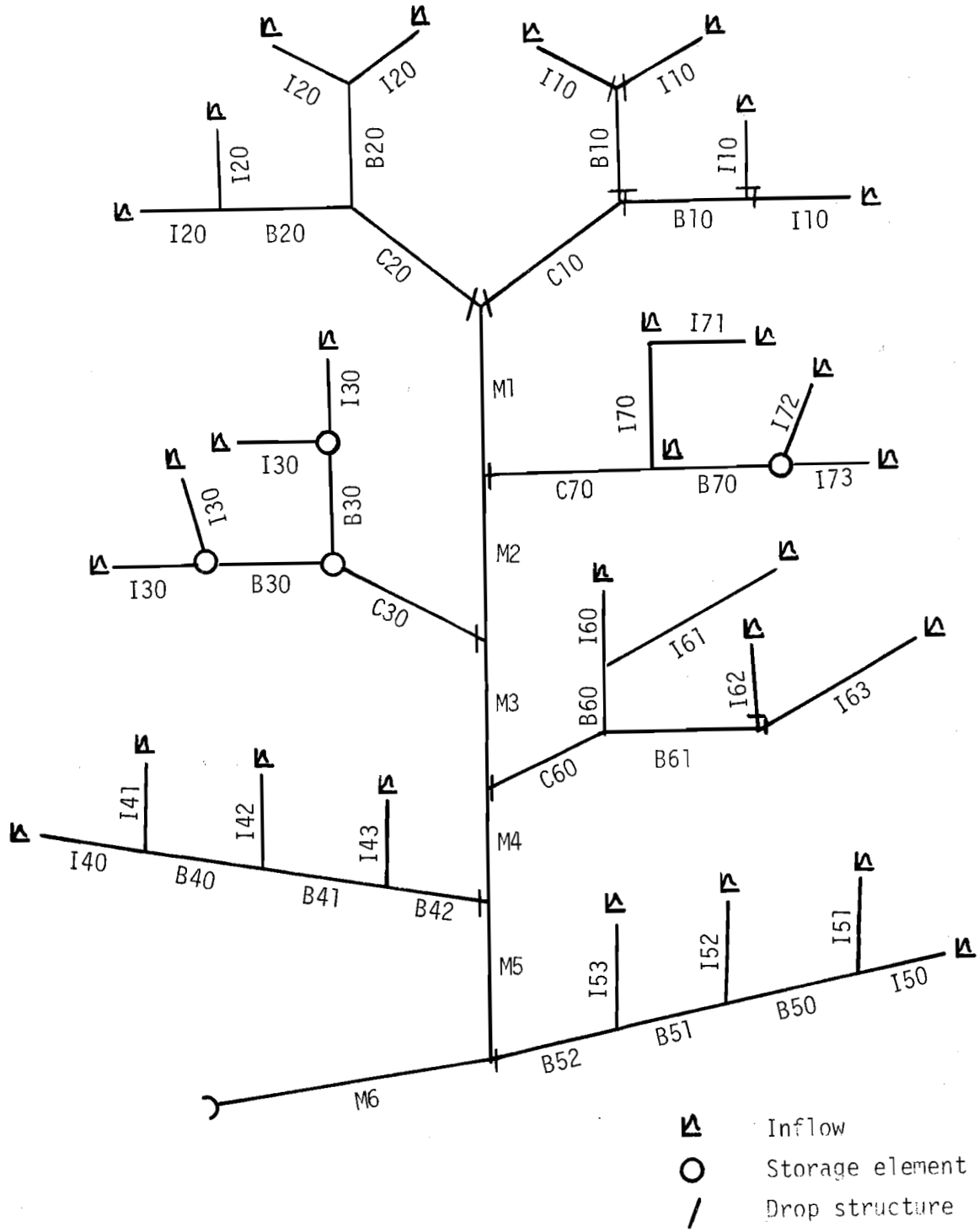

FIG. 27. EXAMPLE SEWER SYSTEM

TABLE 7. - PHYSICAL CHARACTERISTICS OF SEWERS ANALYZED

Sewer	Length L (ft)	Slope S_o (10^{-4})	Diameter D (ft)	Roughness k (10^{-3} ft)	Downstream Drop Z (ft)
I10	1000	12	2.5	10	3
I20	1000	12	2.5	10	
I30	1000	12	2.5	10	
I40	2000	10	2.5	10	
I41	1000	10	2.5	10	
I42	1000	10	2.5	10	
I43	1000	10	2.5	10	
I50	2000	10	2.5	10	
I51	1000	10	2.5	10	
I52	1000	10	2.5	10	
I53	1000	10	2.5	10	
I60	750	10	2.5	7	
I61	1500	10	2.5	7	
I62	750	10	2.5	7	3
I63	1500	10	2.5	7	3
I70	1200	8	3.0	8	
I71	750	10	3.0	10	
I72	750	8	3.0	5	
I73	750	10	3.0	10	
B10	1400	10	3.0	10	3
B20	1400	10	3.0	10	
B30	1400	10	3.0	10	
B40	2000	12	3.0	10	
B41	2000	12	3.5	10	
B42	2000	12	4.0	10	4
B50	2000	12	3.0	10	
B51	2000	12	3.5	10	
B52	2000	12	4.0	10	
B60	1150	8	3.0	7	
B61	1500	8	3.0	7	
B70	1200	10	3.5	6	
C10	2000	8	4.0	10	4
C20	2000	8	4.0	10	4
C30	2000	8	4.0	10	4
C60	1800	8	3.5	6	4
C70	1500	100	3.5	10	4
M1	2000	8	5.0	10	
M2	1800	12	6.0	10	
M3	2000	10	6.0	10	
M4	2000	8	7.0	10	
M5	2000	8	7.0	10	
M6	2200	8	7.0	10	4

The sewers in the networks are identified by a letter and two numerals. The letters I, B, and C represent respectively the first, second, and third order sewers. The first (left) numeral identifies the network, and the second (right) numeral differentiates those sewers having the same order but different physical characteristics in a network. For example, B41 represents the second-order sewer in Network 4, which has different physical characteristics from B40 or B42. The main sewers are identified by the letter M followed by a number representing their relative location along the mainline.

Networks 1, 2, and 3 are identical in physical as well as input characteristics but having different junction properties. Each of these three networks is symmetric in layout and hence identical sewers bear the same identification code; e.g., the four I20 sewers in Network 2. Networks 4 and 5 are physically identical but receiving different inflows. At the downstream end of each network where it joins the main sewers a drop is assumed to exist. This is to ensure that for the range of flow considered each network acts independently and is free from the backwater effects from the main sewers or other networks and consequently the factors affecting sewer runoffs can be studied and compared individually.

VII-2. Presentation and Interpretation of Results

Hypothetical flood waves entering through the 28 inlets and a junction have been routed through the example sewer system (Fig. 27) by using the ISS Model. The input flood-wave hydrographs are of triangular shape above a baseflow which has a constant discharge ranging from 1 to 3 cfs. The peak inflow rate of the flood ranges from 15 to 25 cfs, and the duration ranges from 12 to 24 min. For the conditions tested, due to the flat slope of all the sewers in the system except that of Sewer C70, the flows in these sewers are in subcritical regime. These mild slopes are selected purposely in order to investigate the mutual interaction (backwater effects) of the flows at

various junctions throughout the networks and along the main sewers. On the other hand, each of the networks acts independently from others permitting separated analysis and comparison for each network.

(A) Networks 1, 2, and 3.

As described in Sec. VII-1, Networks 1, 2 and 3 have identical layout of the first, second and third order sewers as shown in Fig. 27 and Table 7. They have, however, different junction characteristics. In Network 1, a drop of 3 ft is specified at the downstream end of each sewer and the sewers are linked by point-type junctions so that for the range of flow conditions considered the flows in all the sewers are cascading into the storageless junctions free from backwater effects. In Network 2, the joining sewers are linked by a point-type junction with a common invert elevation, and hence the flow in each of the sewers experiences the backwater effect of the junction. In Network 3, the joining sewers are linked by a reservoir-type junction of 500 sq ft cross-sectional area and with a common invert elevation. In this case the flow in each sewer is subject to both the backwater and storage effects of the junction.

Identical and concurring inflow hydrographs at the inlets are routed through each of these three networks. The results are shown in Figs. 28, 29 and 30 in the form of discharge hydrograph and velocity and depth graphs at the entrance to the first, second and third order sewers of the networks. The maximum values of discharge, velocity and depth, and their times of occurrence, being of primary importance in design and operation, are also listed in Table 8.

As shown in Figs. 28, 29 and 30, each of the discharge hydrographs and hence the velocity and depth graphs has a single peak. This is due to the propagation of identical flood waves through identical sewers upstream from each junction in each of the symmetric networks. An inspection of these single-peak graphs indicates the existence of a loop-type discharge rating curve. At a given location in a sewer, the same discharge occurs at a smaller depth and

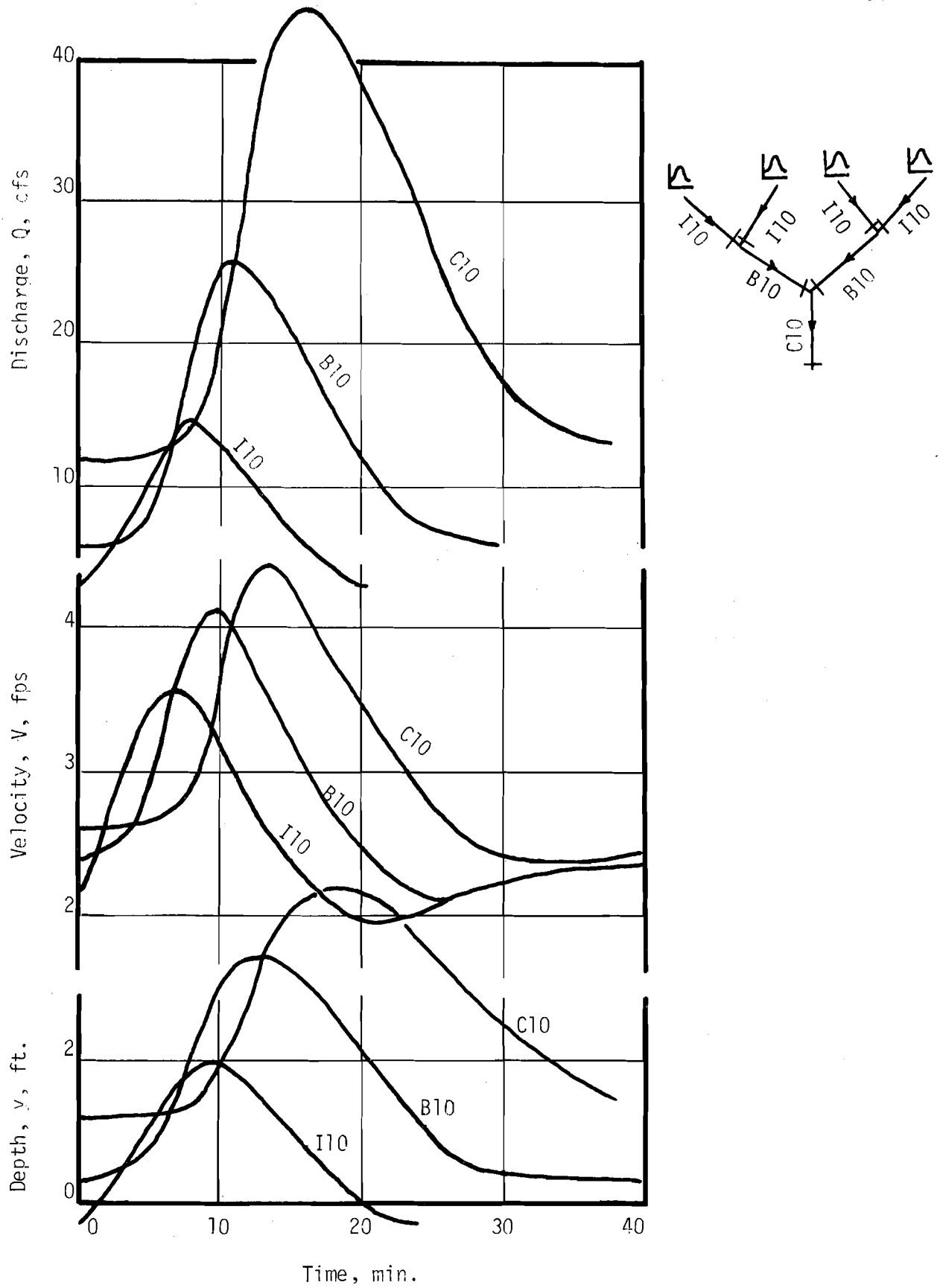

FIG. 28. FLOW AT ENTRANCE OF SEWERS IN NETWORK 1

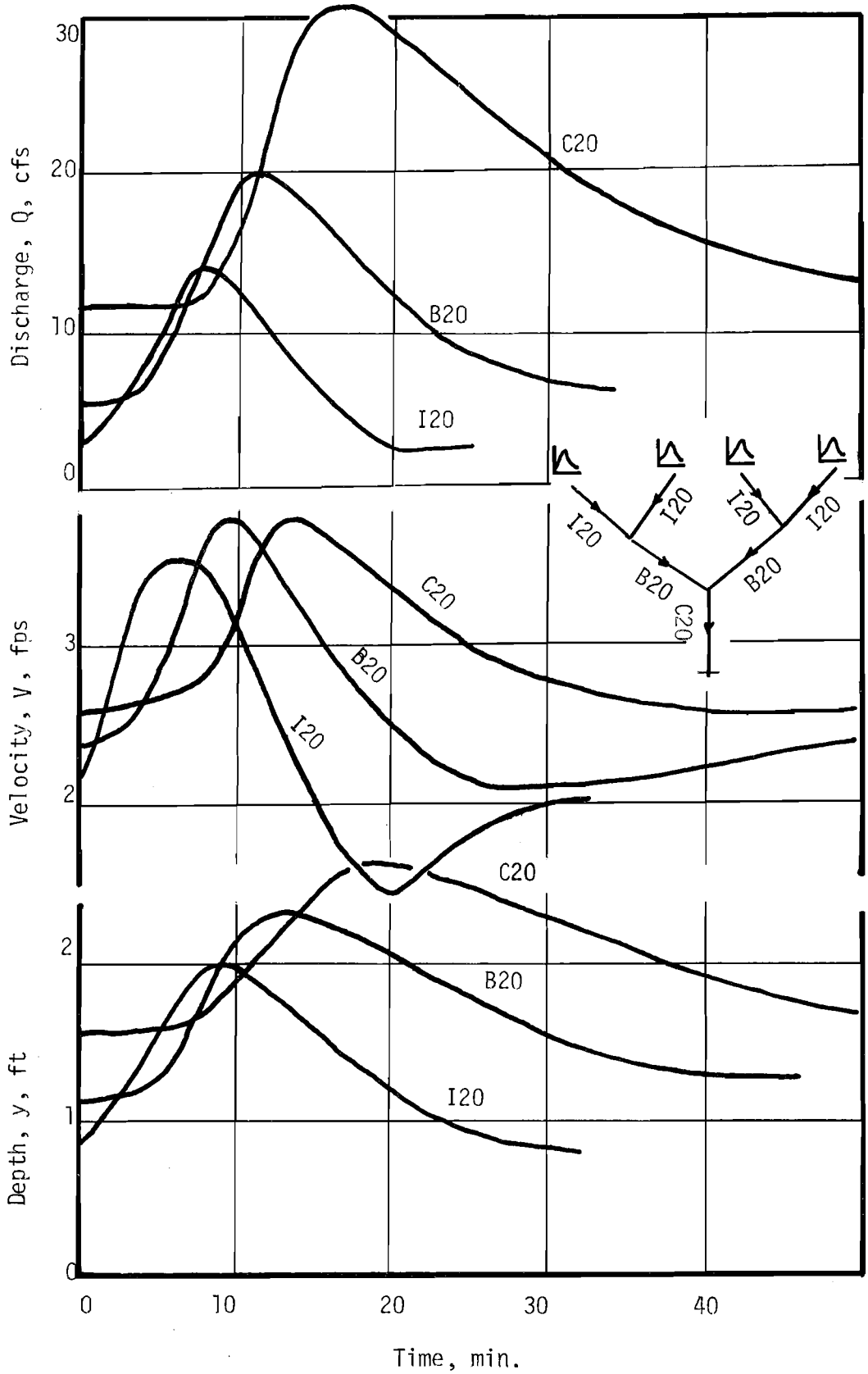

FIG. 29. FLOW AT ENTRANCE OF SEWERS IN NETWORK 2

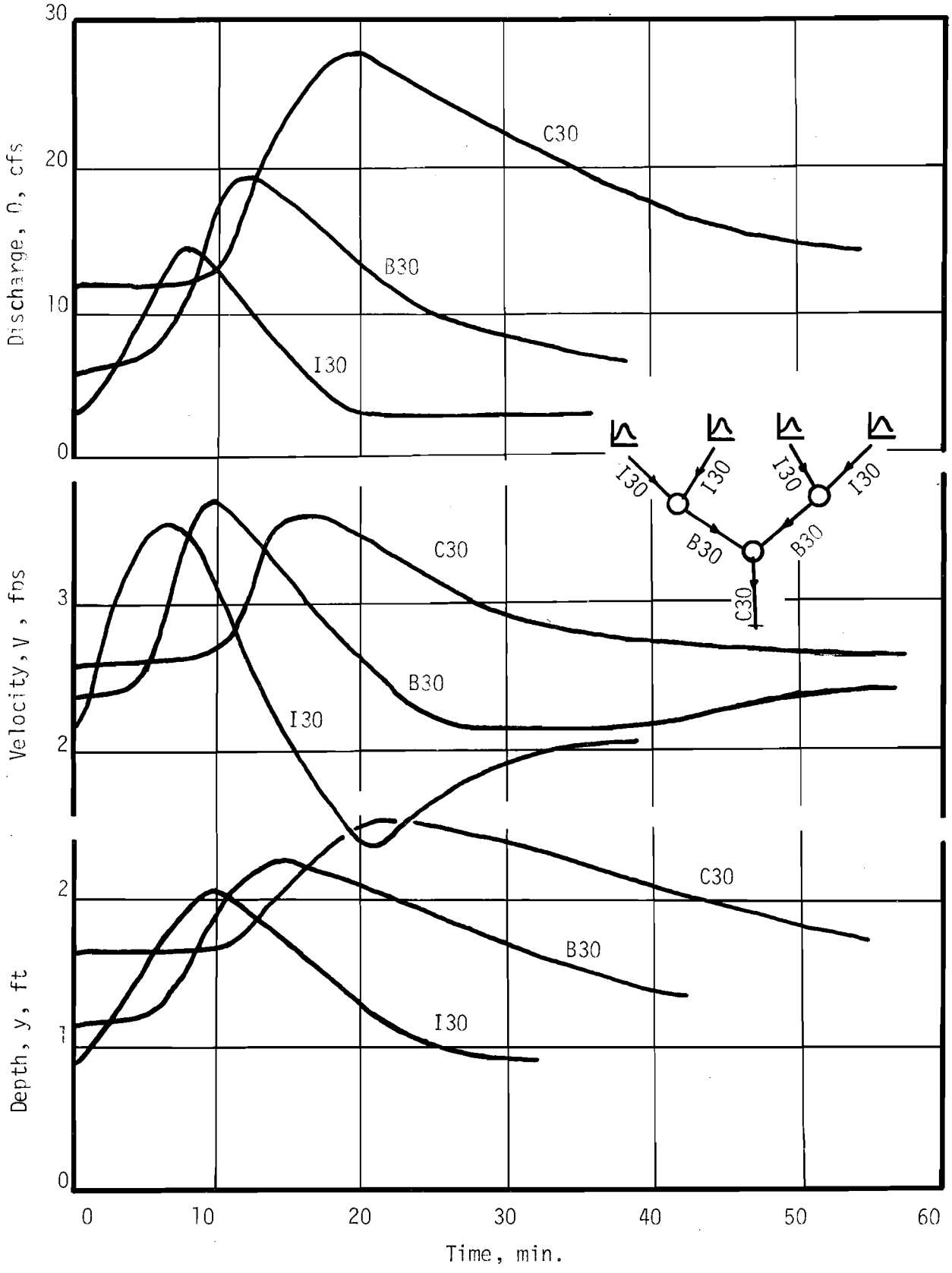

FIG. 30. FLOW AT ENTRANCE OF SEWERS IN NETWORK 3

higher velocity during the rising part than during the recession part of the discharge hydrographs. Furthermore, maximum values of velocity, discharge and depth occur, following that order, at different times.

A comparison of the flow conditions at the corresponding points of Networks 1 and 2 demonstrates the relative importance of backwater effects in storm sewer networks. At the upstream end of the first-order sewers, i.e., at the entrances of Sewers I10 and I20, the same flow conditions prevail for approximately first ten minutes for the inflow hydrographs tested. After that the flow at the entrance of I20 starts to experience the backwater effect of the junction. Thus, at a given instant for the same rate of inflow, lower velocity and higher depth are observed at the entrance of I20 than at that of I10. As would be expected, flood waves in Network 1, being free from backwater effects of the junctions, propagate faster and experience less attenuation than those in Network 2. Therefore, as indicated in Table 8, considerably higher values of maximum discharge, velocity and depth occur at earlier times at the entrance of Sewers B10 and C10 as compared to those at B20 and C20.

The increasing rate of attenuation due to backwater is, of course, accompanied by an increasing rate of dispersion of the flood waves. Thus, as shown in Figs. 28 and 29, the discharge hydrographs and hence the velocity and depth graphs in Network 2 have longer runoff durations than the corresponding ones in Network 1. This increased duration is particularly pronounced at the recession part of the graphs for Network 2 which represents the period during which the backwater detention storage in the sewers is gradually drained away.

A similar comparison of flow conditions between the corresponding points of Networks 3 and 2 indicates the different effects of reservoir and point-type junctions on the propagation of flood waves. As can be seen from Figs. 29 and 30, at the entrance to the first-order sewers, I20 and I30, flow

TABLE 8. - MAXIMUM VALUES OF FLOW AND THEIR TIME OF OCCURRENCE AT ENTRANCE OF SEWERS FOR NETWORKS 1, 2, and 3

Sewer	Discharge		Velocity		Depth	
	Max. value (cfs)	Time to peak (sec)	Max. value (fps)	Time to peak (sec)	Max. value (ft)	Time to peak (sec)
I10	15.0	480	3.60	420	2.03	600
I20	15.0	480	3.60	420	2.03	600
I30	15.0	480	3.60	420	2.03	600
B10	26.2	660	4.18	570	2.76	750
B20	20.8	690	3.87	580	2.33	800
B30	19.3	740	3.75	590	2.23	850
C10	43.8	910	4.50	780	3.28	1100
C20	31.0	970	3.82	840	2.65	1140
C30	28.0	1160	3.62	940	2.52	1260

conditions are practically identical. With identical inflow hydrographs at a given instant, the flow at the entrance of I30 occurs at slightly lower velocity and higher depth as compared to that at the entrance of I20. This is due to the fact that for flows having low values of Froude number the energy compatibility condition, Eq. 32, for a reservoir junction and the kinematic compatibility condition, Eq. 28, for a point junction do not differ significantly, and hence the flows at the entrance of I20 and I30 experience similar backwater effects from point- and reservoir-type junctions, respectively.

As would be expected, flood waves being subject to the reservoir action of junctions in Network 3 propagate at slower rates and experience greater attenuation and dispersion than those in Network 2. Consequently, the values of maximum discharge, velocity and depth at the entrance of Sewers B30 and C30 are smaller and occurring at later times than those of Sewers B20 and C20, as indicated in Table 8.

In order to reveal the different detention storage mechanisms and to assess the reliability of the mathematical simulation, the amount of detention storage in Networks 1, 2 and 3 is analyzed. For the sake of simplicity, the third-order sewers are excluded from the analysis and the amount of detention storage is calculated as the difference between the cumulative inflow at the upstream end of the first-order sewers and the cumulative inflow at the upstream end of the third-order sewers, C10, C20 and C30, of Networks 1, 2 and 3, respectively. The computed detention storages at various instants within the networks are shown in Fig. 31 in a nondimensional form as the percentage of the total volume of the flood waves above the baseflow.

As expected, Fig. 31 indicates that the detention storage in Network 3 is greater than that in Network 2, which is in turn greater than that in Network 1. The difference in the detention storages between Network 2 and 1

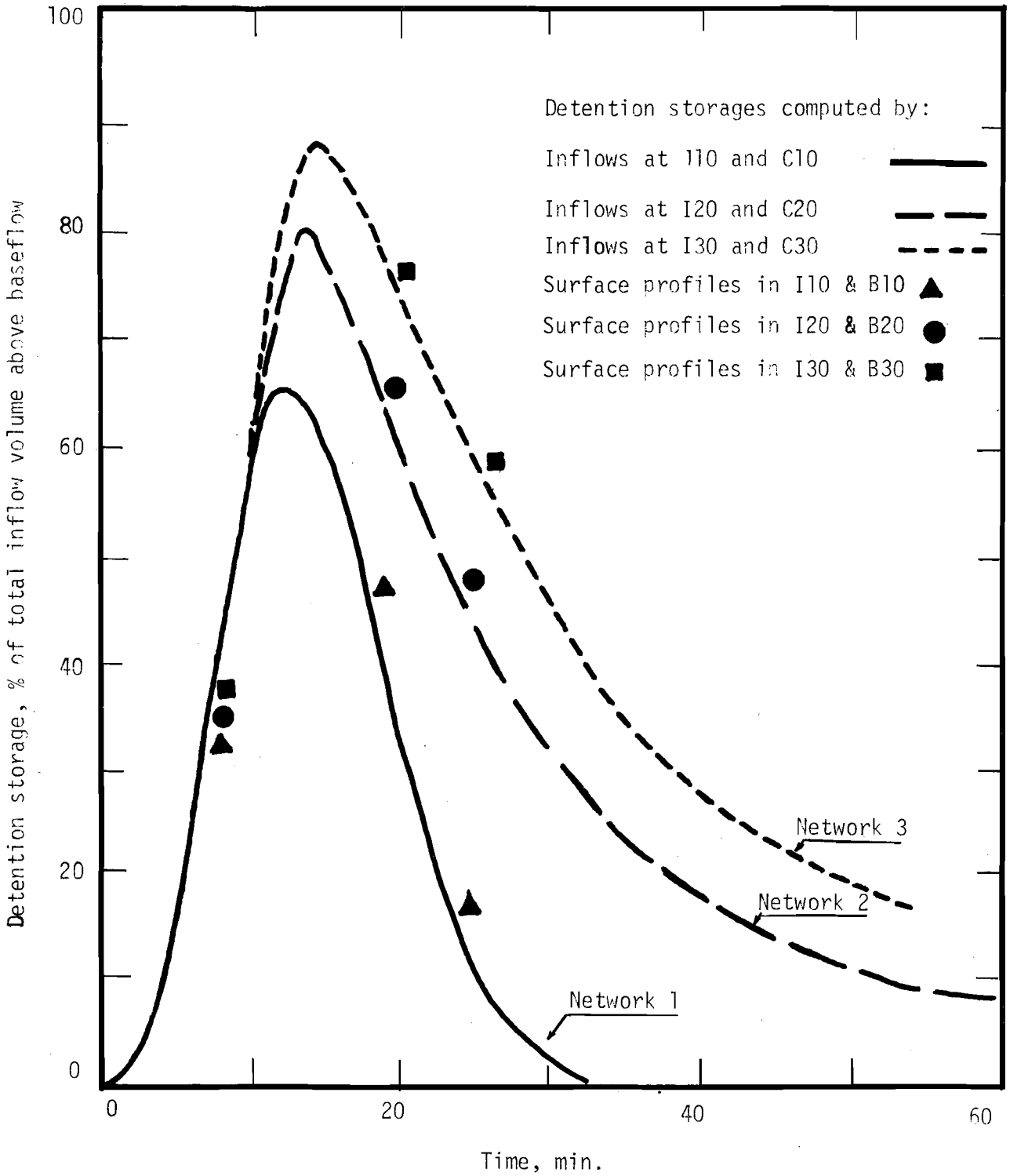

FIG. 31. TIME VARIATION OF DETENTION STORAGES IN NETWORKS 1, 2, AND 3

represents the so called "backwater storage." For a simple case of steady nonuniform subcritical flow, this storage would be equal to the volume of water between M1 and M2 type water surface profiles in a storm sewer. In the present case of unsteady nonuniform flow it is difficult to give such a simple quantitative description for backwater storage. For as will be discussed later, its magnitude is controlled by various mechanisms including the possibility of reverse flow through the downstream end of a sewer.

The difference in detention storages between Networks 3 and 2, on the other hand, represents mainly the amount of water stored in the junctions of Network 3. It should be noted here that, the 500-sq ft cross sectional area for each of the junctions in Network 3 is much too big for prototype storm sewer junctions or manholes. Therefore, the magnitude of the junction storage which is approximately one tenth of the total flood volume as shown in Fig. 31 is only for the purpose of illustration and is not representative of the storage capability of storm sewer junctions and manholes.

In an effort to test the reliability of the mathematical simulations, the detention storages in the first- and second-order sewers and junctions of the three networks are also calculated from the computed water surface profiles at three instants as shown in Fig. 31. The difference between the amount of detention storages computed by the two procedures at the same instant is an indication of the error in the conservation of volume. This error, as can be seen from Fig. 31, is found to be less than 0.5% of the total volume of the inflow above baseflow, i.e., the volume of the flood, in all the networks, and hence the results appeared to be reliable.

(B) Networks 4 and 5.

Networks 4 and 5 are identical in geometrical characteristics as shown in Fig. 27 and Table 7. However, they receive identical inflow hydrographs at different times at their inlets. In Network 4 identical flood

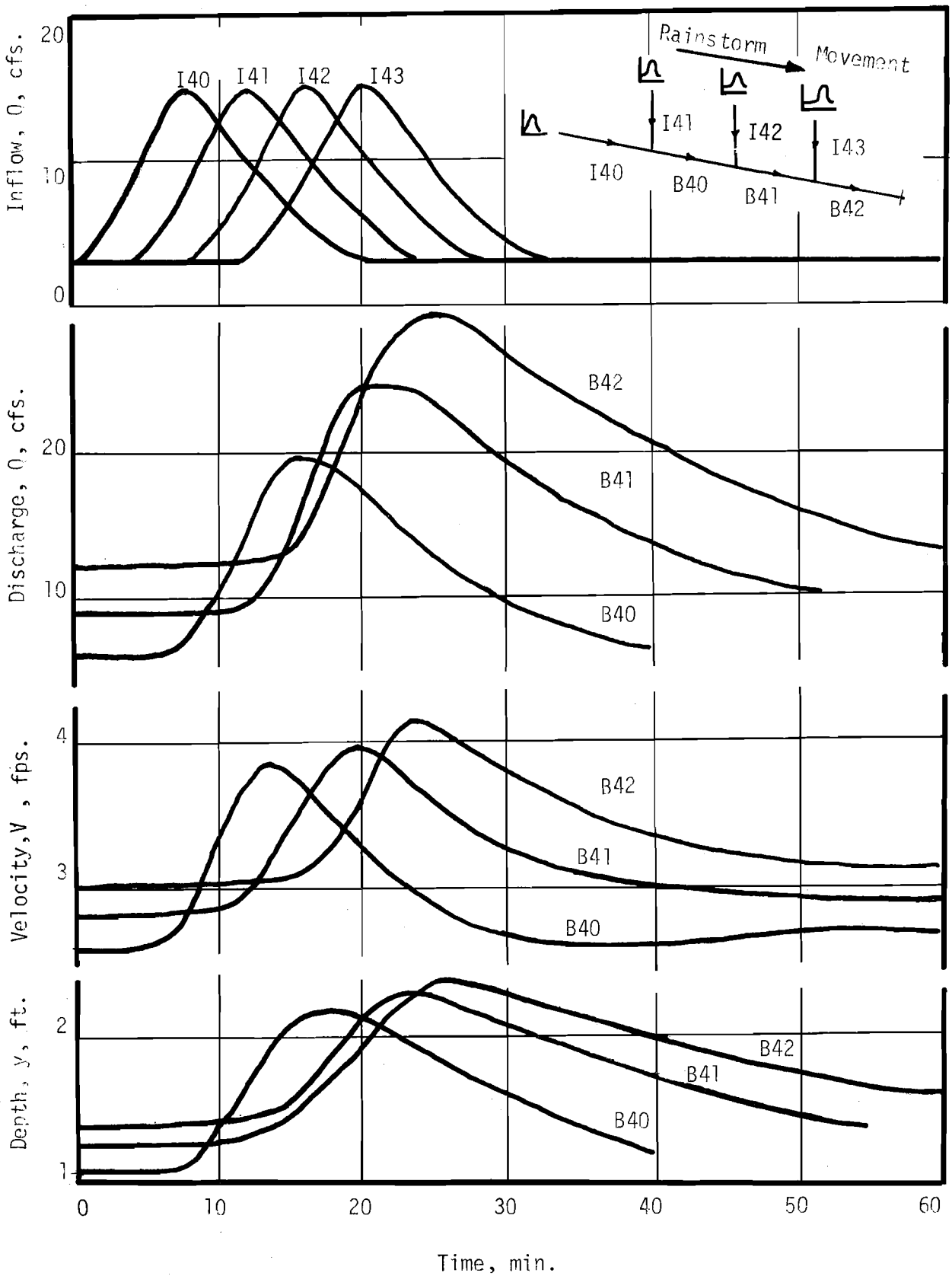

FIG. 32. FLOW AT ENTRANCE OF SEWERS IN NETWORK 4

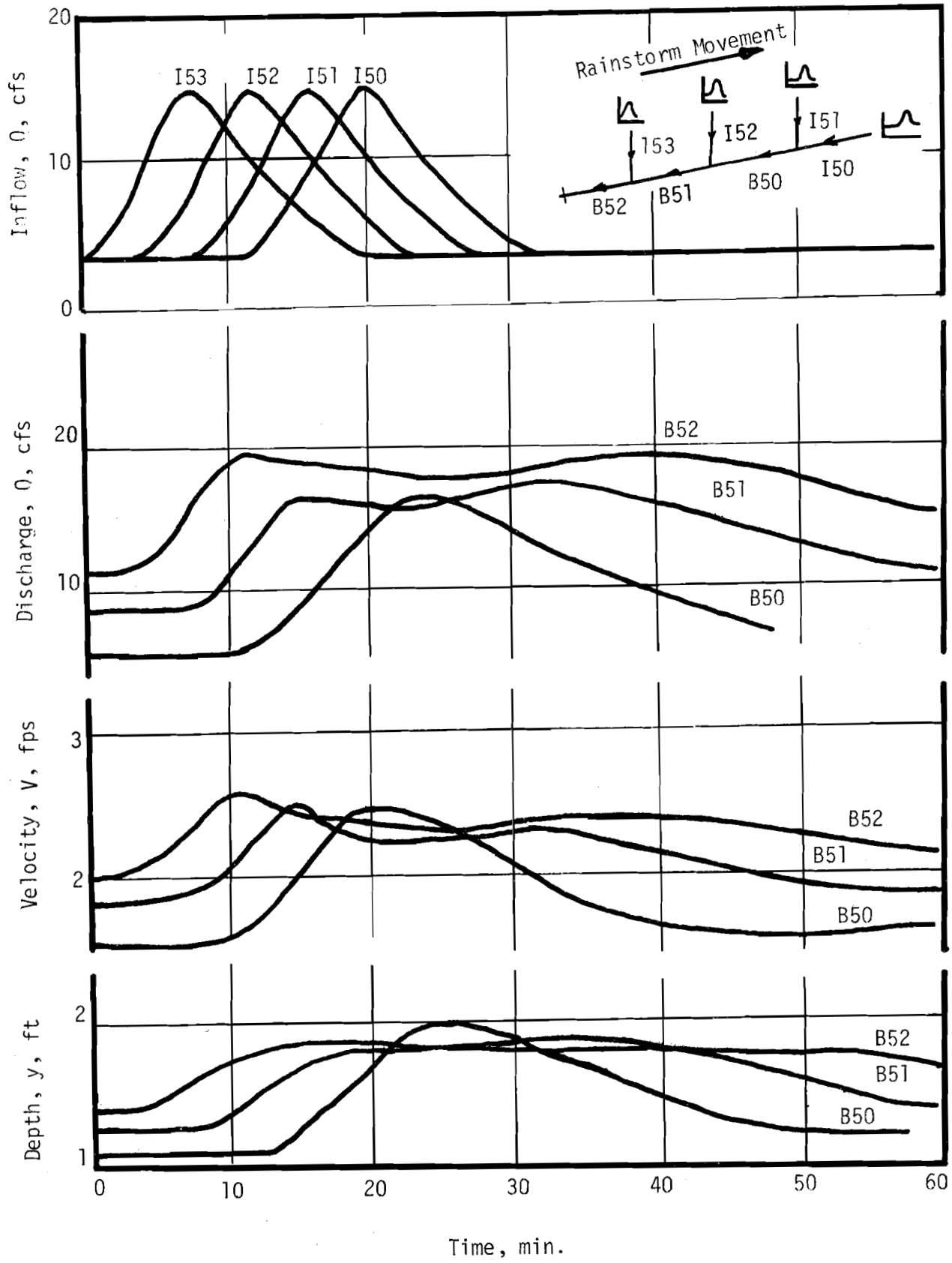

FIG. 33. FLOW AT ENTRANCE OF SEWERS IN NETWORK 5

inflows enter successively into Sewers I40, I41, I42 and I43, at t = 0, 4, 8 and 12 min, respectively, representing an hypothetical rainstorm movement towards downstream along the general direction of the network as shown in Fig. 32. In Network 5, contrarily, the same inflows enter successively into Sewers I53, I52, I51 and I50 at t = 0, 4, 8 and 12 min, respectively, representing a rainstorm moving towards upstream as shown in Fig. 33.

Computed flow depth, velocity, and discharge at the entrance of the second-order sewers of Networks 4 and 5 are given in Figs. 32 and 33, respectively. A comparison of the flow conditions at the corresponding locations in the two networks reveals the importance of the effect of time lag of the inflow hydrographs at the inlets. In Network 4, flood waves from the upstream sewers arrive at the junctions at almost the same times, consequently the cumulative effect of the flows results in short-duration and single-peak discharge, velocity, and depth graphs at the entrance of Sewers B40, B41 and B42. In Network 5, contrarily, flood waves arrive at the junctions at different delayed times yielding long-duration and low-peak discharge, velocity and depth graphs at the entrance of B50, B51 and B53. The result of this comparison indicates that from sewer design viewpoint a downstream moving rainstorm is more important than an upstream moving one as the former gives higher maximum values for depth, velocity and discharge.

(C) Network 6.

Network 6 is an asymmetric network in which sewers of the same order joining to the same junction have different lengths but are otherwise identical, as shown in Fig. 27 and Table 7. The network receives identical flood waves first through the inlets of I60 and I62 at t = 0 and then with a time lag of 10 min through the inlets of I61 and I63. These inflow flood waves together with the computed flow depth, velocity and discharge at the entrance to the second- and third-order sewers of the network are presented in Fig. 34.

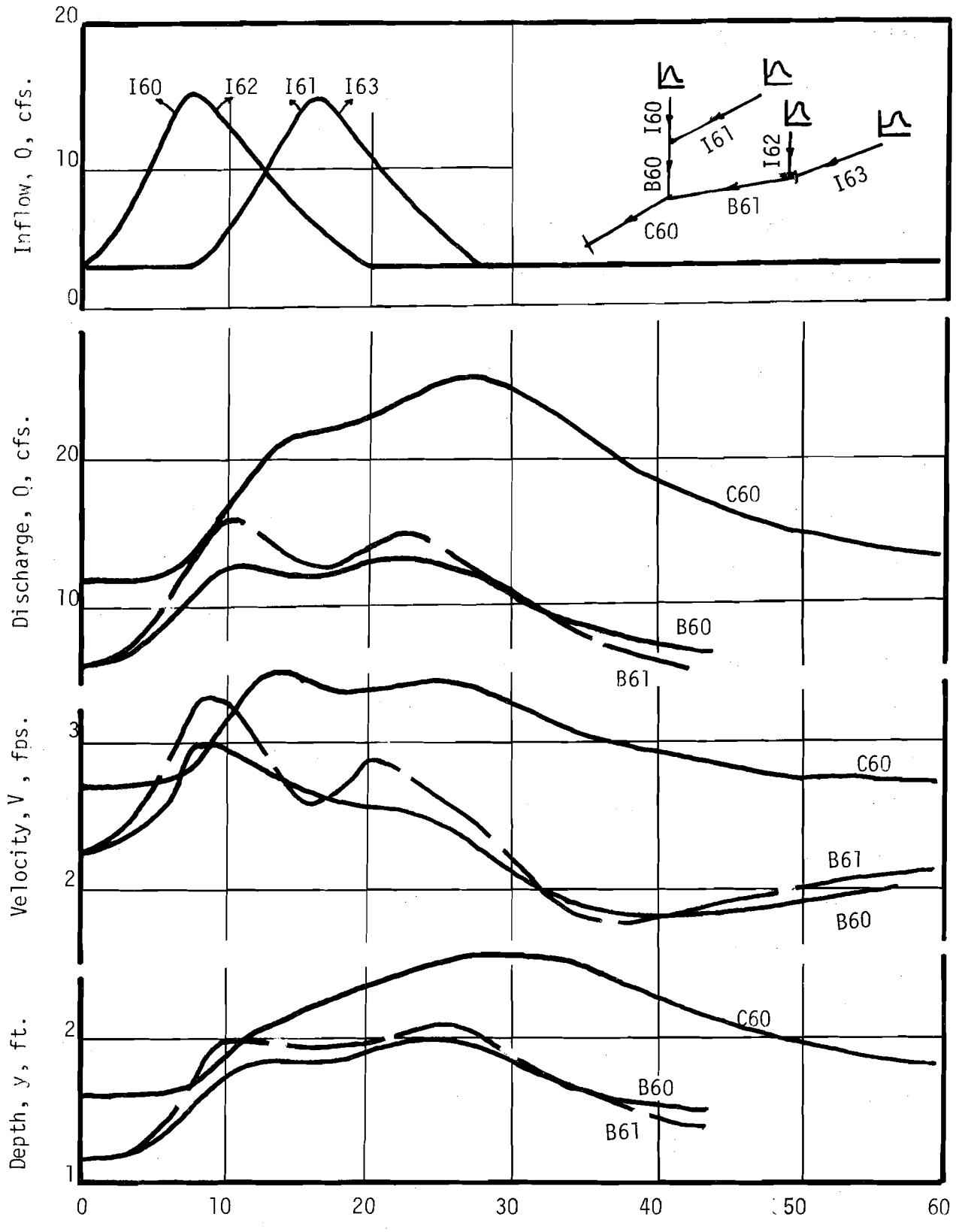

FIG. 34. FLOW AT ENTRANCE OF SEWERS IN NETWORK 6

As expected, the flood waves in the shorter sewers I60 and I62 arrive at the second-order sewers B60 and B61 earlier than the delayed flood waves from the longer sewers I61 and I63. Thus as shown in Fig. 34, the discharge hydrographs, and hence the velocity and depth graphs, at the entrance of Sewers B60 and B61 have double peaks. These double-peak flood waves then propagate through identical second-order sewers of different lengths, B60 and B61, and when they meet at their junction with Sewer C60, they yield an irregular shape inflow hydrograph and hence velocity and depth graphs at the entrance of Sewer C60.

The sequence of events in a "backwater cycle" at a sewer junction can be seen by studying the discharge, depth, and velocity graphs at the upstream and downstream ends of Sewers I60 and I61 (Fig. 35). The kinematic compatibility condition at the junction implies that the depths of flow at the exit of Sewers I60 and I61 are equal. However, the discharges and velocities at these points at a given instant are quite different (Fig. 35). As the earlier flood wave which is from the shorter sewer I60 arrives at the junction the water surface elevation there starts to rise and consequently the depth near the downstream end of Sewer I61 increases. Due to backwater effect the discharge and velocity around the downstream end of Sewer I61 decreases, and they both become negative for a short period, i.e., water flows towards upstream in the downstream part of Sewer I61. After the flood peak from Sewer I60 passes through the junction, the discharge and velocity near the downstream end of Sewer I61 begins to increase in response to an increasing water surface slope towards downstream in the sewer, and eventually return to positive values for draining of the detention storage. Both the discharge and velocity are further increased rapidly with the approaching of the flood wave from Sewer I61 to the junction, and the backwater effect now starts to influence the receding flow in Sewer I60. During the passage of

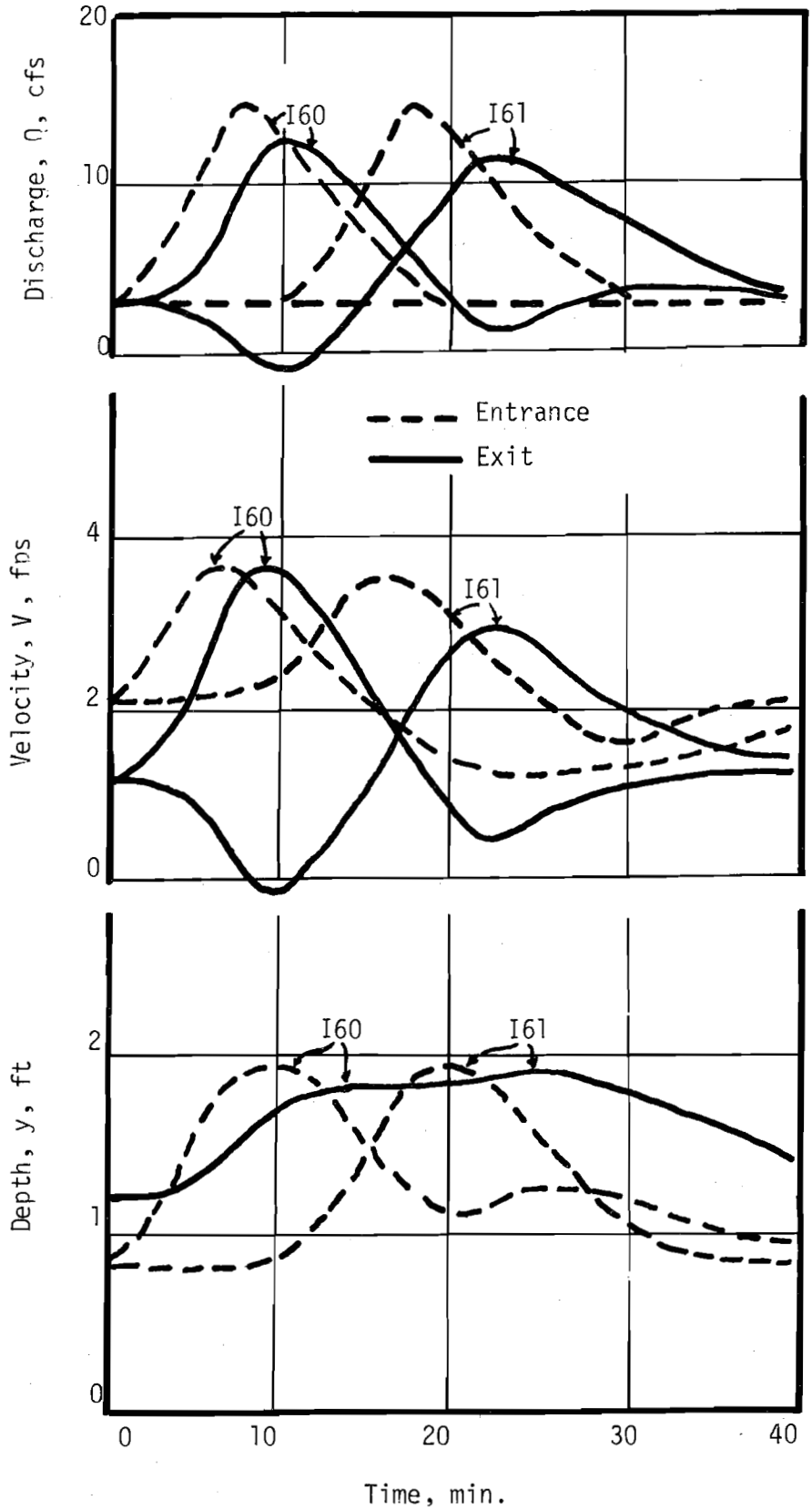

FIG. 35. FLOW AT ENTRANCE AND EXIT OF SEWERS I60 and I61

this second flood peak through the junction the discharge at the downstream end of Sewer I60 decreases temporarily below the rate of inflow at its entrance. Therefore, during this period, part of the inflow is temporarily retained within Sewer I60 as the so called backwater storage. After the second flood peak passes through the junction, the flow at the downstream end of Sewer I61 starts to recede, and the discharge and velocity at the downstream end of Sewer I60 increase. The backwater storage in the sewers is of practical importance in view of the recent attempts to use sewer conduits as a place for detention storage of rainstorm runoffs.

(D) Network 7.

Network 7 has an irregular layout which is most likely to be observed in real storm sewer systems. As shown in Fig. 27 and Table 7, each sewer in the network has different physical characteristics. Flood waves enter to the network at inlets of the first-order sewers I70, I71, I72, I73, as well as directly at the junction of the sewers I70, B70 and C70. These inflow flood waves together with the computed discharge, velocity, and depth at a few selected locations in the network are presented in Fig. 36.

The effects of direct inflows at the junctions of Sewers I70 and I71 and of Sewers I70, B70 and C70 can be seen from an inspection of the computed velocity, depth and discharge hydrographs. The inflow at the junction of Sewers I71 and I70 creates a backwater effect to the flow in Sewer I71, as clearly shown by the dips in the velocity and discharge at the exit of that sewer. Similarly, the inflow at the junction of Sewers I70, B70, and C70 creates backwater effects on the flows in Sewers I70 and B70, causing the velocity and discharge at the exit of these sewers to drop temporarily below the corresponding initial steady flow values.

The dip in the velocity graph at the entrance of Sewer I70 occurs at around t = 20 min, while the direct inflow at the junction of Sewers I70,

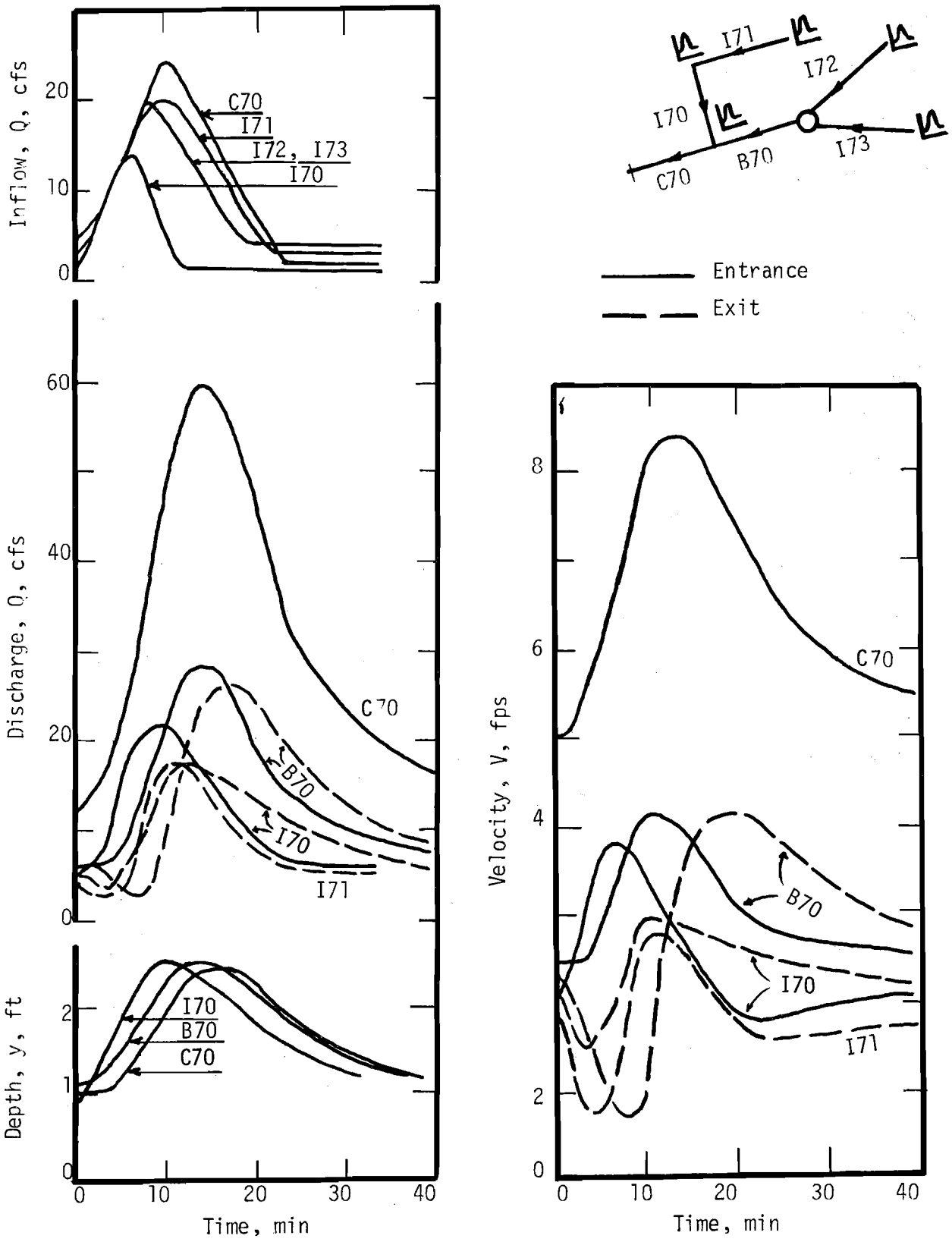

FIG. 36. FLOW AT SELECTED LOCATIONS IN NETWORK 7

B70, and C70 is receding, and the flood peak from Sewer B70 is passing through the junction. Therefore, this later backwater, which propagates up to the entrance of Sewer I70, is created by the flow in Sewer B70, rather than by the direct inflow at the junction of Sewers I70, B70, and C70.

The flow in Sewer C70 is supercritical with the values of Froude number ranging from 1.05 to 1.3. Hence, the flow in this sewer is controlled by the flow condition at its entrance.

Reliability of the computed flow conditions in Network 7 is checked by computing the error in volume conservation, as has been done for Networks 1, 2 and 3. The net inflow volume is computed as the difference of cumulative inflow (at the inlets of Sewers I70, I71, I72, I73 and at the junction upstream of Sewer C70) and the cumulative outflow (at the downstream end of Sewer C70) from the network. The detention storage in the network is calculated from the computed water surface profiles. The errors in the volume balance as indicated by the difference between the net inflow volume and the detention storage at t = 10, 20 and 40 min are found to be 0.5, 1.2 and 0.9 percent, respectively, of the total inflow volume above the base flow.

(E) Main-Sewer Line.

As shown in Fig. 27, the main line of the sewer system is formed by a series of six sewers. Three of the sewers, M1, M2, and M3, have different geometries and the remaining three, M4, M5, and M6 are identical (Table 7). The main-sewer line receives flood waves from the seven networks cascading through drops at their exits at six point-type junctions along the main-sewer line and it conveys the water to the outlet of the system where critical flow condition, i.e., a free fall, is assumed. The computed time variations of discharge and depth at the entrance of the main sewers and at the outlet of the system are shown in Fig. 37.

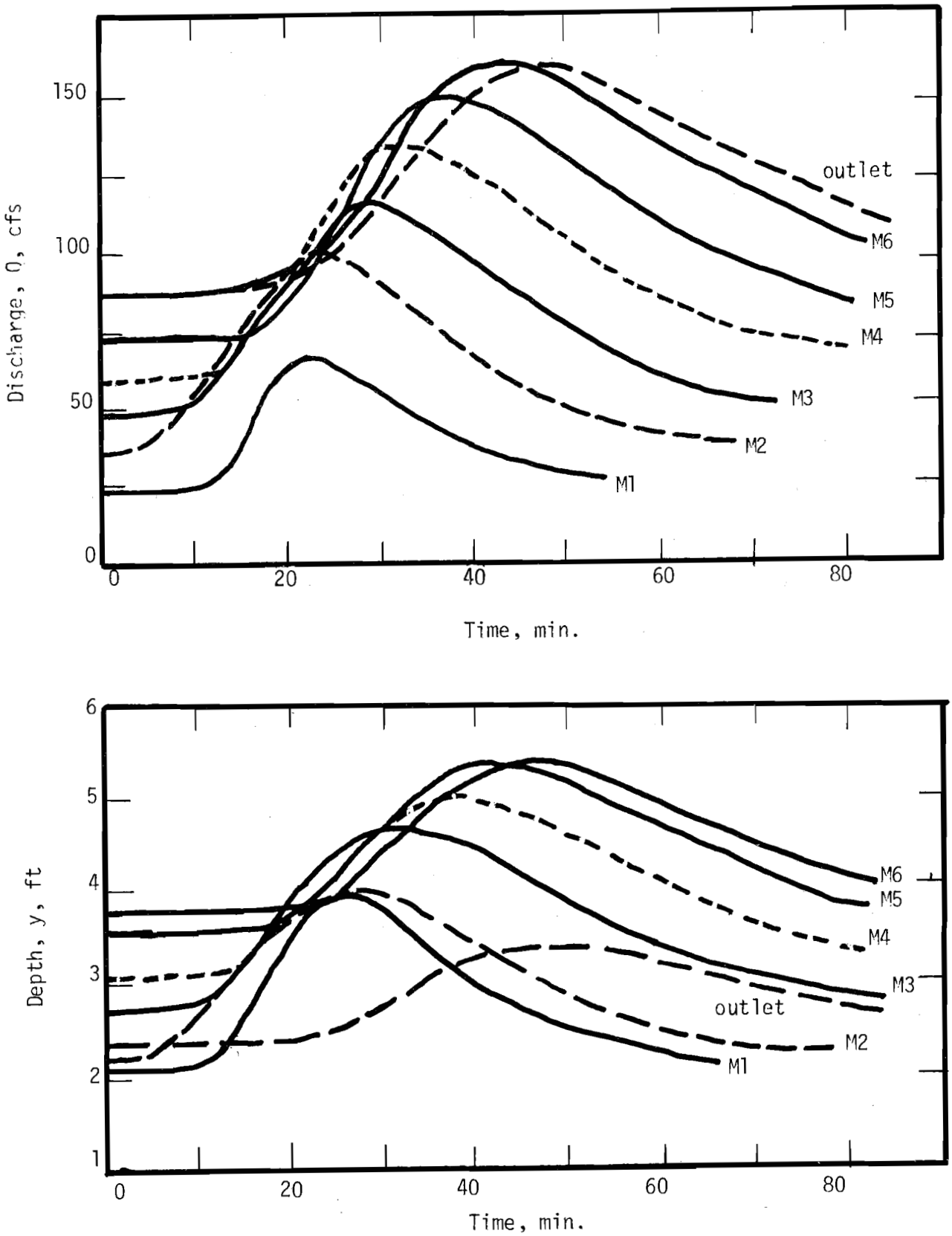

FIG. 37. FLOW AT ENTRANCE OF MAIN SEWERS

As shown in Fig. 37 both the peak flow and duration of the flood in the main sewers increase along the downstream direction. The discharge at the entrance of Sewer M1 is the sum of the outflows from Networks 1 and 2. This flow propagates through Sewer M1, joined by the outflow from Network 7, to give a longer duration hydrograph at the entrance of Sewer M2 with a higher peak discharge than that for M1. In a similar manner, the discharge hydrograph at the exit of M2 is joined by the outflow hydrograph of Network 3 at the entrance of M3, then propagates downstream and is joined successively by the outflows from Networks 6, 4, and 5 at the entrance of M4, M5, and M6, respectively. The flood wave then propagates through Sewer M6 and reaches to the outlet of the system with a slight attenuation, as shown in Fig. 37. The variations of flow depth with both time and space follow the variation of discharge, with the time of occurrence of maximum depth being preceded by that for the peak discharge at all the points along the main sewer line.

Backwater effects in the main sewers can be illustrated by studying the discharge, depth, and velocity graphs at the entrance and exit of Sewer M1. These graphs are presented in Fig. 38 together with the outflow hydrograph for Network 7, which joins to the downstream and of Sewer M1. As shown by the discharge graphs, the flood from Network 7 arrives early and cascades freely through a drop into the point-type junction, causing the water surface at the junction to rise as indicated by the depth graphs. The backwater effect in Sewer M1 due to this increase in depth at the junction is evidenced by a decrease in velocity as well as discharge at the downstream end of the sewer. This backwater effect prevails until the flood peak from Network 7 passes through the junction and a significant amount of water is temporarily detented in Sewer M1. The backwater effect in Sewer M1 diminishes as the flood entering at the upstream end of Sewer M1 passes through the junction, while the flow from Network 7 is receding.

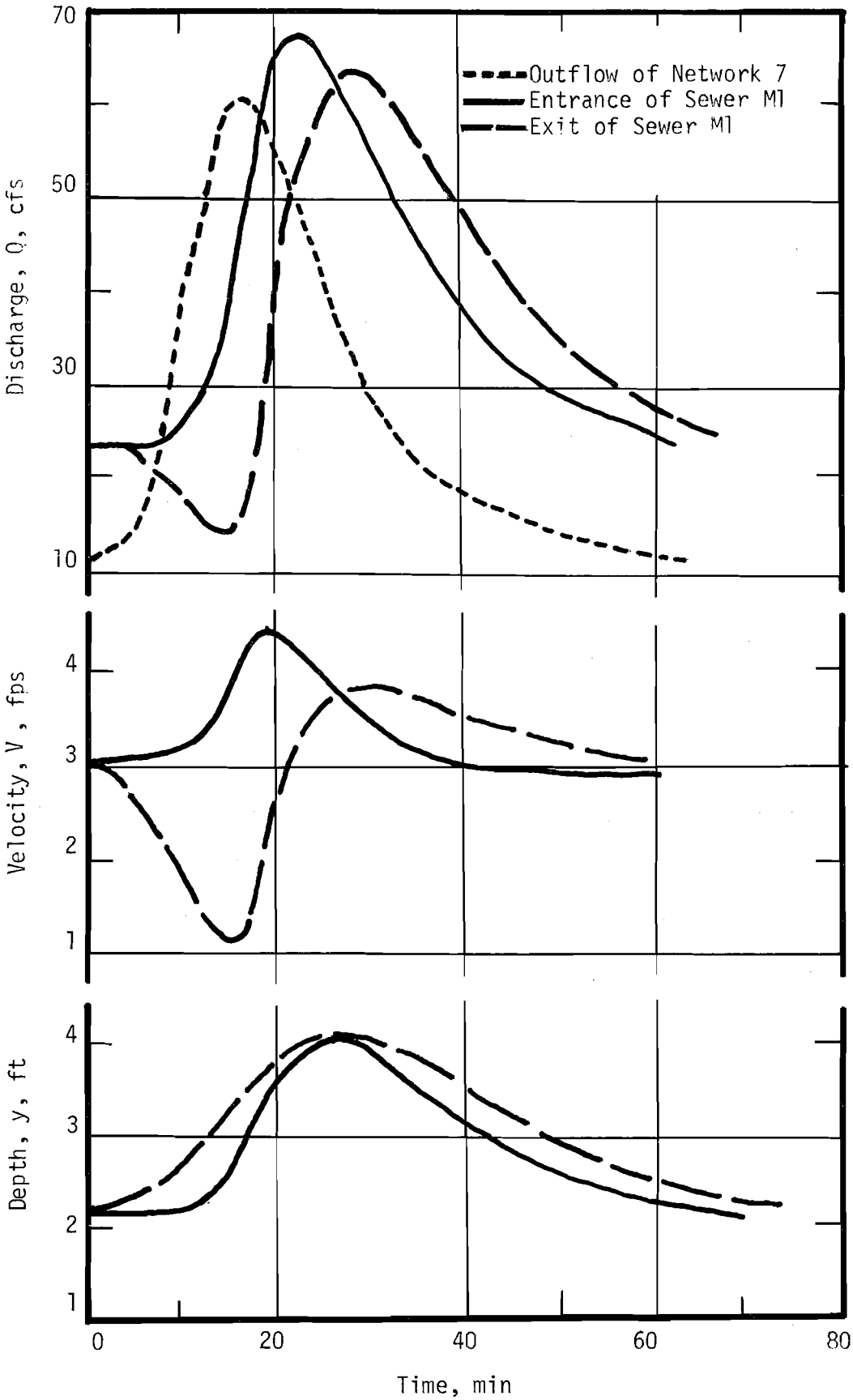

FIG. 38. FLOW AT ENTRANCE AND EXIT OF SEWER M1

Because of continuity of water surface at the junctions, the variation of depth along the sewers indicates that in a main sewer the largest flow depth occurs at the exit rather than at the entrance of the sewer. In Sewer M2, maximum flow depth at the entrance is 4 ft, whereas that at its exit is 4.8 ft. Similarly, the maximum depths at the exit of Sewers M3 and M4 are 5 and 5.4 ft, respectively, and those at the corresponding upstream ends are 4.8 and 5 ft.

VII-3. Further Remarks.

The computed results of the ISS model applied to the example sewer system presented in the preceding section appear to be in good agreement with the expectations based on physical reasoning. A limited number of volume balance calculations for Networks 1, 2, 3, and 7 further indicates the error in conservation of volume to be negligible for all practical purposes. Therefore, the results seem to be correct and substantiate, at least qualitatively, the importance of mutual interaction of flood waves and the resulting backwater effects and detention storages in the sewers and junctions of the system.

In fact, the results indicate that, in routing flood waves, if the junction condition is not carefully selected to approximate closely the actual condition, considerable errors can occur which may completely nullify the effort of elaborated flow equations and numerical schemes for the individual sewers (Sevuk and Yen, 1973b). This is perhaps best indicated by the comparison of results in Networks 1, 2 and 3, as discussed previously.

From a design viewpoint, on the other hand, the results indicate the possible occurrence of a largest flow depth at the downstream rather than at the upstream end of a sewer due to backwater effects. Therefore, the common practice of computing sewer diameters from the peak discharge of the unattenuated flood wave at the upstream end is questionable if pressurized sewer flow is not allowed.

In engineering applications, the ISS Model can be used not only for design purposes but also for flow prediction and for identification of important parameters of storm sewer systems. For example, the Model can be used to test the effectiveness of detention of rainstorm water at various points in a sewer system and its potential on optimal design and pollution control practices. It can be used to predict the effects of urbanization. Or, it can be used to pin-point the bottle-necks of existing sewer systems for improvement and modifications.

Needless to say, complicated as it is, much improvement and refinement can and should be made on the ISS Model. For instance, the extension to include pressurized full conduit flow and hydraulic jumps and surges are desirable. Modification to account for noncircular sewers in a simple but accurate manner would greatly broaden the usefulness of the Model. Furthermore, from the computational economic viewpoint, it appears desirable to modify the Model into two, namely, one for design purposes and the other for flow prediction for which the layout, slope and size of the sewers are known.

It may be appropriate to mention here that the computer time required for the proposed model to operate on the IBM 360/75 system of the University of Illinois at Urbana-Champaign to simulate the flow in the example sewer system is approximately 20 min. If the same system were to be designed, i.e., the sewer diameters were to be determined so as to restrict the maximum flow depth in each sewer between 0.8D and 0.9D, a conservative estimate for the computer time would be one hour.

VIII. DETERMINATION OF DESIGN RAINFALL AND NEW APPROACH TO DESIGN SEWERS BASED ON RISK ANALYSIS

During the early stage of this research a careful re-examination of the then current status of knowledge in urban storm drainage revealed several fundamental weaknesses in conventional design strategy. One of these weaknesses is on the determination of design rainfall and the subsequent sewer design without considering the probability of failure. For a design involving probabilistic quantities of future events, there is always a risk or probability of failure associated with the design (Yen, 1970). For instance, the inlet hydrographs for the worst rainstorm throughout the expected service period of the sewer, say 50 years, is subject to chance in nature. Uncertainties also exist in the mathematical modeling of the sewer system, in the adoption of an idealized and simplified method of solution, and in construction workmanship and material quality. No hydraulic structure can be built absolutely safe, although some important projects may carry a very low risk of failure.

A hydraulic project can be built relatively safe but expensive. The same project may also be built less safe but much cheaper. There is a trade-off point between cost and safety. Also, the public should be informed on the level of protection and the risk of the projects they are involved in or concerned about. In fact, a rational design should have a balanced consideration of cost, benefit, and risk. This is particularly true for urban storm drainage systems because of the manner to finance such projects and the two different types of failure. The recurring type flood protection failure, which results in temporal flooding of low land and basements and interruption of traffic because of inadequacy in capacity of the drainage system, with subsequent property damages and inconvenience but without any structural failure which would impair and damage the functioning of the system. The other is the

catastrophic type failure which involves structural functioning failure such as overloading and damaging of sewage pumps or treatment plants.

In traditional design practice, neither the type of failure nor the risk is explicitly considered. The design rainfall is determined by some rules-of-thumb based on past experiences. For instance, as specified in commonly used technical manuals or reference books such as the ASCE Manual No. 37 (1969), facilities to protect from flooding damages should be designed for rainfall with a return period of 2 to 5 years and for major equipment like pumps and treatment plants 10 to 50 years. Not only is it often difficult to determine exactly what return period should be used within the suggested range but also that in many cases the recommended range of return period is actually unsatisfactory and unscientific. Also, the frequency of rainstorm has been implicitly assumed to be the same as that of the storm runoff, although they are actually different in view of infiltration and other abstractions together with the effect of flow unsteadiness.

In this research project it has been pointed out that the design rainfall return period can be determined scientifically based on risk analysis. First, the simple calculated hydrologic risk is considered (Yen, 1970). In hydrologic design of an engineering project such as storm sewers with an expected life of n years based on a return period T years of the hydrologic event, there always exists an associated risk. By using simple probability theory on independent recurring events and the definition of return period, the risk of failure for the n-year period can be derived as

$$P(X > Q) = 1 - (1 - \frac{1}{T})^n \qquad (35)$$

in which $P(X > Q)$ is the probability of occurrence of an hydrologic event X greater than the design magnitude Q during the entire n years under consideration. Here failure is assumed to occur once the event X, such as rainfall and flood, exceeds the design value Q.

Conversely, if the expected life of the project and the acceptable risk is predetermined, then the corresponding return period can be determined by using Eq. 35. Figure 39 is a plot of Eq. 35 for convenience in engineering uses. If n/T is much smaller than unity, by expanding Eq. 35 into series it can be shown that the risk can be approximated by $P(X > Q) \approx n/T$.

Equation 35 or Fig. 39 can also be used to determine the risk for the remaining n - n' year of a project designed with a return period of T years after it has successfully survived n' years of its expected life of n years.

The simple risk involved for projects designed with T = n > 2 can be found from Eq. 35 or Fig. 39 to be slightly more than 60%. Equation 35 or Fig. 39 can also be used to evaluate the uncertainty involved for rank 1 (maximum) event in limited record of data. For an event with rank m the probability of occurrence $X > Q_m$ equal to or more than m times in n year period can be derived from binomial distribution as

$$P_m(X > Q_m) = 1 - \sum_{r=0}^{m-1} \frac{n!}{r!\,(n-r)!} \left(\frac{1}{T_m}\right)^r \left(1 - \frac{1}{T_m}\right)^{n-r} \qquad (36)$$

The evaluation of the simple risk by Eq. 35 or Fig. 39 depends on neither the type of distribution nor the plotting position of the hydrologic data. Only when either the value or the probability density function of Q is to be determined from statistical data that knowledge on distribution and plotting position of the hydrologic data is required.

In addition to the simple risk just discussed, there are other risks and uncertainties involved which should be considered in hydrologic design of engineering projects. These risks and uncertainties include the risk due to limited record of data available which can be evaluated by using Eqs. 35 and 36 or Fig. 39, and the uncertainties arising from transformation of rainfall data to runoff information, from using a point record to represent an area information, and from the uncertainty of the mathematical techniques in handling

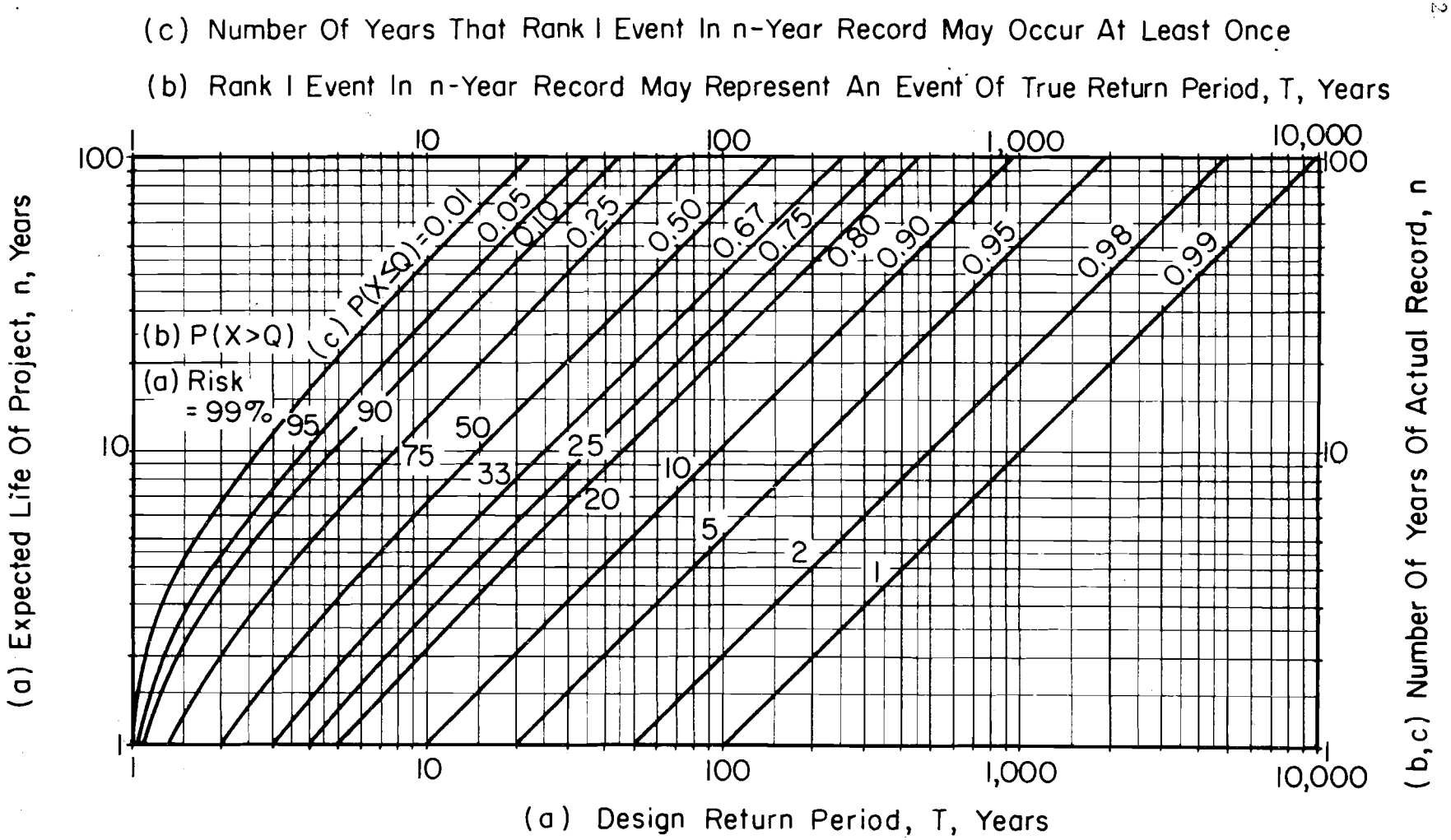

FIG. 39. DESIGN RETURN PERIOD AS FUNCTION OF EXPECTED PROJECT LIFE FOR VARIOUS RISK LEVELS

the data and measurement errors. Furthermore, there are uncertainties concerning the reliability of the hydraulic equations and friction factors used, and non-hydraulic uncertainties like the actual conduit size, surface roughness, alignment and elevation for sewers, and the future changes in physical conditions of the drainage area with time. Some of these uncertainties have no quantitative factual information and must be handled subjectively based on judgement, experience, and intuition. Traditionally, in engineering design a safety factor is introduced to account for the subjective uncertainties. Yet there is no scientific rational method to determine the safety factor for a hydraulic project.

A method based on the extended reliability concept to account for the uncertainties has been proposed in this research project (Yen and Aug, 1971). In probabilistic analysis of hydraulic projects, the design of the engineering system may be subdivided into three components; namely, the hydrologic analysis, hydraulic analysis, and structural analysis, In the hydrologic analysis, a collection of runoff data for a finite period is usually available, either from direct measurement or through transformation from precipitation data or other synthetic means. Based on frequency analysis with an assumed distribution of the data, a reference runoff rate Q can be found for design consideration. For a given return period $T = 1/P(X > Q)$ of the flood X, with an expected life of n years for the project, the probability of of failure can be obtained from Eq. 35. From the assumed distribution of the presumably random variable X, the value of Q can be found since

$$P(X > Q) = \int_{Q}^{\infty} p(X)\, dX \tag{37}$$

where p(X) is the probability density function of the flood (Fig. 40).

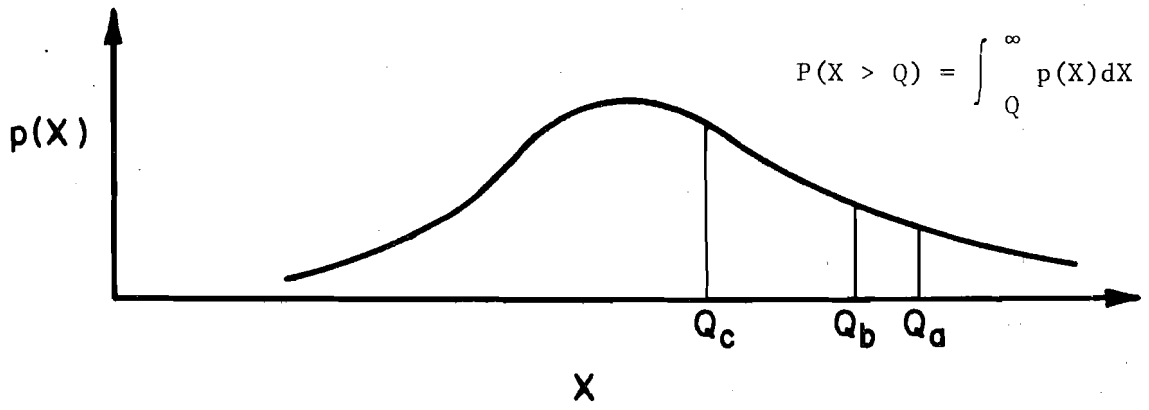

FIG. 40. PROBABILITY DENSITY FUNCTION OF HYDROLOGIC EVENT

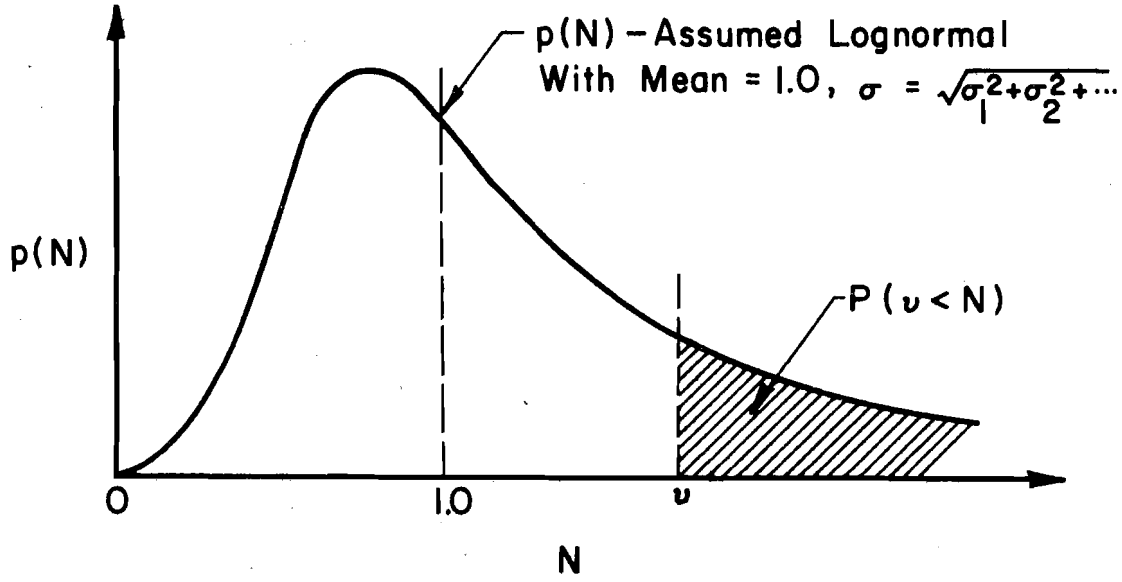

FIG. 41. ASSUMED DENSITY FUNCTION OF THRESHOLD SAFETY NUMBER N

With the value of Q known, further hydrologic and hydraulic analysis can be made. Usually the design flow capacity Q_b is taken to be greater than Q to account for the subjective uncertainties. Thus, the adopted safety factor (or judgement factor) in hydrologic and hydraulic design is equal to $Q_b/Q = w$.

Failure of hydraulic design may be defined as $(X > Q_b/w) \cap (N > w)$, in which N is the safety factor required by virtue of the subjective uncertainties. In order to permit a probabilistic analysis, N is considered as a random variable. Accordingly, the risk of failure is

$$\alpha_h = P(X > Q_b/w) \cdot P(N > w) \tag{38}$$

in which $P(N > w)$ is necessarily a subjective probability. In practice it will suffice to assume N to be a lognormal variate with mean equal to 1.0 and standard deviation σ representing a measure of the subjective uncertainties (Fig. 41). Thus, if the subjective uncertainties consist of error in data sampling, inaccuracy in converting precipitation data to runoff information, and others, which are determined on the basis of judgement to be σ_1, σ_2, ..., respectively, then σ is given (approximately at least) by $\sigma_N = (\sigma_1^2 + \sigma_2^2 + \ldots)^{1/2}$.

Since w can be related to σ_N, the probability $P(N > w)$ can be calculated for a given w to account for the subjective uncertainties. Conversely, if $P(N > w)$ is specified, the appropriate value of w can be evaluated. Hence, in an engineering design, if the appropriate and acceptable values of $P(X > Q)$ and w are specified and if the probability distribution of X is known or assumed, the corresponding values of Q and Q_b can be determined.

Since the true probability distribution of X (or Q) is usually unknown, often a certain distribution function is assigned to it. Hence, ideally, the probabilistic hydrologic and hydraulic design should not be sensitive to the type of the assumed distribution functions. It has been shown (Yen and Ang,

1971) that when the probability of failure is smaller than 10^{-3} it becomes sensitive to the type of distribution function. Therefore, from Eq. 38, $P(X > Q)$ can be kept greater than 10^{-3} by incorporating with the appropriate value of $P(N > w)$. It should be noted here that in most of the conventional design of minor hydraulic structures the values of $P(X > Q)$ are much greater than 10^{-3}, i.e., corresponding to an average flood return period much shorter than once every one thousand years. However, for major hydraulic structures, the acceptable risk of failure would be in the order of 10^{-6} or smaller.

Moreover, often the actual capacity of the hydraulic structure, Q_a, is greater than Q_b due to practical reason. For instance, in sewer design the computed diameter is usually an odd size and hence the next commercially available size of pipe is used. In effect, this provides an additional safety factor of $(Q_a - Q_b)/Q$. Hence, the actual safety factor is equal to $w + (Q_a - Q_b)/Q = Q_a/Q$.

The reliability analysis just described provides not only a scientific approach in determining the safety factor but also a rational basis for design of storm sewers and other hydraulic structures. Examples on application of the risk analysis for design of storm sewers for both the recurring type flood protection failure and catastrophic type failure have been presented elsewhere (Yen and Ang, 1971). Further studies have also been carried out under the OWRR Title II Project C-4123 (Tang and Yen, 1972).

IX. PRELIMINARY INVESTIGATION ON OPTIMAL DESIGN OF STORM SEWER SYSTEM

From a practical viewpoint, the most useful end results of any research on urban storm runoff problems, like this project, are an accurate but relatively simple flow prediction method and an optimal design method accounting for all the influential factors. The ISS Model, or a simplified version of it if desired, satisfies the former objective. As to the optimal design method, non-engineering factors such as cost, damages, and benefits should also be considered. Because in this research project efforts are concentrated on the hydraulic and hydrologic aspects of storm drainage systems, the ISS Model provides a scheme for optimization in terms of hydraulic considerations. With the limitations of time, manpower, and financial resources, and scope of this research project, only a preliminary feasibility investigation on the over-all optimal design method for storm sewer systems has been initiated. Such a high accuracy system cost-benefit optimization would not only be useful by direct application to storm drainage systems but also provide a means to verify the limitations on less accurate but less expensive design models which would be useful for small low cost storm drainage systems.

From flow optimization viewpoint, one possible objective is to minimize the peak discharge at certain given locations such as a pumping station or the effluence to a treatment plant. Certain constraints are, of course, necessary for the components of the drainage system upstream from the location of interest. Otherwise the trivial solution of a large upstream storage would be resulted. It has been found that such a flow optimization can be approximately achieved by using the ISS Model with the aid of a large computer. It should be mentioned here that based on the experience obtained in this study, from computational efficiency viewpoint, it is desirable

to modify the ISS Model in the future into two different models; namely, one for flow prediction with the physiographic characteristics of the sewer system known or determined; the other a design model with the size and/or slope of the sewers and junctions to be determined but the requirement for the accuracy of flow calculations can be somewhat relaxed. However, such a modified design-oriented model by considering only the hydraulics and hydrology of storm runoff has not been further pursued in this research project partly because the ISS Model can do the job and mostly because the risk-cost-benefit consideration is an important factor in design strategy and cannot be neglected.

Nevertheless, it has been found that the ISS Model, and presumably its design-oriented modification, is not suitable to be incorporated directly into the over-all optimal design method because of the large computer capability and time required for the model. With the size of computers at present, the ISS Model by using the St. Venant equations leaves little room for a compatible considerations on risk, cost, damage, and benefit. Hence, a simplified flow evaluation model should be used in developing the method for cost-benefit optimization.

An investigation is first made on an approximate system-cost optimization by using the Manning's formula to describe approximately the flow. The cost is assumed to be described mathematically by two functions, one for the cost of materials and the other for the cost of installation. Of course, maintenance cost and risk functions should eventually be added but are not considered at this stage. It has been found that with these assumptions the system optimization is possible although difficult. It has also been found that a similar simplified approximate system cost optimization scheme by using Manning's formula was proposed in a rarely known report entitled "Sewer System Cost Estimation Model" by Alan M. Voorhees & Associates, Inc. (1969) for the Baltimore Regional Planning Council with a grant from HUD. Hence,it was

decided that the feasibility of a high level accuracy system-cost optimization scheme by considering the effects of flow unsteadiness and sewer storage be investigated.

As pointed out in Chapter II, instead of using the completed St. Venant equations to describe the unsteady flow in the sewers, simpler models can be used if high accuracy is not required. Among the various approximate models, the linear diffusion-wave model and the nonlinear kinematic-wave model appear to be most promising.

The nonlinear kinematic-wave model has the advantage of simplicity, is more widely known, and has been promoted for use in overland flow and channel flow by Wooding (1965), Eagleson (1970), and many others. But it fails to attenuate the storm hydrographs and simply routes them through sewers with no modification except a time lag. Its accuracy is relatively much less than that by the linear diffusion-wave model. The linear diffusion-wave model is capable to account for storm flood flow attenuation and is more accurate with only a slight increase in computor time as compared to the kinematic-wave method. However, for unsteady nonuniform flow such as storm runoff in sewers, the determination of the linealization parameters is tricky and sometimes difficult.

A possible alternative approach to incorporate the unsteady flow in sewers in the optimization is to utilize the nondimensional relationships between the peak discharge as well as its time of occurrence and the sewer and inflow characteristics as shown in Figs. 7 and 8. However, a method must be developed to account for the time difference of the peak discharges of the joinging sewers.

Obviously, the development of a system cost-benefit optimization design method is extremely complicated and difficult. The preliminary feasibility investigation indicates that further study is worthwhile. With

the background information obtained from this project as well as from elsewhere, attempts are being made to develop an optimal design approach for storm sewer system under another research project, OWRR C-4123.

X. CONCLUSIONS

As stated in the original project proposal, "The main objective of this research is to develop methods for quantitative prediction of a storm flow at various locations of an urban drainage system by utilizing the modern development in hydrology, fluid mechanics, and systems concepts, and by considering the urban surface areas, the gutter and inlet devices, the sewer branches, junctions, manholes, and other related structures as an integrated storm drainage system." This objective has been achieved and fulfilled with the development of the method to predict the time distribution of surface runoff into inlet catch basins and the ISS Model to route the inlet hydrographs through sewer network systems. The equations describing flow of storm runoffs and the methods of solutions have been critically reviewed for selection of the most desirable equations and solution methods to solve storm runoff problems. The reliability of the St. Venant flow equations and solution method adopted in this study has been verified by comparing the computed results with available laboratory data for single sewers. Example of application of the ISS Model to sewer network is illustrated by using an example sewer system showing the velocity, depth, and discharge of the flow at any time and any desired locations in the system. The result reveals that conventional flow prediction methods are inadequate because they either fail to account for the backwater effects in the mutually influenced sewers or give only an approximated peak flow rate.

In addition, a method has been developed based on risk analysis for determination of design rainstorm, and then further extended for a scientific approach to determine the factor of safety in hydraulic and hydrologic design. The research result also indicates that a new engineering design method based on risk-cost-benefit consideration is promising.

REFERENCES

Abdel-Razaq, A. Y., W. Viessman, Jr., and J. W. Hernandez, "A Solution to the Surface Runoff Problem," J. Hyd. Div., ASCE, Vol. 93, No. HY6, pp. 335-352, Nov. 1967.

Ackers, P., and A. J. M. Harrison, "Attenuation of Flood Waves in Partfull Pipes," Proc., Inst. Civil Engrs., London, Vol. 28, pp. 361-382, July 1964.

Alan M. Voorhess & Associates, Inc., "Sewer System Cost Estimation Model," McLean, Va., available as PB 183 981, NTIS, Dept. Comm., Springfield, Va., 1969.

Amein, M., and C. S. Fang, "Streamflow Routing With Applications to North Carolina Rivers," Water Resources Research Institute Rept. No. 17, Univ. of North Carolina, 72 p., Jan., 1969.

American Public Works Association, "Urban Drainage Practices, Procedures and Needs," Special Rept. No. 31, Chicago, Dec. 1966.

ASCE Urban Water Resources Research Program, "Urban Water Resources Research," Rept., New York, Sept. 1968.

ASCE Urban Water Resources Research Program, "Basic Information Needs in Urban Hydrology," Rept., p. 5, New York, April 1969.

ASCE and Water Pollution Control Federation, "Design and Construction of Sanitary and Storm Sewers," ASCE Manual No. 37, New York, 1969.

Baltzer, R. A., and C. Lai, "Computer Simulation of Unsteady Flows in Waterways," J. Hyd. Div., ASCE, Vol. 94, No. HY4, pp. 1083-1117, July, 1968.

Behlke, C. E., "The Mechanics of Overland Flow," Dissertation, Dept. of Civil Eng., Stanford Univ. 1957.

Ben-Zvi, A., "On the Relationship Between Rainfall and Surface Runoff on Laboratory Watersheds," Dissertation, Dept. of Civil Eng., Univ. of Illinois at Urbana-Champaign, 1970.

Bowers, C. E., G. S. Harris, and A. F. Pabst, "The Real-Time Computation of Runoff and Storm Flow in the Minneapolis-St. Paul Interceptor Sewers," Memo. M-118, St. Anthony Falls Hyd. Lab., Univ. of Minnesota, Dec. 1968.

California Department of Public Works Division of Highways, "California Culvert Practice," 2nd ed., 1953.

Chen, C. L., and V. T. Chow, "Hydrodynamics of Mathematically Simulated Surface Runoff," Civil Eng. Studies Hydraulic Eng. Ser. 18, Univ. of Illinois at Urbana-Champaign, 132 p., Aug. 1968.

Chen, C. W., and R. P. Shubinski, "Computer Simulation of Urban Storm Water Runoff," J. Hyd. Div., ASCE, Vol. 97, No. HY2, pp. 289-301, Feb. 1971.

Chow, V. T., "Hydrologic Determination of Waterway Areas for the Design of Drainage Structures in Small Drainage Basins," Bull. 462, Eng. Exp. Sta., Univ. of Illinois at Urbana-Champaign, 1962.

Chow, V. T., ed., Handbook of Applied Hydrology, McGraw-Hill Book Co., New York, 1964.

Crawford, N. H., and R. K. Linsley, "Digital Simulation in Hydrology: The Stanford Watershed Model IV," Tech. Rept. 39, Dept. Civil Eng., Stanford Univ., 210 p., 1966.

Dronkers, J. J., "Tidal Computations in Rivers and Coastal Waters," John Wiley & Sons, New York, 1964.

Dronkers, J. J., "Tidal Computations for Rivers, Coastal Areas, and Seas," J. Hyd. Div., ASCE, Vol. 95, No. HY1, pp. 29-77, Jan. 1969.

Eagleson, P. S., Dynamic Hydrology, pp. 326-363, 379, McGraw-Hill Book Co., New York, 1970.

Eagleson, P. S., "Dynamics of Flood Frequency," Water Resources Research, Vol. 8, No. 4, pp. 878-898, Aug. 1972.

Espey, W. H., C. W. Morgan, and F. O. Masch, "A Study of Some of the Effects of Urbanization on Storm Runoff from a Small Watershed," Tech Rept. HY00-7-6501, CRWR-2, Dept. Civil Eng., Univ. of Texas, Austin, 1965.

Evelyn, J. B., V. V. D. Narayana, J. P. Riley, and E. K. Israelsen, "Hydrograph Synthesis for Watershed Subzones from Measured Urban Parameters," Rept., Water Research Lab., Utah State Univ., Aug. 1970.

Fread, D. L., "Technique for Implicit Routing In Rivers with Tributaries," Water Resources Research, Vol. 9, No. 4, pp. 918-926, Aug. 1973.

Gilcrest, B. R., "Flood Routing," Chapter X of Engineering Hydraulics (H. Rouse, ed.) John Wiley & Sons, New York, pp. 635-710, 1950.

Golany, P., and C. L. Larson, "Effects of Channel Characteristics on Time Parameters for Small Watershed Runoff Hydrographs," Bulletin 31, Water Resources Research Center, Univ. of Minnesota, 130 p., May 1971.

Grace, R. A., and P. S. Eagleson, "The Modelling of Overland Flow," Water Resources Research, Vol. 2, pp. 393-403, 1966.

Gunaratnam, D. J., and F. E. Perkins, "Numerical Solution of Unsteady Flows in Open Channels," Rept. 127, R. M. Parsons Lab for Water Resources and Hydrodynamics, MIT, 260 p, July, 1970.

Hamilton, C. L., and H. G. Jepson, "Stock-Water Development: Wells, Springs, and Ponds," US Dept. Agr. Farmers Bull. 1859, p. 39, 1940.

Harley, B. M., F. E. Perkins, and P. S. Eagleson, "A Modular Distributed Model of Catchment Dynamics," Rept. 133, R. M. Parsons Lab. for Water Resources and Hydrodynamics, MIT, 537 p, Dec. 1970.

Harris, G. S., "Real Time Routing of Flood Hydrographs in Storm Sewers," J. Hyd Div., ASCE, Vol. 96, No. HY6, pp. 1247-1260, June 1970a.

Harris, G. S., "Development of a Computer Program to Route Runoff in the Minneapolis-St. Paul Interceptor Sewers," Memo. M-121, St. Anthony Falls Hyd. Lab., Univ. of Minnesota, June 1970b.

Henderson, F. M., and R. A. Wooding, "Overland Flow and Groundwater Flow from a Steady Rainfall of Finite Duration," J. Geophys. Res., Vol. 69, No. 8, pp. 1531-1540, 1964.

Hicks, W. I., "A Method of Computing Urban Runoff," Trans. ASCE, Vol. 109, pp. 1217-1253, 1944.

Horn, D. R., and N. Dee, "Synthesis of the Inlet Hydrograph from Small Pervious and Combination Pervious-Impervious Drainage Areas," Storm Drainage Res. Proj. Tech. Rept. 7, Johns Hopkins Univ., Nov. 1967.

Horton, R. E., "The Interpretation and Application of Runoff Plot Experiments, with Reference to Soil Erosion Problems," Proc. Soil Sci. Soc. Am., Vol. 3, pp. 340-349, 1938.

Hydrocomp Incorporated, "Hydrocomp Simulation Programming: Operation Manual," 2nd Ed., Palo Alto, Calif. 1969.

Illinois Technical Advisory Committee on Water Resources, "Water for Illinois, a Plan for Action," State of Illinois, March 1967.

Isaacson, E. J., J. J. Stoker, and B. A. Troesch, "Numerical Solution of Flood Prediction and River Regulations Problems," Inst. Math. and Mechanics, New York Univ., Rept. 2, IMM-NYU205, Jan. 1954; Rept. 3, IMM-NYU235, Oct. 1956.

Iwagaki, Y., "Theory of Flow on Road Surface," Memoirs of the Faculty of Engineering, Kyoto, Univ., Japan, Vol. 13, pp. 139-147, 1951.

Iwagaki, Y., "Fundamental Studies on the Runoff Analysis by Characteristics," Bull. No. 10, Disaster Prevention Research Inst., Kyoto Univ., Japan, 25 p., 1955.

Izzard, C. F., "Hydraulics of Runoff from Developed Surfaces," Proc. Highway Res. Board, Vol. 26, pp. 129-146, 1946.

James, L. D., "An Evaluation of Relationships Between Streamflow Patterns and Watershed Characteristics Through the use of OPSET: A Self Calibrating Version of the Stanford Watershed Model," Res. Rept. 36, Water Resources Inst., Univ. of Kentucky, 1970.

Kaltenbach, A. B., "Storm Sewer Design by the Inlet Method," Public Works, Vol. 94, No. 1, pp. 86-89, Jan. 1963.

Kareliotis, S. J., and V. T. Chow, "Computer Solution of a Hydrodynamic Watershed Model (IHW Model II)," Civil Eng. Studies Hyd. Eng. Ser. 25, Univ. of Illinois at Urbana-Champaign, 128 p, Mar. 1971.

Keifer, C. J., and H. H. Chu, "Synthetic Storm Pattern for Drainage Design," J. Hyd. Div., ASCE, Vol. 83, No. HY4, Aug. 1957.

Larson, C. L., T. C. Wei, and C. E. Bowers, "Numerical Routing of Flood Hydrographs Through Open Channel Junctions," Water Resources Research Center Bull. 40, Univ. of Minnesota, 67 p, Aug. 1971.

Liggett, J. A., and D. A. Woolhiser, "Difference Solutions of Shallow-Water Equation," J. Eng. Mech. Div., ASCE, Vol. 93, No. EM2, pp. 39-71, Apr. 1967.

Linsley, R. K., "A Critical Review of Currently Available Hydrologic Models for Analysis of Urban Stormwater Runoff," Rept., Hydrocomp Internat., Inc., Palo Alto, Calif., 83 p., Aug. 1971.

McPherson, M. B., "Some Notes on the Rational Method of Storm Drain Design," Tech Memo 6, ASCE Urban Water Resources Program, Jan. 1969.

Metcalf & Eddy, Inc., University of Florida, and Water Resources Engineers, Inc., "Storm Water Management Model," EPA Water Poll. Cont. Res. Ser. 11024 DOC, Vol. 1-4, 1971.

Morgali, J. R., and R. K. Linsley, "Computer Analysis of Overland Flow," J. Hyd. Div., ASCE, Vol. 91, No. HY3, pp. 81-100, May 1965.

Narayana, V. V. D., J. P. Riley, and E. K. Israelsen, "Analog Computer Simulation of the Runoff Characteristics of an Urban Watershed," Rept. Water Research Lab., Utah State Univ., 1969.

Onstad, C. A., and D. G. Jamison, "Subsurface Flow Regimes of a Hydrologic Watershed Model," Proc. 2nd Seepage Symp. USDA AR S41-147, pp. 46-55, 1960.

Papadakis, C., and H. C. Preul, "University of Cincinnati Urban Runoff Model," J. Hyd. Div., ASCE, Vol. 98, No. HY10, pp. 1789-1804, Oct. 1972.

Pinkayan, S., "Routing Storm Water Through a Drainage System," J. Hyd. Div., ASCE, Vol. 98, No. HY1, pp. 123-135, Jan. 1972.

Potter, W. P., "Peak Rates of Runoff from Small Watersheds," BPR Bull. Hyd. Design Ser. 2, Apr. 1961.

Ragan, R. M., "The Determination of Local Inflows Entering a Channel," Proc. Int'l Hydrology Symp., Colo. State Univ., pp. 235-243, Sept. 1967.

Rao, R. A., J. W. Delleur, and S. P. Sarma, "Conceptual Hydrologic Models for Urbanizing Basins," J. Hyd. Div., ASCE, Vol. 98, No. HY7, pp. 1205-1220, 1972.

Rawls, W. J., and J. W. Knapp, "Methods for Predicting Urban Drainage Costs," J. Hyd. Div., ASCE, Vol. 98, No. HY9, pp. 1575-1585, Sept. 1972.

Richtmyer, R. D., "A Survey of Difference Methods for Non-steady Fluid Dynamics," NCAR Technical Notes 63-2, National Center for Atmospheric Research, Boulder, Colorado, 1962.

Rockwood, D. M., "Columbia Basin Streamflow Routing by Computer," J. Waterways and Harbors Div., ASCE, Vol. 84, pp. 1-15, Dec. 1958.

Rockwood, D. M., "Application of Stream Flow Synthesis and Reservoir Regulation --SSARR -- Program to the Mekong River," Pub. 90, Internat. Assoc. for Sci. Hydrology, pp. 329-244, 1968.

Schaake, J. C., "Synthesis of the Inlet Hydrograph," Storm Drainage Res. Proj. Tech. Rept. 3, Johns Hopkins Univ., 105 p., June 1965.

Schaake, J. C., J. C. Geyer, and J. W. Knapp, "Experimental Examination of the Rational Method," J. Hyd. Div., ASCE, Vol. 93, No. HY6, pp. 353-370, Nov. 1967.

Sevuk, A. S., "Unsteady Flow in Sewer Networks," Dissertation, Dept. Civil Eng., Univ. of Illinois at Urbana-Champaign, 1973.

Sevuk, A. S., and B. C. Yen, "A Comparative Study on Flood Routing Computation," Proc. IAHR Internat. Symp. River Mechanics, Bangkok, Vol. 3, pp. 275-290, Jan. 1973a.

Sevuk, A. S., and B. C. Yen, "Comparison of Four Approaches in Routing Flood Wave Through Junction," Proc., Intern. Assoc. Hyd. Res. 15th Congr., Vol 5, pp. 169-172, Istanbul, Sept. 1973b.

Sevuk, A. S., B. C. Yen, and G. E. Peterson, "Illinois Storm Sewer System Simulation Model: User's Manual," Research Rept. No. 74, Water Resources Center, Univ. of Illinois, Urbana, Illinois, 1973.

Shubinski, R. P., and L. A. Roesner, "Linked Process Routing Models," paper presented at the 54th Annual Meeting of the Am. Geophys. Union, Washington, D.C., April 1973.

Stall, J. B. and M. L. Terstriep, "Storm Sewer Design -- An Evaluation of the RRL Method," EPA Environment Protection Technology Ser. R2-72-068, Oct. 1972.

Strelkoff, T., "Numerical Solution of Saint-Venant Equations," J. Hyd. Div., ASCE, Vol. 96, No. HY1, pp. 223-252, Jan. 1970.

Sugawara, M., "On the Analysis of Runoff Structure About Several Japanese Rivers," Jap. J. Geophysiology, Vol. 2, 1961.

Tang, W. H., and B. C. Yen, "Hydrologic and Hydraulic Design Under Uncertainties," Proc., Internat. Symp. on Uncertainties in Hydrologic and Water Resource Systems, Vol. 2, pp. 868-882, Tucson, Ariz., Dec. 1972.

Terstriep, M. L., and J. B. Stall, "Urban Runoff by Road Research Laboratory Method," J. Hyd. Div., ASCE, Vol. 95, No. HY6, pp. 1809-1834, Nov. 1969.

Tholin, A. L., and C. J. Keifer, "The Hydrology of Urban Runoff," Trans. ASCE, Vol. 125, pp. 1308-1379, 1960.

U.S. Soil Conservation Service, "SCS National Engineering Handbook, Section 4, Hydrology," pp. 10.1-10.24, Jan. 1971.

University of Cincinnati, Civil Engineering Dept., "Urban Runoff Characteristics," EPA Water Poll. Cont. Res. Ser. 11024 DOU, Oct. 1970.

Van de Nes, Th. J., and M. H. Hendriks, "Analysis of a Linear Distributed Model of Surface Runoff," Rept. 1, Hydraulics and Catchment Hydrology Lab., Wageningen Agricultural Univ., The Netherlands, 129 p, Jan. 1971.

Watkins, L. H., "The Design of Urban Sewer Systems," Road Res. Tech. Paper 55, Road Research Lab., British Dept. Sci. and Ind. Res., 96 p., 1962.

Wells, D. M., T. A. Austin, and B. C. Cook, "Variation of Urban Runoff with Duration and Intensity of Storms," Completion Rept., OWRR Proj. B-064-Tex, Water Resources Center, Texas Tech Univ., Aug. 1971.

Wooding, R. A., "A Hydraulic Model for the Catchment-Stream, Problem I, Kinematic Wave Theory, Problem II, Numerical Solution," Jour. Hydrology, Vol. 3, pp. 254-282, 1965.

Wright-McLaughlin Engineers, "Urban Storm Drainage Criteria Manual," Vol. 1 and 2, Denver, Colo., 1969.

Wylie, E. B., "Unsteady Free-Surface Flow Computations," J. Hyd. Div., ASCE, Vol. 94, No. HY11, pp. 2241-2251, Nov. 1970.

Yen, B. C., "Risks in Hydrologic Design of Engineering Projects," J. Hyd. Div., ASCE, Vol. 96, No. HY4, pp. 959-966, April 1970; (Closure Vol. 97, No. HY9, pp. 1525-1526, Sept. 1971).

Yen, B. C., "Spatially Varied Open-Channel Flow Equations," Research Rept. 51, Water Resources Center, Univ. of Illinois at Urbana-Champaign, 63 p., Dec. 1971.

Yen, B. C., "Open-Channel Flow Equations Revisited," Jour. Eng. Mech. Div., ASCE, Vol. 99, No. EM5, Oct. 1973.

Yen, B. C., and A. H.-S. Ang, "Risks Analysis in Design of Hydraulic Projects," Stochastic Hydraulics, Proc. Internat. Symp. Stochastic Hydraulics, Pittsburgh, pp. 694-709, 1971.

Yen, B. C., H. G. Wenzel, Jr., and Y. N. Yoon, "Resistance Coefficients for Steady Spatially Varied Flow," J. Hyd. Div., ASCE, Vol. 98, No. HY8, pp. 1395-1410, Aug. 1972.

Yevjevich, V., and A. H. Barnes, "Flood Routing Through Storm Drains, Parts I to IV," Hydrology Papers No. 43-46, Colorado State Univ., Nov. 1970.

Zovne, J. J., "The Numerical Solution of Transient Supercritical Flow by the Method of Characteristics with a Technique for Simulating Bore Propagation," Dissertation, School of Civil Eng., Georgia Inst. Tech., 1970.

APPENDIX 1

Project Publications

A list of publications wholely or partially supported by the research project and excluding this report is given as follows. Copies of the first eight have been submitted to OWRR. The last three will be submitted to OWRR when reprints are available.

(1) Yen, B. C., "Risks in Hydrologic Design of Engineering Projects," Jour. Hyd. Div., ASCE, Vol. 96, No. HY4, pp. 959-966, April, 1970; Closure Vol. 97, No. HY9, pp. 1525-1526, Sept. 1971.

(2) Yen, B. C., discussion of "Real Time Routing of Flood Hydrographs in Storm Sewers," by G. S. Harris, Jour. Hyd. Div., ASCE, Vol. 97, No. HY2, pp. 368-369, Feb. 1971.

(3) Yen, B. C. and A. H.-S. Ang, "Risks Analysis in Design of Hydraulic Projects," Stochastic Hydraulics, Proceedings of the International Symposium on Stochastic Hydraulics, Univ. of Pittsburgh, pp. 694-709, 1971.

(4) Yen, B. C., "Spatially Varied Open-Channel Flow Equations," Water Resources Center Research Rept. No. 51, Univ. of Illinois, 63 p., Dec. 1971.

(5) Yen, B. C., H. G. Wenzel, Jr. and Y. N. Yoon, "Resistance Coefficients for Steady Spatially Varied Flow," Jour. Hyd. Div., ASCE, Vol. 98, No. HY8, pp. 1395-1410, Ang. 1972.

(6) Sevuk, A. S., and B. C. Yen, "A Comparative Study on Flood Routing Computation," Proc, International Symposium on River Mechanics, Vol. 3, pp. 275-290, Bangkok, Thailand, Jan. 1973.

(7) Sevuk, A. S., "Unsteady Flow in Sewer Networks," dissertation, Dept. of Civil Eng., Univ. of Illinois at Urbana-Champaign, 142 p, 1973.

(8) Akan, A. O., "Unsteady Gutter Flow into Grate Inlets," M.S. thesis, Dept. of Civil Eng., Univ. of Illinois at Urbana-Champaign, 88 p, 1973.

(9) Sevuk, A. S., and B. C. Yen, "Comparison of Four Approaches in Routing Flood Wave Through Junction," Proc., 15th Congress, International Association for Hydraulic Research, Vol. 5, pp. 169-172, Istanbul, Turkey, Sept. 1973.

(10) Sevuk, A. S., B. C. Yen, and G. E. Peterson, "Illinois Storm Sewer System Simulation Model: User's Manual," Water Resources Center Research Rept. No. , Univ. of Illinois, 1973.

(11) Yen, B. C., "Open-Channel Flow Equations Revisited," Jour. Eng. Mech. Div., ASCE, Vol. 99, No. EM5, Oct. 1973.

More papers to report the research results are planned to be submitted to technical journals for publications. The abstracts of the publications listed except that for publication No. 2 are reproduced in the following pages.

(1) 7229 RISKS IN HYDROLOGIC DESIGN

KEY WORDS: design; floods; hydraulics; hydrology; probability theory; risk

ABSTRACT: By using the probability theory it has been shown that for any hydrologic design with a certain return period and expected life of a project there is always a calculated risk of failure involved. For a time invariant hydrologic system this simple risk can be computed. Conversely, if the expected project life and the simple risk are known, the corresponding design return period can be determined. Such a determination of the return period is independent of the type of distribution and the plotting position of the hydrologic data. Furthermore, there are additional risks and uncertainties involved which should be considered in hydrologic design of engineering projects such as those due to limited record of data available, using rainfall records to synthesize runoff information, stochastic nature of the hydrologic system, and the techniques utilized in the mathematical processing of the data.

REFERENCE: Yen, Ben Chie, "Risks in Hydrologic Design of Engineering Projects," Journal of the Hydraulics Division, ASCE, Vol. 96, No. HY4, Proc. Paper 7229, April, 1970, pp. 959-966.

(3)

RISKS ANALYSIS IN DESIGN OF HYDRAULIC PROJECTS

By Ben Chie Yen and A. H.-S. Ang
Department of Civil Engineering
University of Illinois
Urbana, Illinois, U.S.A.

SYNOPSIS

In engineering design of hydraulic projects it is often necessary to make use of statistical data. Two types of uncertainties are involved in the design; namely, the objective and subjective uncertainties. Traditionally, in hydraulic projects the reliability of the project as a system is not estimated due mainly to the difficulty in estimating the subjective uncertainties. In this study, a new approach for reliability design of hydraulic projects is proposed. The approach is based on the probabilistic reliability theory, which has been used extensively in structural and systems analyses, with appropriate extension and modification. The total acceptable project risk is subdivided among the project components for design purposes. The risks associated with the subjective and objective uncertainties are handled separately. The design of a storm sewer is used as an example. Alternatively, the proposed approach can be used to estimate the project reliability implied in conventional design procedures and provides a scientific basis for evaluating the proper safety factor required.

STOCHASTIC HYDRAULICS

Proceedings of the First
International Symposium on
Stochastic Hydraulics
(Pittsburgh, May 31-June 2, 1971)
pp. 694-709

(4) ABSTRACT

SPATIALLY VARIED OPEN-CHANNEL FLOW EQUATIONS

Recent development and improvement in numerical techniques and computer capability enables more accurate numerical solutions of spatially varied flow problems such as various phases of urban storm runoffs. Consequently, it is desirable to re-examine fundamentally the competibility of the flow equations used in solving unsteady spatially varied flow problems. To achieve this goal, the continuity, momentum, and energy equations for unsteady nonuniform flow of an incompressible viscous nonhomogeneous fluid with lateral flow into or leaving a channel of arbitrary geometry in cross section and alignment are formulated in integral form for a cross section by using the Leibnitz rule. The resulted equations are then transformed into one-dimensional form by introducing the necessary correction factors and these equations can be regarded as the unified open-channel flow equations for incompressible fluids. The flow represented by these equations can be turbulent or laminar, rotational or irrotational, steady or unsteady, uniform or nonuniform, gradually or rapidly varied, subcritical or supercritical, with or without spatially and temporally variable lateral discharge. Flow equations for certain special cases are deduced from the derived general equations for the convenience of possible practical uses. Conventionally used various equations for open-channel flows are shown to be simplifications and approximations of special cases of the general equations. The inherent difference between the flow equations derived based on the energy and momentum concepts is discussed. Particular emphasis is given to the differences among the energy dissipation coefficient, the frictional resistance coefficient, and the total-head loss coefficient. Common hydraulic practice of using the Chezy, Manning, or Weisbach formulas to evaluate the dissipated energy gradient or the friction slope is only an approximation.

Yen, Ben Chie
SPATIALLY VARIED OPEN-CHANNEL FLOW EQUATIONS
Technical Report to Office of Water Resources Research, Department of the Interior, Washington, D.C., December 1971, vii + 63 pp.
KEYWORDS—*energy equation/ flow resistance/ fluid mechanics/ homogeneous fluid/ hydraulics/ momentum equation/ nonhomogeneous fluid/ nonuniform flow/ *open-channel flow/ *spatially varied flow/ unsteady flow/ water flow

(5)

9107 COEFFICIENTS FOR STEADY SPATIALLY VARIED FLOW

KEY WORDS: **Flow resistance; Friction; Head losses; Hydraulics; Nonuniform flow; Open channel flow; Overland flow; Rainfall; Water flow**

ABSTRACT: In spatially varied flow three coefficients in Weisbach f form are involved which are sometimes termed resistance coefficients. They are the frictional resistance coefficient, the dissipated energy coefficient, and the total head-loss coefficient. In general these three coefficients are not equal whether there is lateral flow or not. Only for steady uniform flow without lateral flow are these three coefficients equal to one another and to the corresponding f in the Moody diagram. Theoretical solution of steady two-dimensional Stokes flow with lateral flow is obtained to show the difference among these three coefficients. Experimental data for steady two-dimensional sheet flow under simulated rainfall are also analyzed to illustrate numerically the variations of these coefficients. In practice, hydraulic engineers should keep in mind the difference in these different resistance coefficients, to avoid unnecessary errors.

REFERENCE: Yen, Ben Chie, Wenzel, Harry G., Jr., and Yoon, Yong Nam, "Resistance Coefficients for Steady Spatially Varied Flow," *Journal of the Hydraulics Division,* ASCE, Vol. 98, No. HY8, **Proc. Paper 9107**, August, 1972, pp. 1395-1410

(6)

INTERNATIONAL ASSOCIATION FOR HYDRAULIC RESEARCH
INTERNATIONAL SYMPOSIUM ON RIVER MECHANICS
9-12 January 1973 Bangkok, Thailand

A COMPARATIVE STUDY ON FLOOD ROUTING COMPUTATION

AHMET SUHA SEVUK
Graduate Research Assistant
Department of Civil Engineering
University of Illinois
Urbana, Illinois 61801 USA

BEN CHIE YEN
Associate Professor of Civil Engineering
University of Illinois
Urbana, Illinois 61801 USA

SYNOPSIS

Hydrologic routing of floods involves only the continuity equation of the flow whereas in hydraulic routing usually the momentum equation and sometimes the energy equation is also used. The most commonly used flow equations in hydraulic routing are the St. Venant equations for which no explicit solution exists. Previously proposed computational techniques to obtain numerical solutions for the St. Venant equations can be categorized into the explicit finite difference schemes, implicit finite difference schemes, and method of characteristics. A comparative investigation has been made in this study on the relative merits of these three schemes with respect to convergence and computational speed. Improved computational methods have been proposed for the latter two schemes with computer results plotted for comparison. Through numerical examples it is shown that a second order formulation of the method of characteristics and an implicit scheme canonical formulation of the characteristic equations are superior to other schemes.

(7) UNSTEADY FLOW IN SEWER NETWORKS

Ahmet Suha Sevük, Ph.D.
Department of Civil Engineering
University of Illinois at Urbana-Champaign, 1973

The objective of this study is to develop a mathematical simulation model for unsteady free-surface flows in urban storm sewer systems with prescribed inflows. The model is intended to serve a dual purpose, flow prediction in existing sewer systems and systematic hydraulic design of the size of the sewers of an entire sewer system. In the developed model one-dimensional equations of continuity and momentum for gradually varied, unsteady, free-surface flow, i.e., the St. Venant equations, are used to describe the sewer flows. A comparative study of the various numerical methods of solution for these equations for flow in single sewers is made in an effort to select the most appropriate numerical solution technique, and the numerical solutions are verified with available experimental data for unsteady flow in single channels. The selected first-order scheme of the method of characteristics for numerical solution is then incorporated with point- and reservoir-type junctions for extension and application to tree-type sewer networks with no closed loops. To account for the mutual influence of flows in the sewers and junctions, the network is considered to be composed of a number of overlapping Y-segments. Following an appropriate sequence these segments are solved one at a time and then the solutions are pieced together to give the time variations of discharge depth and velocity throughout the entire network. In view of the computational difficulties, backwater from a junction is assumed to be confined within the immediate adjacent sewers, and there are no hydraulic jumps or surges inside the sewers.

Computational algorithm of the proposed model which includes a systematic procedure for the design of sewer sizes has been programmed in PL/1 language. The program can be executed on any disk supported digital computer system of the size of IBM 360/75 or larger. The proposed model has been applied to an example sewer system for the prediction of flow conditions. The flood waves are found to attenuate significantly while propagating along the individual sewers. The backwater effects and subsequently the detention storage in sewers have been found important in routing storm inflows through the sewer system. Furthermore, from a design viewpoint, it is significant to find that the backwater effects may cause the occurrence of the largest flow depth at the exit rather than at the entrance of a sewer. The results also indicate the importance of proper representation of the junction hydraulic characteristics on determining correctly the flow in the sewer system. The computed depth, velocity and discharge hydrographs for various locations of the example sewer system are in agreement with the physical expectation.

(8)

UNSTEADY GUTTER FLOW INTO GRATE INLETS

A. O. Akan

ABSTRACT

Runoff from gutters into inlets is usually an unsteady flow phenomenon and is investigated theoretically in this study. The St. Venant equations describing unsteady gutter flows are solved numerically by using the method of characteristics. The discharge into the grate inlet is then determined approximately with the aid of previous experimental results. Design curves are proposed for a given type of gutter and grate inlet to determine the runoff intercepted by the inlet, and the use of of these curves is illustrated by an example.

(9)

INTERNATIONAL ASSOCIATION FOR HYDRAULIC RESEARCH

COMPARISON OF FOUR APPROACHES IN ROUTING FLOOD WAVE THROUGH JUNCTION

By A. Suha SEVUK, Graduate Research Assistant,
and Ben Chie YEN, Associate Professor

Department of Civil Engineering
University of Illinois at Urbana-Champaign
Urbana, Illinois 61801 USA

SYNOPSIS

In routing floods through junctions of open-channels, the computed propagation of the flood wave depends on the assumption made concerning the physical conditions of the junctions. Numerical results of flood wave propagation through a tree type channel network for four different assumed junction conditions are given as an example to illustrate the effect.

(10)

ABSTRACT

ILLINOIS STORM SEWER SYSTEM SIMULATION MODEL: USER'S MANUAL

The Illinois Storm Sewer System Simulation Model is a mathematical model for sewer design and flow prediction utilizing the St. Venant equations to route unsteady flows through tree-type sewer networks. An overlapping segment scheme is used in the numerical solutions to account for the backwater effects and mutual influences of the sewers and junctions. The program is written in PL/1 and assembler Language consisting of more than 3000 statements and can be executed on most large IBM 360 and 370 systems. User oriented information is provided in this report. An example on sewer design is also given.

Sevuk, A. Suha, Yen, Ben Chie, and Peterson, Gordon E.
ILLINOIS STORM SEWER SYSTEM SIMULATION MODEL: USER'S MANUAL
Technical Report to Office of Water Resources Research, Department of the Interior, Washington, D.C., Research Report No. 74 , Water Resources Center, University of Illinois, Urbana, Illinois, September 1973
KEYWORDS--*computer models, drainage systems, flood routing, hydraulics, *hydraulic design, hydrograph, mathematical model, open-channel flow, *simulation, *storm sewers, unsteady flow, *urban runoff

(11) OPEN-CHANNEL FLOW EQUATIONS REVISITED

ABSTRACT

Increasing sophistication in the manner of solving open-channel flow problems together with recent development and improvement in computer capabilities and numerical techniques promotes a fundamental re-examination of the open-channel flow equations. Equations of continuity, momentum, and energy in integral form are here formulated by integrating over the cross section the corresponding equations for a point and then transformed into one-dimensional form by introducing the necessary correction factors. These one-dimensional equations can be regarded as the unified general open-channel flow equations. The channel can have arbitrary cross sectional shape and alignment with fixed or erodible and impervious or pervious bed. The fluid can be homogeneous or nonhomogeneous, compressible or incompressible, and viscous or inviscid. The flow can be turbulent or laminar, rotational or irrotational, steady or unsteady, uniform or nonuniform, supercritical or subcritical, gradually or rapidly varied, and with or without lateral discharge. Based on these equations, the assumptions involved in conventionally used open-channel flow equations such as backwater flow equation and St. Venant equations are examined. The inherent differences between the flow equations derived based on the momentum and energy concepts are compared. The differences among the friction slope, the dissipated energy gradient, and other flow gradients are also discussed.

KEYWORDS: energy equation; flow resistance; fluid mechanics; homogeneous fluid; hydraulics; momentum equation; nonhomogeneous fluid; nonuniform flow; open-channel flow; spatially varied flow; steady flow; unsteady flow; water flow.

REFERENCE: Yen, Ben Chie, "Open-Channel Flow Equations Revisited," Journal of the Engineering Mechanics Division, ASCE, Vol. 99, No. EM5, 1973.

APPENDIX 2

Project Personnel

Many technical and non-technical persons have involved in the project at various times and capacities, including three faculty members (two of them provided free consultations), four graduate research assistants, nine student assistants, and three technicians. Throughout the project period no one person has been supported financially by the project on a full-time basis during the regular academic years. The names of the technical personnel together with their responsibilities and periods of engagement are listed as follows:

Name	Title	Starting Date	Termination Date
B. C. Yen	Principal Investigator, Associate Professor of Civil Engineering	9-1-69	1-31-73
A. H.-S. Ang	Professor of Civil Engineering (free consultation on risk analysis)	9-1-70	1-31-73
V. J. McDonald	Associate Professor of Civil Engineering (free consultation on instrumentation)	9-1-69	1-31-73
Y.-C. Liou	Graduate Research Assistant	9-16-69	1-31-70
A. S. Sevuk	Graduate Research Assistant	2-15-71	1-31-73
Y. H. Tsai	Graduate Research Assistant	9-16-71	6-30-72
A. O. Akan	Graduate Research Assistant	2-1-72	1-31-73
Lawrence Chan	Student Assistant	2-19-71	5-29-71
W. Y. Chen	Student Assistant	5-21-70	10-3-70
D. L. Humpert	Student Assistant	11-1-70	11-2-71
M. Lackpour	Student Assistant	9-21-70	2-20-71
G. E. Peterson	Student Assistant	1-20-72	1-31-73
L. D. Schrof	Student Assistant	6-1-70	8-19-70
A. S. Sevuk	Student Assistant	2-15-70	2-6-71

Name	Title	Starting Date	Termination Date
M. F. Washburn	Student Assistant	2-2-70	6-13-70
D. C. Williams	Student Assistant	7-6-71	8-31-71
J. W. Miller	Physical Science Staff Assistant	9-16-69	1-31-73
G. H. Lafenhagen	Electronic Technician	10-1-70	1-31-73
E. E. Boatz	Draftsman	10-1-69	1-31-73

In addition, the secretary-clerk staff is provided by the Department of Civil Engineering of the University and accounting service is provided by the Water Resources Center of the University of Illinois.